

Phenomenology of Z' -bosons at the LHC

Juri Fiaschi

[Accomando, Belyaev, Fiaschi, Mimasu, Moretti, Shepherd-Themistocleous, JHEP, 01 \(2016\), 127](#)

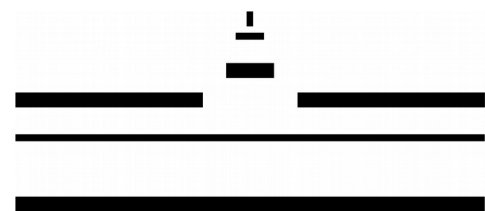
[Accomando, Fiaschi, Moretti, Shepherd-Themistocleous, Phys. Rev. D 96, 075019 \(2017\)](#)

[Accomando, Barducci, De Curtis, Fiaschi, Moretti, Shepherd-Themistocleous, JHEP, 07 \(2016\), 068](#)

[Accomando, Fiaschi, Hautmann, Moretti, Shepherd-Themistocleous, Phys. Rev. D, 95 \(2017\), 035014, Phys. Lett. B, 770 \(2017\), 1-7](#)

UNIVERSITY OF
Southampton
School of Physics
and Astronomy

Particle Physics
Rutherford Appleton Laboratory

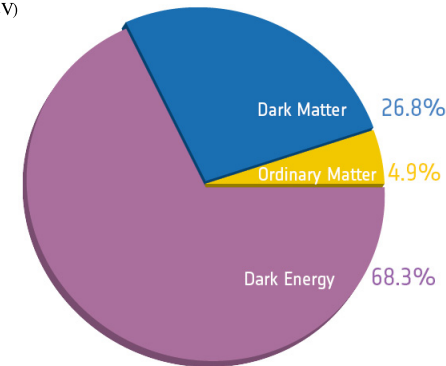
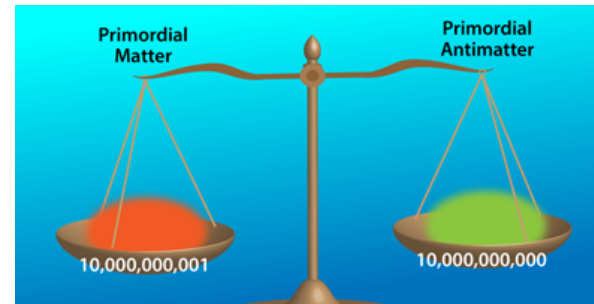
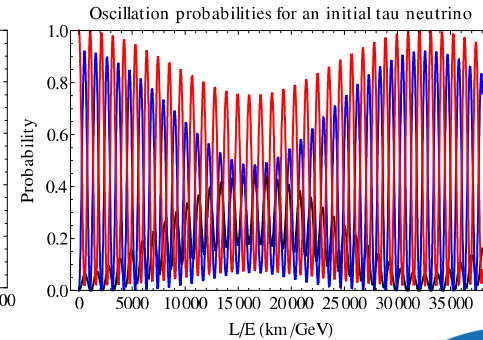
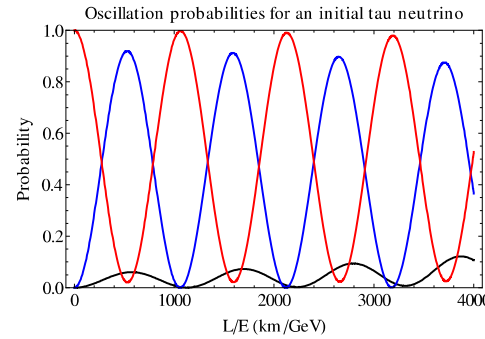


WESTFÄLISCHE
WILHELMS-UNIVERSITÄT
MÜNSTER

Motivations for BSM searches

- We have evidences for BSM physics:

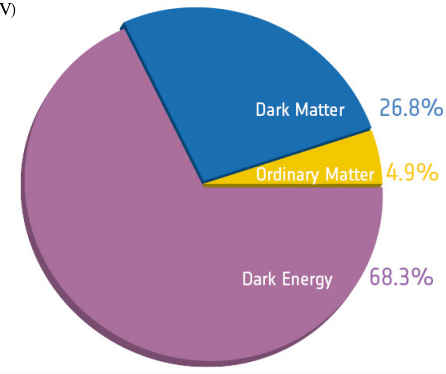
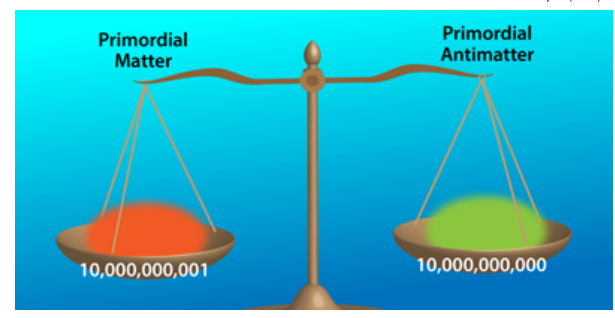
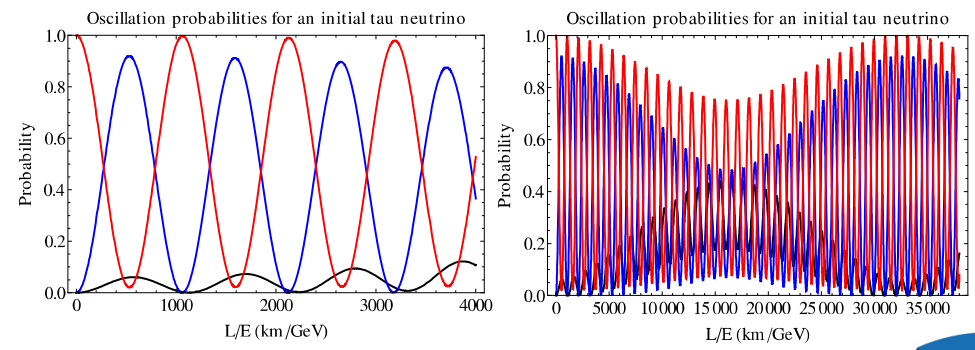
- Neutrino masses
- Matter / antimatter asymmetry
- Dark matter / dark energy



Motivations for BSM searches

- We have evidences for BSM physics:

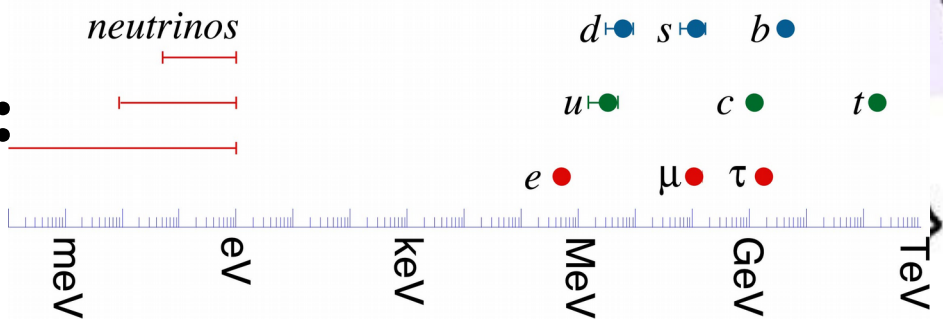
- Neutrino masses
- Matter / antimatter asymmetry
- Dark matter / dark energy



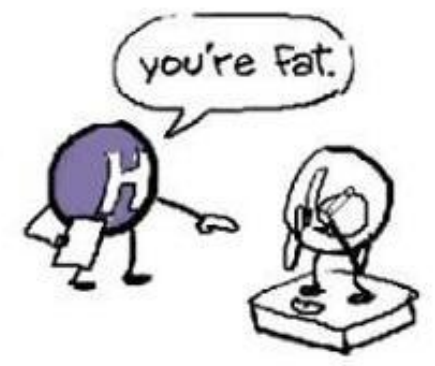
- We have theoretical arguments

- for BSM physics:

- Families of flavour
 - Hierarchy problem
 - Higgs, a fundamental scalar that makes the most important job
- fine tuning $O(10^{34})$ ($M_{Planck} = 10^{19} GeV, M_{Higgs} = 10^2 GeV$)



THE HIGGS IS THE PARTICLE RESPONSIBLE FOR GIVING MASS TO OTHER PARTICLES.



Searches for BSM

Where shall we look for BSM physics?

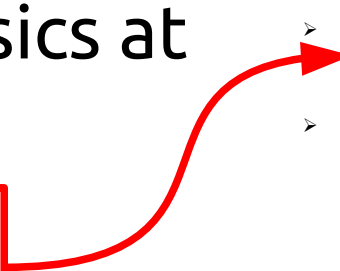
- We want to probe physics at the SM energy scale:
 - Precision measurements can detect BSM effects in low energy observables
 - Determination of the parameters of the Higgs potential to understand the dynamics of Symmetry Breaking
- We want to probe physics at higher energy scale:
 - New heavy particles can be directly produced, and their decay can be observed
 - New signatures can be established as smoking gun of a particular BSM construction

Searches for BSM

Where shall we look for BSM physics?

- We want to probe physics at the SM energy scale:
 - Precision measurements can detect BSM effects in low energy observables
 - Determination of the parameters of the Higgs potential to understand the dynamics of Symmetry Breaking
- We want to probe physics at higher energy scale:
 - **New heavy particles can be directly produced, and their decay can be observed**
 - New signatures can be established as smoking gun of a particular BSM construction

In this talk



Analysis of two opposite sign leptons in the final state: $pp \rightarrow \ell^+ \ell^-$

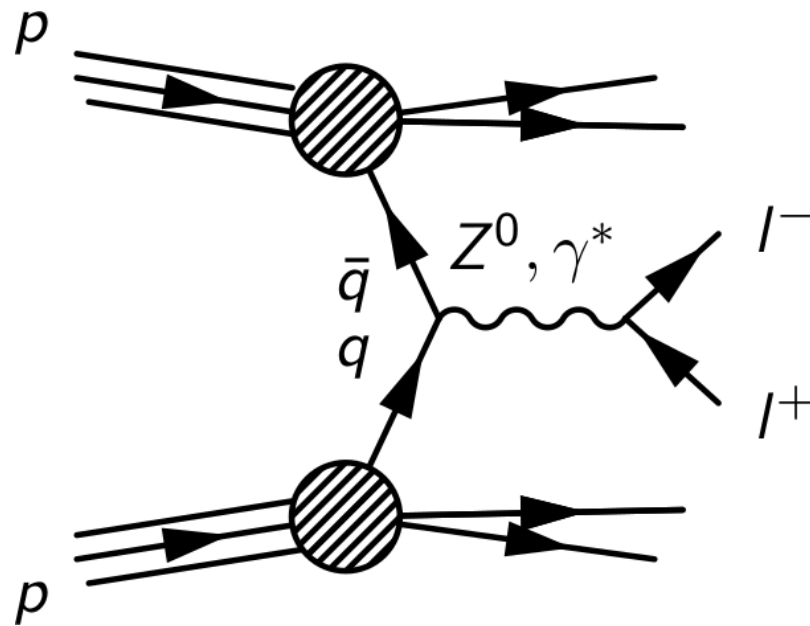
Observing leptons in the final state is a good idea!

- ✓ They can be generated only through Electro-Weak interactions (free of QCD background)
- ✓ They are easy to detect (efficient triggers and clean signature)
- ✓ Detectors are capable of very precise measurements of the kinematics

Topics of this talk

- **Z' bosons: theory → pheno → experiment**
 - Z's from GUT
 - Parametrising Z' interactions
 - LHC updates in the di-lepton channel
- **Experimental searches and their caveats**
 - Narrow resonances
 - Wide resonances
 - Effects of photon-initiated processes
 - Multiple resonances
- **Conclusions**

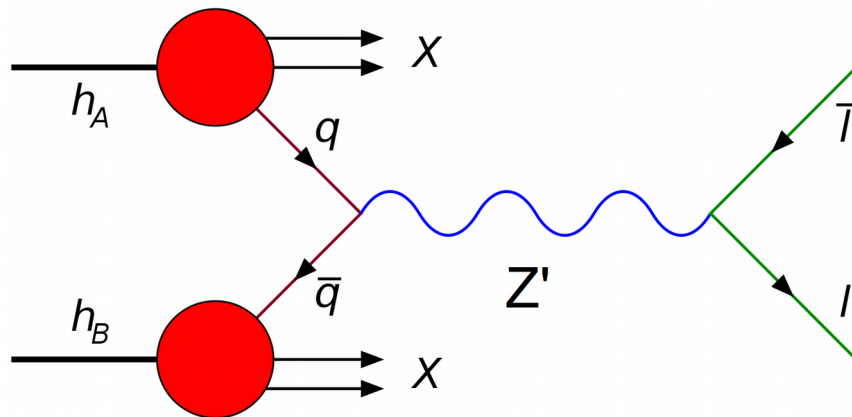
The Drell-Yan channel



Drell-Yan (DY) process, i.e. production of two leptons in the final state from the interactions of two quarks

The mediator of this interaction must be a **neutral** particle coupled to the **Electro-Weak (EW)** sector

In the SM the **photon** and the **Z-boson** do this job



Many BSM constructions predict an extra contribution to the DY due to a new heavy mediator, a **Z'-boson**

The *di-electron* and *di-muon* final states are the golden channel for the detection of **Z'** resonances

Z's at the GUT scale

E_6 class

$$\begin{aligned} E_6 &\rightarrow SO(10) \times U(1)_\psi \\ &\rightarrow SU(5) \times U(1)_\chi \times U(1)_\psi \\ &\rightarrow SM \times U(1)' \end{aligned}$$

*From the theory
point of view*



$$U(1)' = U(1)_\chi \cos \theta + U(1)_\psi \sin \theta$$

Generalised Left-Right class (GLR)

$$\begin{aligned} &SU(2)_L \times SU(2)_R \times U(1)_{B-L} \\ &\rightarrow SU(2)_L \times U(1)_Y \times U(1)' \end{aligned}$$

$$U(1)' = U(1)_R \cos \phi + U(1)_{B-L} \sin \phi$$

Generalised Standard Model class (GSM)

$$U(1)' = U(1)_L \cos \alpha + U(1)_Q \sin \alpha$$

*(Just a heavier
copy of the SM)*

Z's at low energy

We have an effective description

From the pheno point of view

$$SU(3)_C \times SU(2)_L \times U(1)_{em} \times U(1)_{Z'}$$

$$\mathcal{L} \supset g' Z'_\mu \bar{\psi} \gamma^\mu (a_V - a_A \gamma_5) \psi$$

The structure of the interaction is fixed. The only the free parameters are:

- Fermions' chiral couplings
- Mass and Width of the **Z'**-boson

Parameters of the interaction

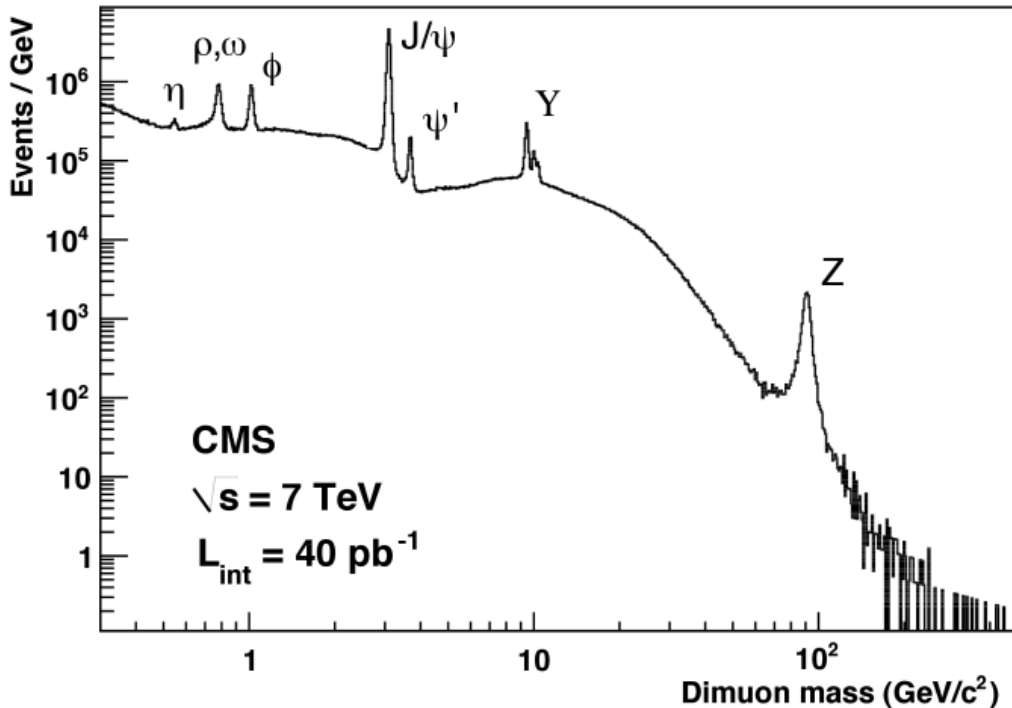
Single Z' benchmarks

*From the pheno
point of view*

$U(1)'$	Parameter	a_V^u	a_A^u	a_V^d	a_A^d	a_V^e	a_A^e	a_V^ν	a_A^ν
$E6(g' = 0.462)$	θ								
χ	0	0	-0.316	-0.632	0.316	0.632	0.316	0.474	0.474
ψ	0.5π	0	0.408	0	0.408	0	0.408	0.204	0.204
η	-0.29π	0	-0.516	-0.388	-0.129	0.388	-0.129	0.129	0.129
S	0.129π	0	-0.130	-0.581	0.452	0.581	0.452	0.516	0.516
I	0.21π	0	0	-0.5	0.5	0.5	0.5	0.5	0.5
N	0.42π	0	0.317	-0.157	0.474	0.157	0.474	0.316	0.316
$GLR(g' = 0.592)$	ϕ								
R	0	0.5	-0.5	-0.5	0.5	-0.5	0.5	0	0
$B - L$	0.5π	0.333	0	0.333	0	-1	0	-0.5	-0.5
LR	-0.130π	0.326	-0.459	-0.591	0.459	-0.06	0.459	0.199	0.199
Y	0.25π	0.589	-0.354	-0.118	0.354	-1.061	0.354	-0.354	-0.354
$GSM(g' = 0.762)$	α								
SM	-0.072π	0.186	0.487	-0.336	-0.487	-0.035	-0.487	0.487	0.487
$T3L$	0	0.5	0.5	-0.5	-0.5	-0.5	-0.5	0.5	0.5
Q	0.5π	1.333	0	-0.667	0	-2	0	0	0

Narrow Z's at the LHC

A "bump" in a smooth background



A signal is observed

The interpretation of an hypothetical Z' signal requires the fit of two independent parameters: the Mass and the Width of the resonance

Narrow Z'
($\Gamma/M < 5\%$)

From the exp
point of view

Scan of the invariant mass spectrum assuming a **Breit-Wigner (BW)** line-shape for the new physics signal standing over an almost null background.

No signal observed

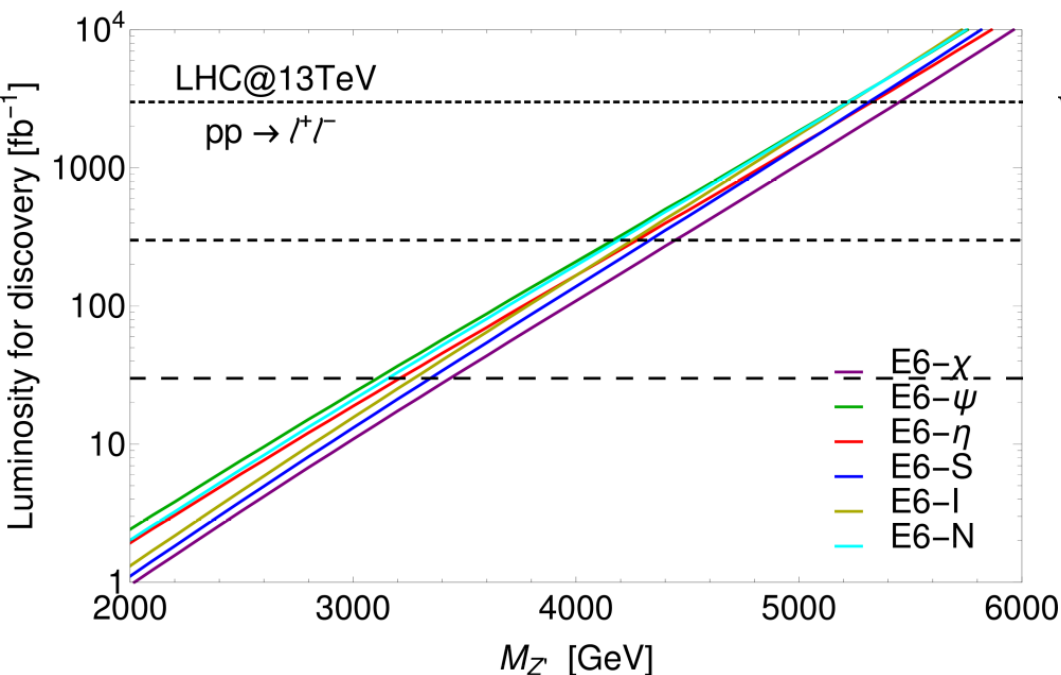
The extraction of Z' mass limits follows model independent procedures, based on the Narrow Width Approximation (**NWA**), or exploiting the invariant mass "optimal cut" $|M_{\parallel} - M_{Z'}| < 5\% E_{\text{LHC}}$

[Accomando, Becciolini, Belyaev, Moretti, Shepherd-Themistocleous, JHEP 10, 2013, 153](#)

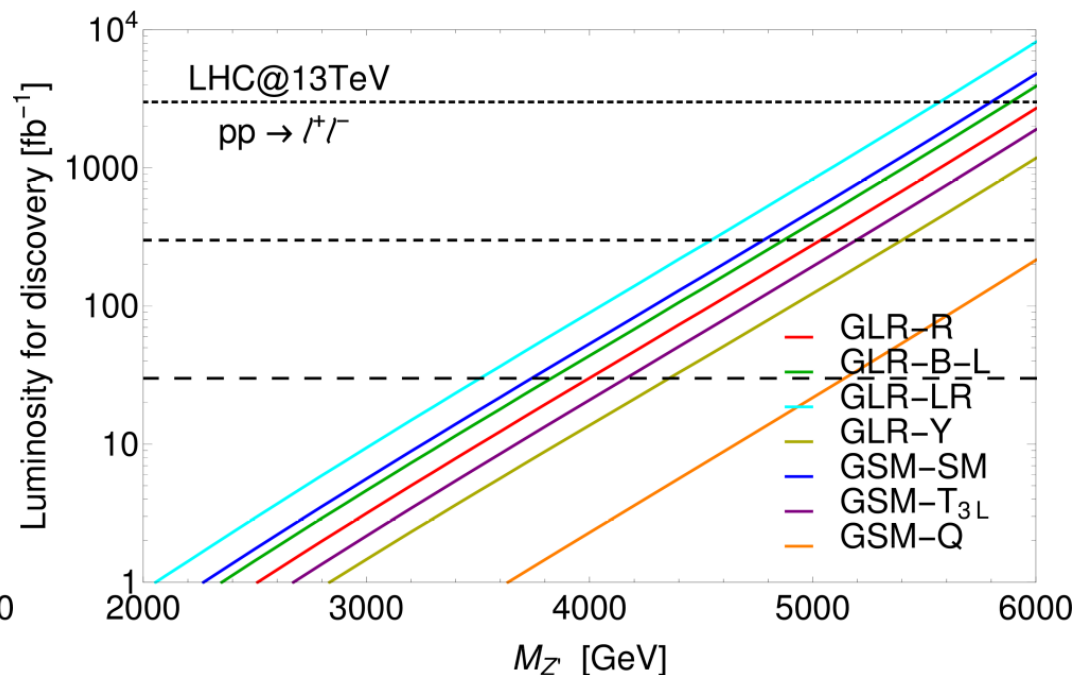
The extracted mass bounds are easy to reinterpret

Narrow Z' discovery projections

The use we would like for the LHC



Luminosity required for Z' discovery as function its mass for popular models



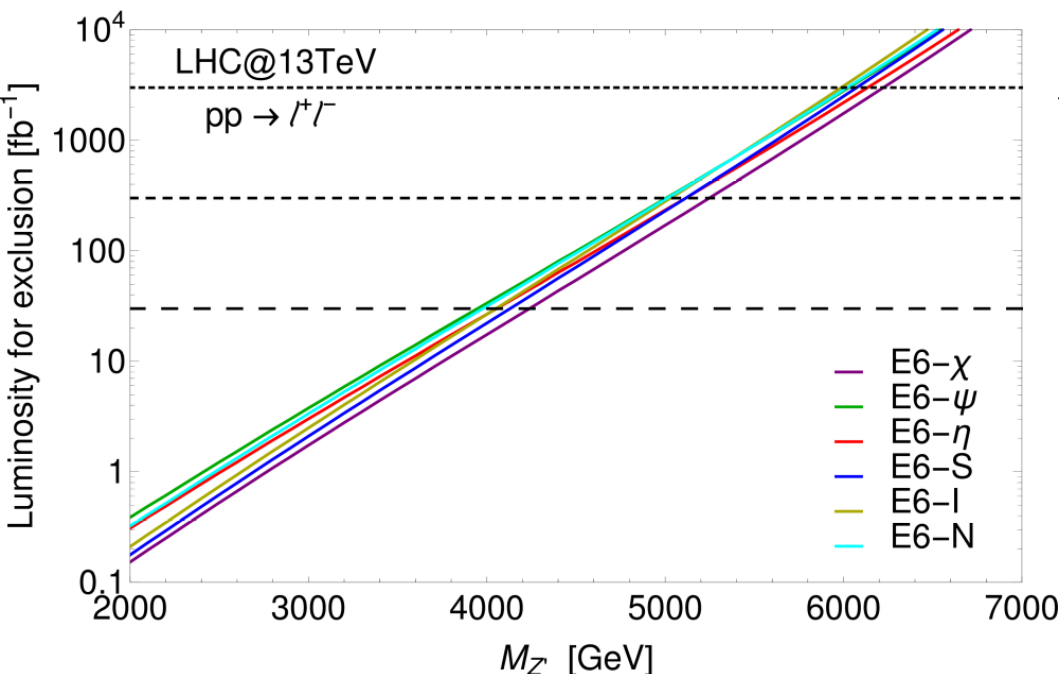
LHC will be sensitive to narrow resonances with masses up to:

- **3 TeV – 4 TeV** at the current luminosity ($\mathcal{L} = 30 \text{ fb}^{-1}$)
- **4 TeV – 5 TeV** by the end of the Run-II stage ($\mathcal{L} = 300 \text{ fb}^{-1}$)
- **5 TeV – 6.5 TeV** by the end of the High Luminosity stage ($\mathcal{L} = 3000 \text{ fb}^{-1}$)

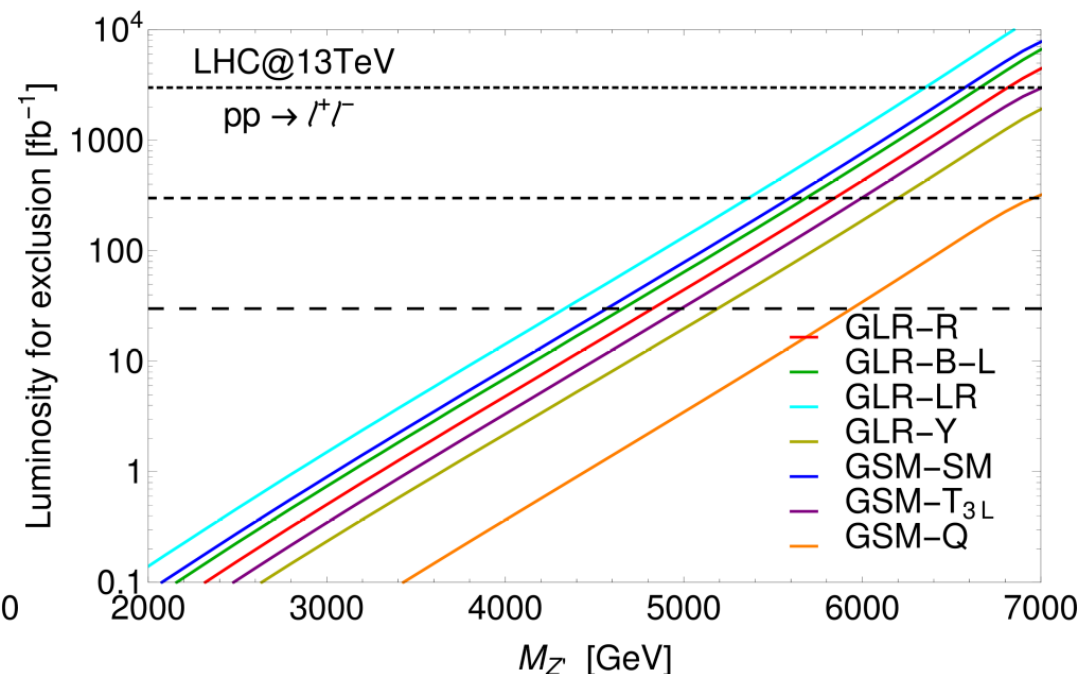
[Accomando, Belyaev, Fiaschi, Mimasu, Moretti, Shepherd-Themistocleous, JHEP, 01 \(2016\), 127](#)

Narrow Z' exclusion projections

The use we make of the LHC



Luminosity required for Z' exclusion as function its mass for popular models

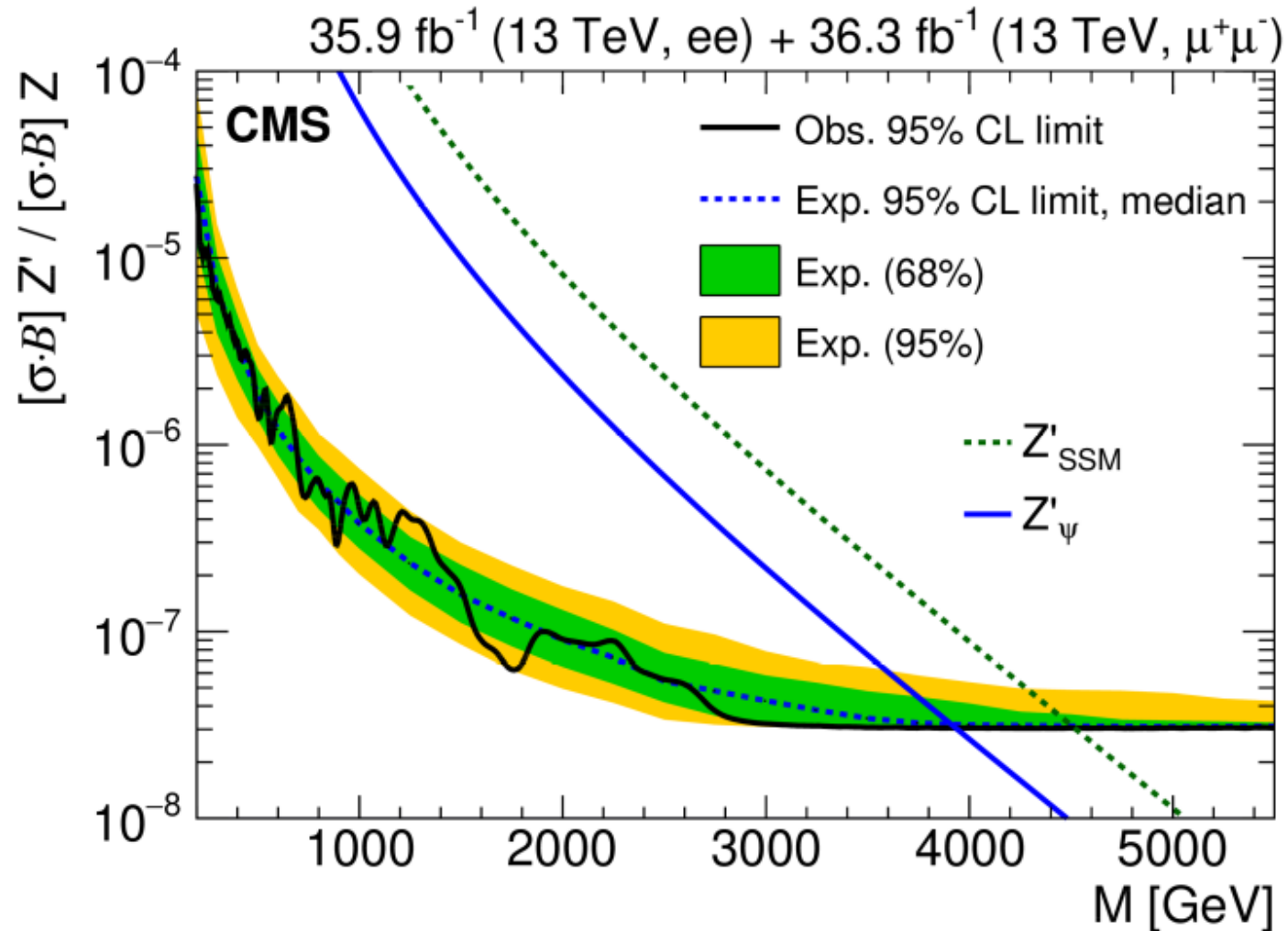
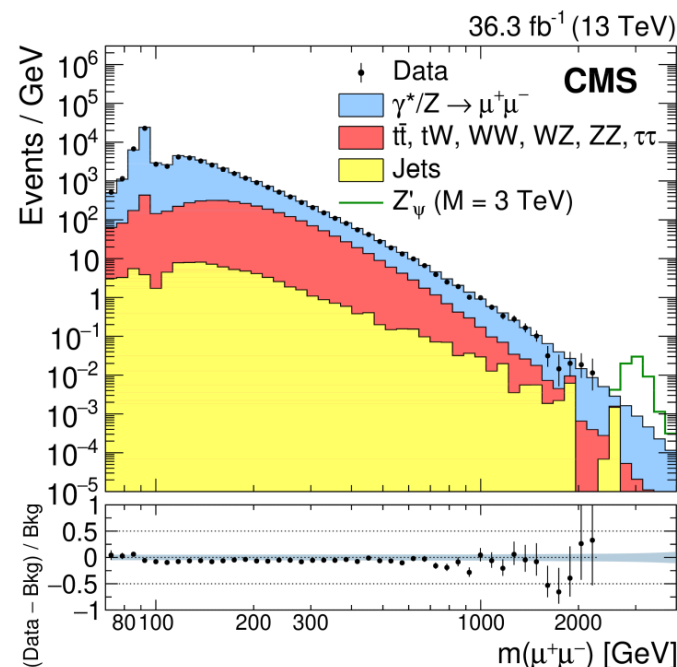
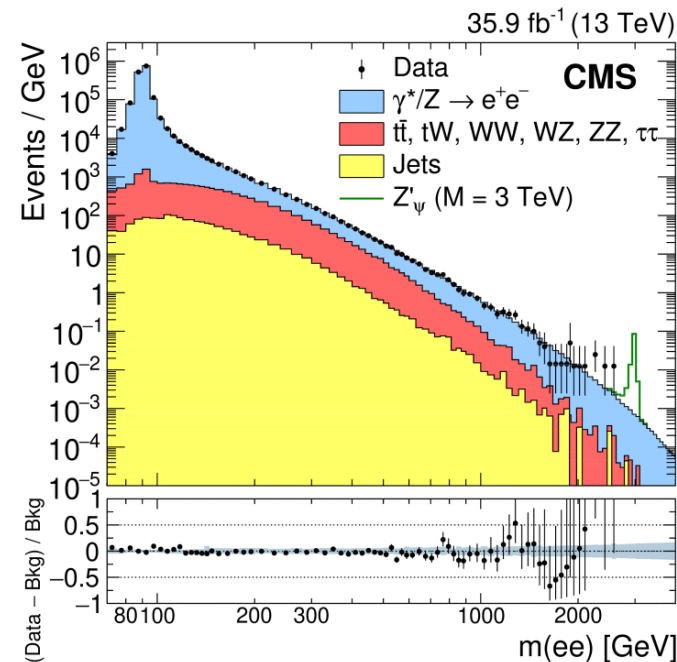


LHC will be able to exclude narrow resonances with masses up to:

- **4 TeV – 5 TeV** at the current luminosity ($\mathcal{L} = 30 \text{ fb}^{-1}$)
- **5 TeV – 6 TeV** by the end of the Run-II stage ($\mathcal{L} = 300 \text{ fb}^{-1}$)
- **6 TeV – 6.5 TeV** by the end of the High Luminosity stage ($\mathcal{L} = 3000 \text{ fb}^{-1}$)

[Accomando, Belyaev, Fiaschi, Mimasu, Moretti, Shepherd-Themistocleous, JHEP, 01 \(2016\), 127](#)

Updates from the LHC

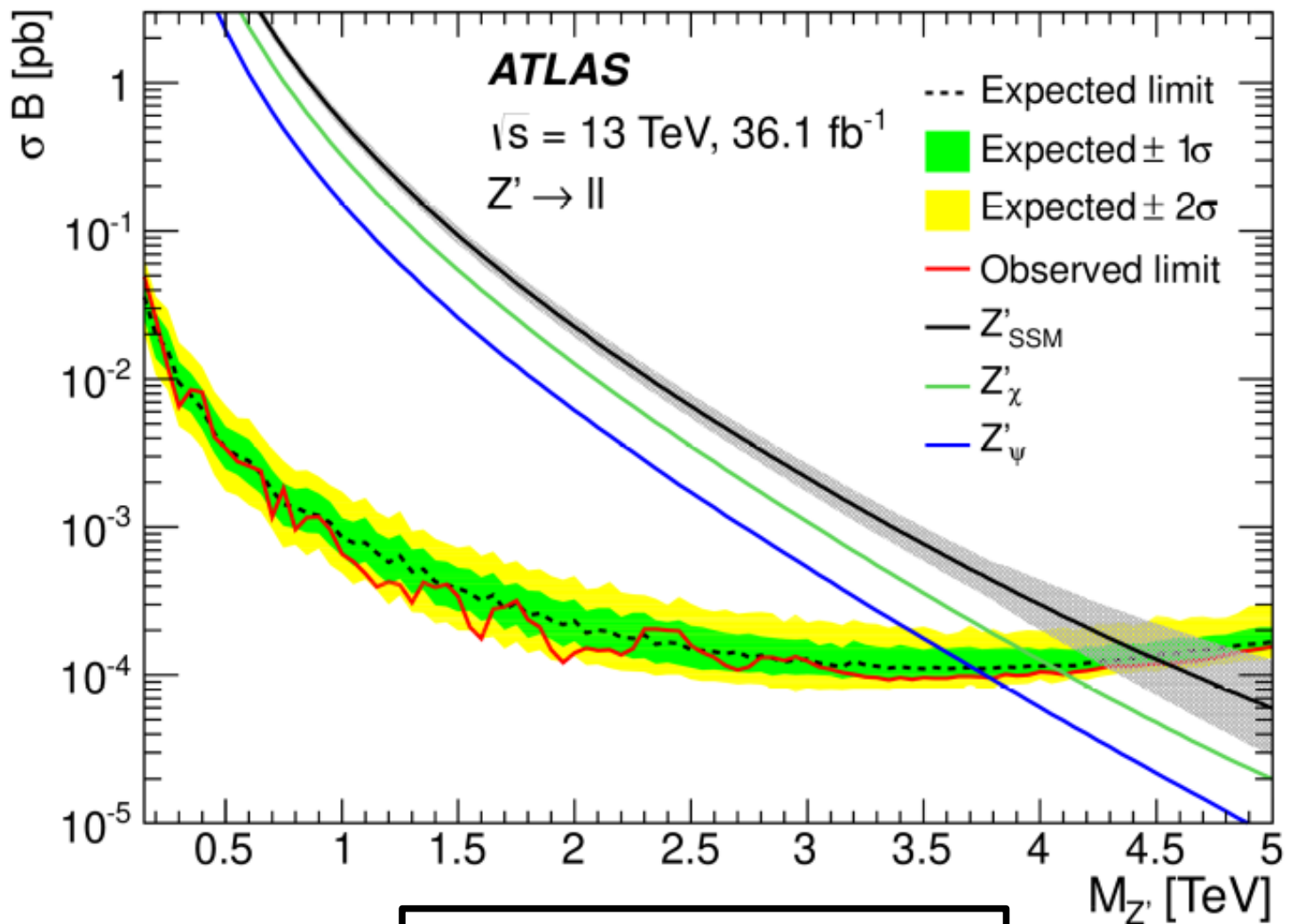
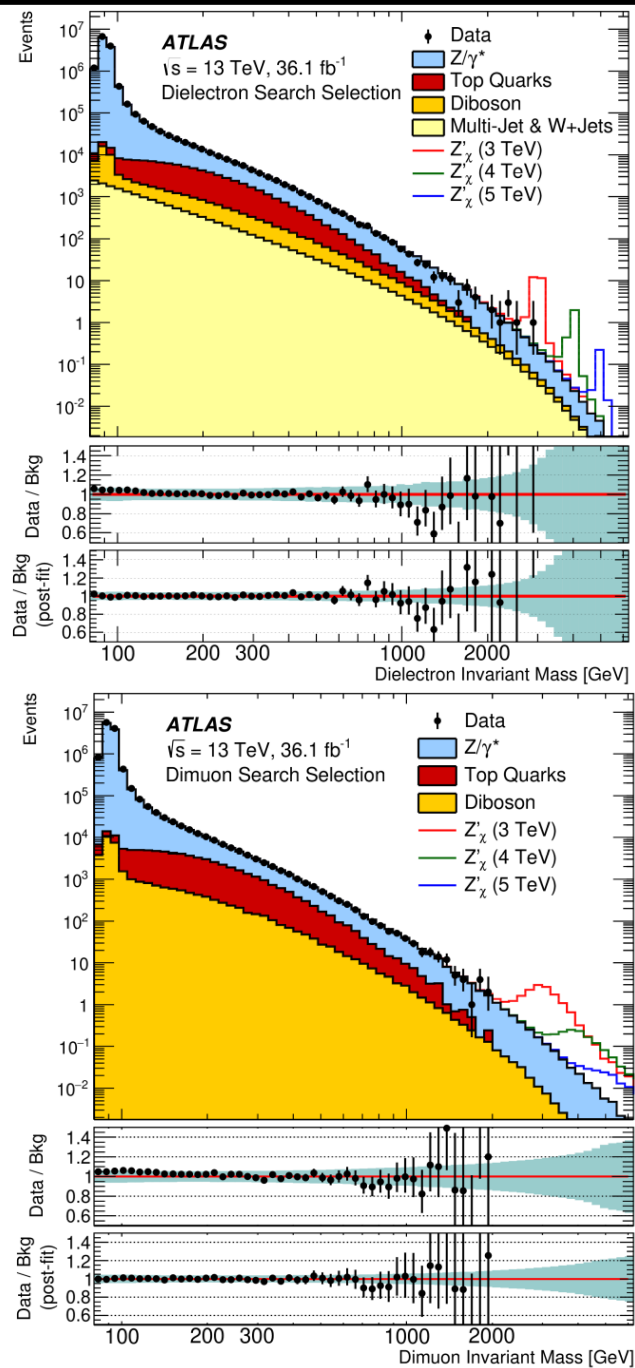


13 TeV data with $\mathcal{L} \sim 36 \text{ fb}^{-1}$

Z' boson masses excluded up to 4 – 4.5 TeV

CMS collaboration,
JHEP 1806 (2018) 120

Updates from the LHC



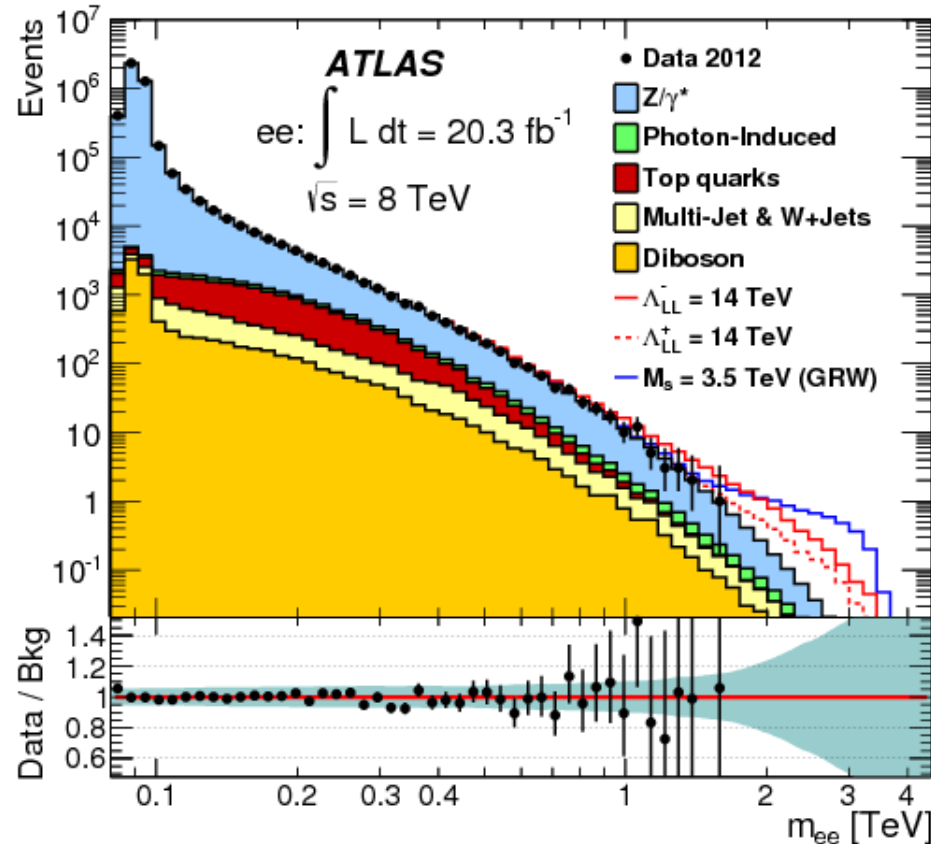
13 TeV data with $\mathcal{L} \sim 36 \text{ fb}^{-1}$

Z' boson masses excluded up to 4 – 4.5 TeV

**ATLAS collaboration,
 JHEP 1710 (2017) 182**

Wide Z's at the LHC

A "shoulder" on an estimated background



Wide Z'
($\Gamma/M > 5\%$)

*From the exp
point of view*

The experimental analysis is essentially a counting experiment where we seek for an excess of events above an estimated SM background

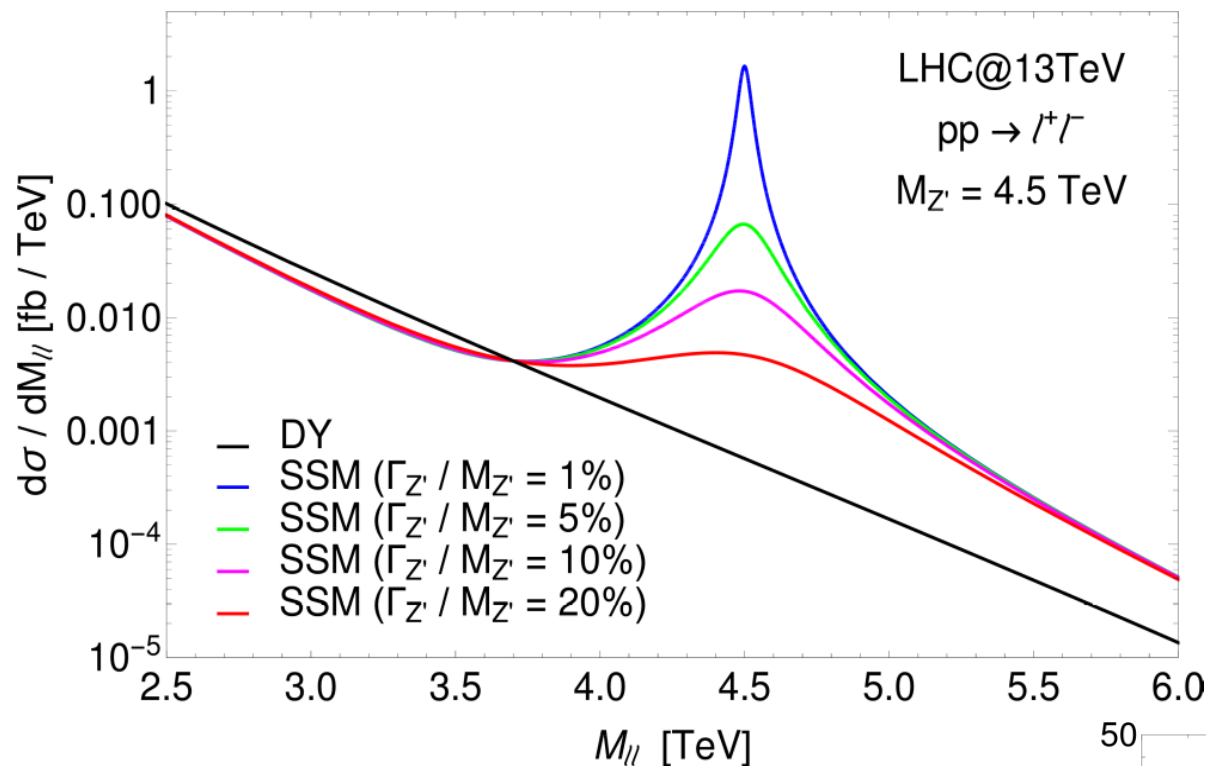
ATLAS Collaboration,
[Eur. Phys. J, C74, \(2014\), no.12, 3134](#)

Other observables can help disentangling a Z' signal:

- The **Forward-Backward Asymmetry (AFB)** maintains a visible line-shape even for large values of the resonance width.
- The **transverse momentum distribution (p_T)** can be used to extract information on the resonance width.

Heavy relying on a good understanding and control of the SM background. Systematic uncertainties in the high invariant mass region (i.e. from **PDFs**) can spoil the extrapolation.

Limits on the XS sensitivity

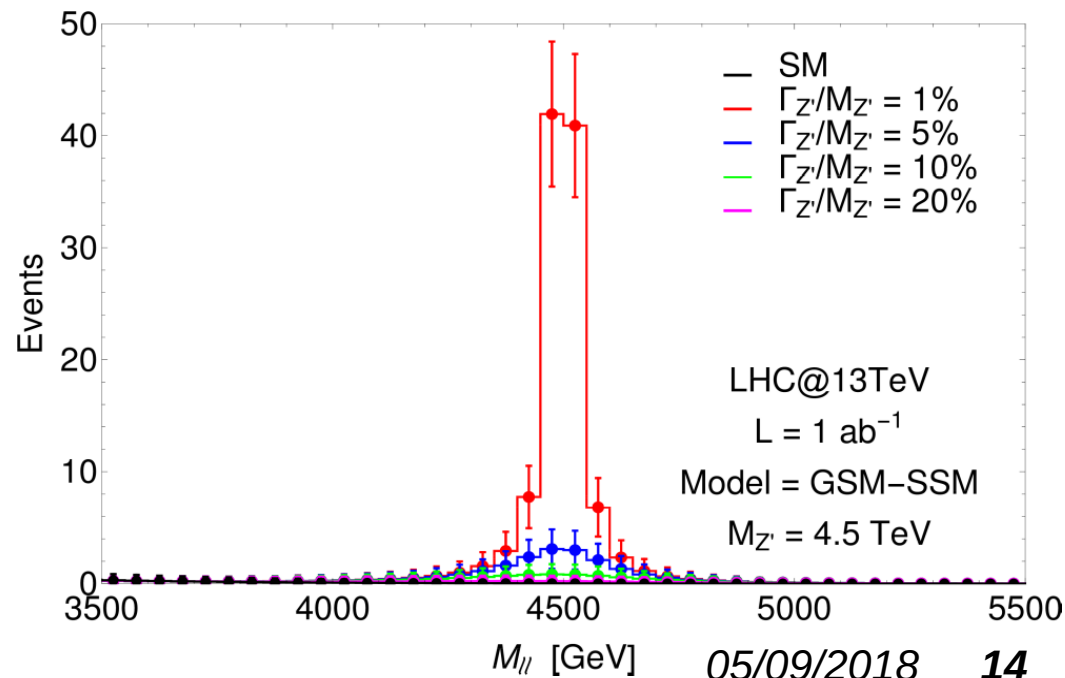


Width is varied by hand (i.e. no rescaling of the couplings):

- σ production is unchanged
- Br scales linearly with of the width

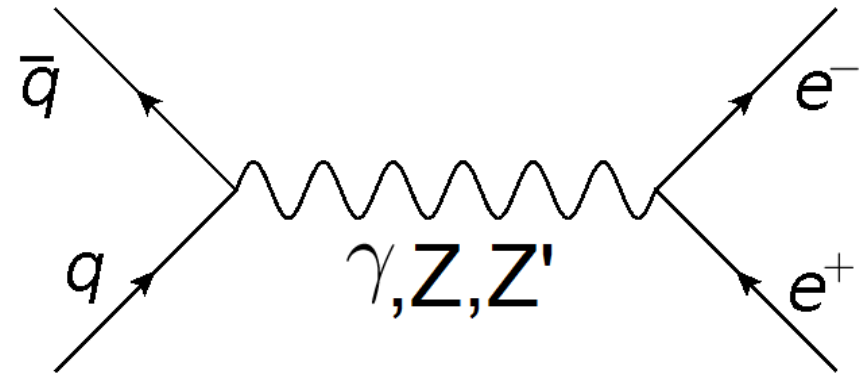
Representative of the case where exotics decay channels are opened

Significant loss of sensitivity in the Cross Section!



The Forward-Backward Asymmetry

The **Forward-Backward Asymmetry (AFB)** is sensitive to different combination of the fermions chiral couplings



$$\sum_{spin, pol} \left| \sum_i \mathcal{M}_i \right|^2 = \frac{\hat{s}^2}{3} \sum_{i,j} |P_i^* P_j| \left[\boxed{(1 + \cos^2 \theta) C_S^{i,j}} + \boxed{2 \cos \theta C_A^{i,j}} \right]$$

Cross section term

AFB term

Where the two coefficients depends on different combinations of the couplings:

$$C_S^{i,j} = (a_{V_i} a_{V_j} + a_{A_i} a_{A_j})_L (a_{V_i} a_{V_j} + a_{A_i} a_{A_j})_Q$$

$$C_A^{i,j} = (a_{V_i} a_{A_j} + a_{A_i} a_{V_j})_L (a_{V_i} a_{A_j} + a_{A_i} a_{V_j})_Q$$

The AFB*

$$A_{FB} = \frac{\sigma_F - \sigma_B}{\sigma_F + \sigma_B}$$

$$\sigma_F = \int_0^1 \frac{d\sigma}{d\cos\theta} d\cos\theta$$

$$\sigma_B = \int_{-1}^0 \frac{d\sigma}{d\cos\theta} d\cos\theta$$

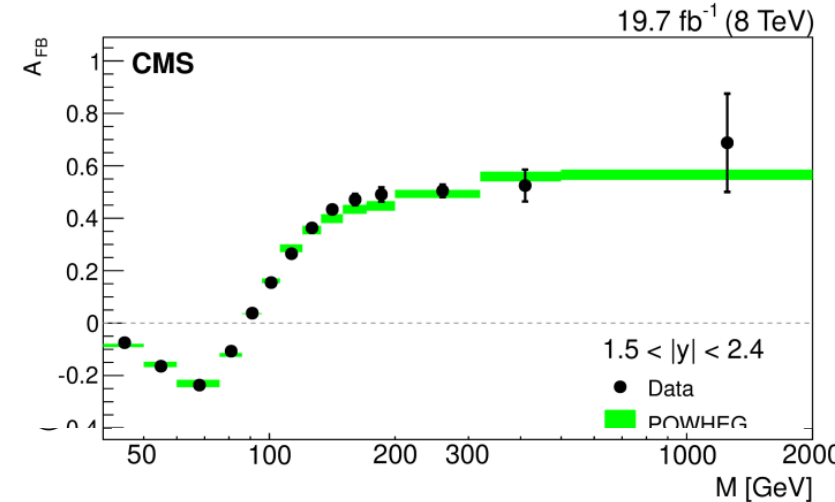
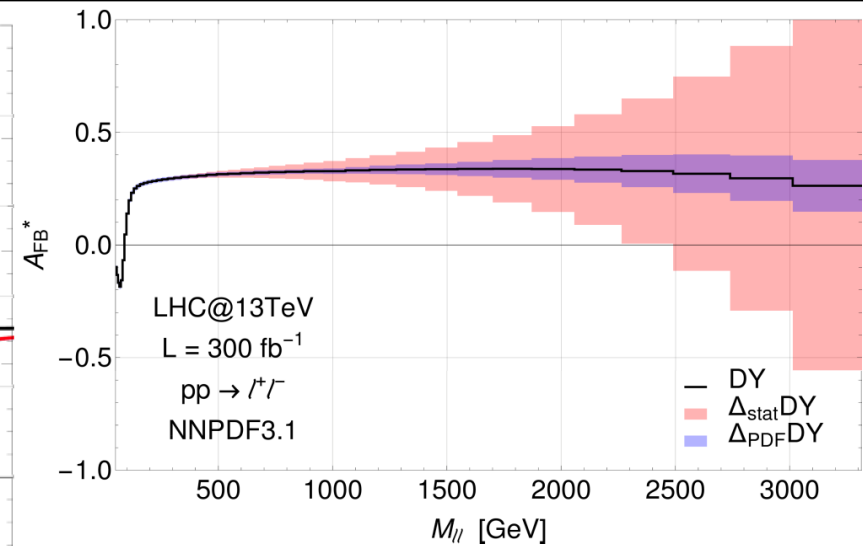
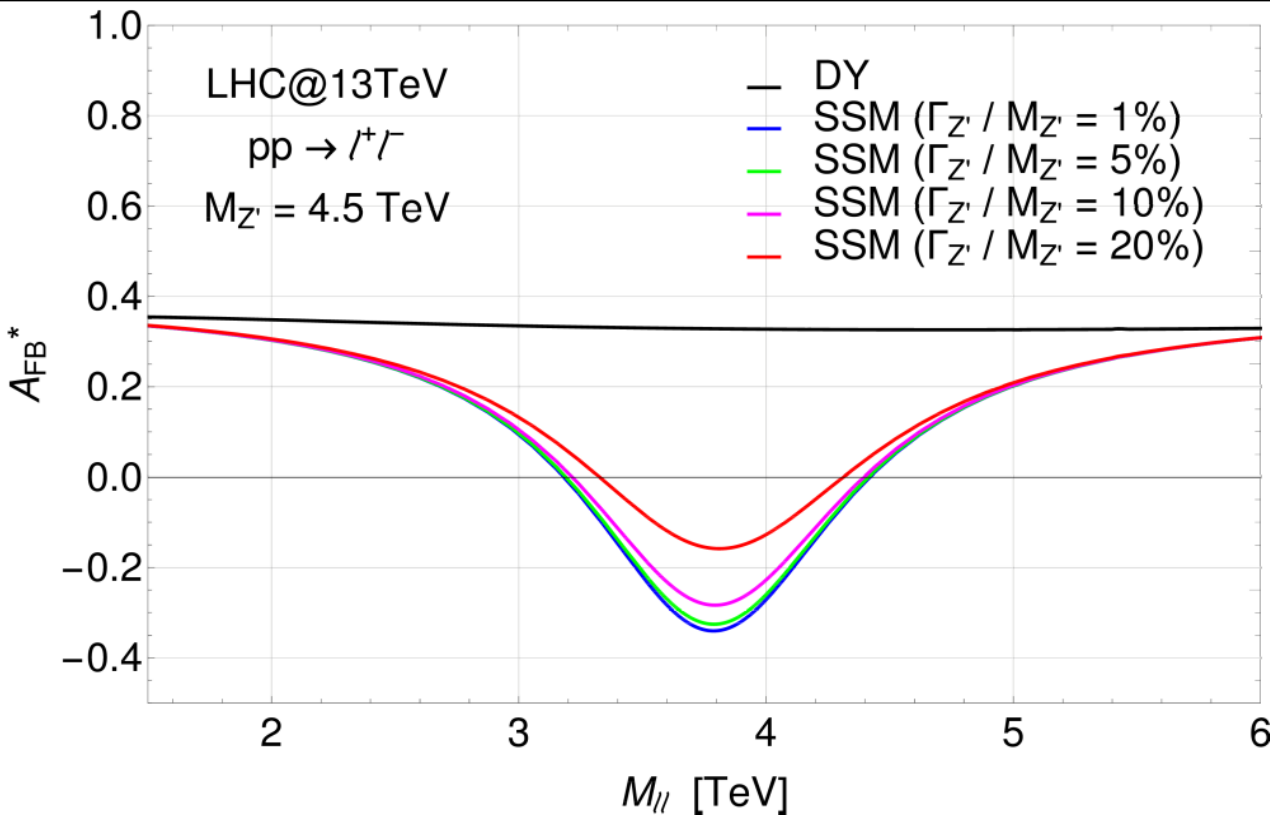
The θ angle is defined in the partonic center of mass

**In proton-proton collisions
no access to c.o.m. frame!**

Convention: the direction of the incoming quark is defined by the boost of the di-lepton system

**At LHC we can observe the
reconstructed AFB or **AFB*****

The AFB*



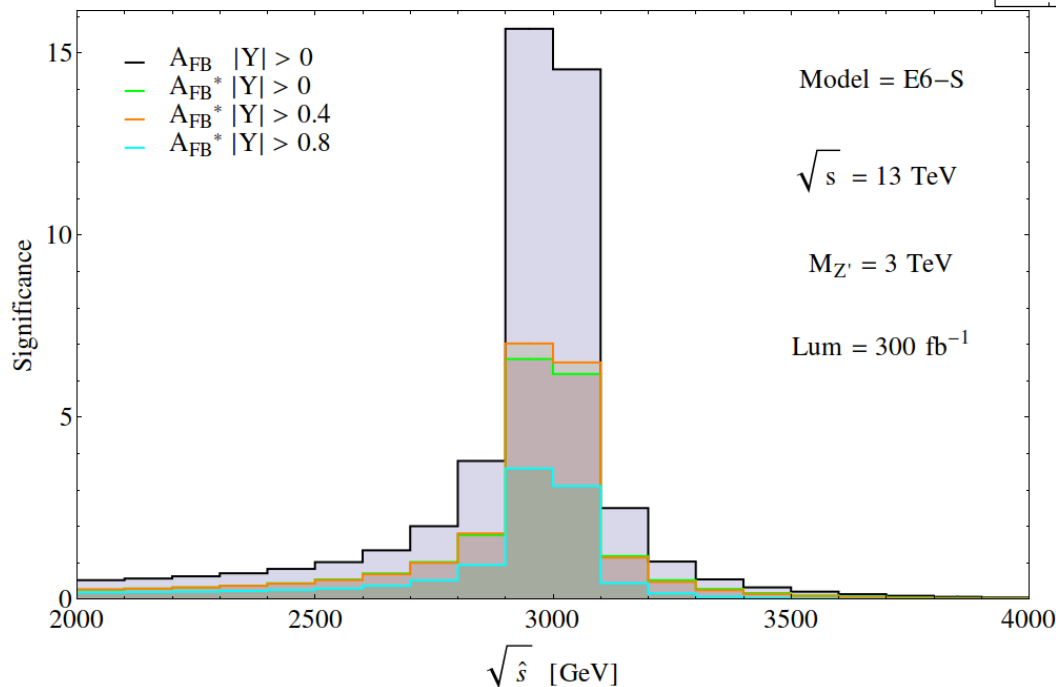
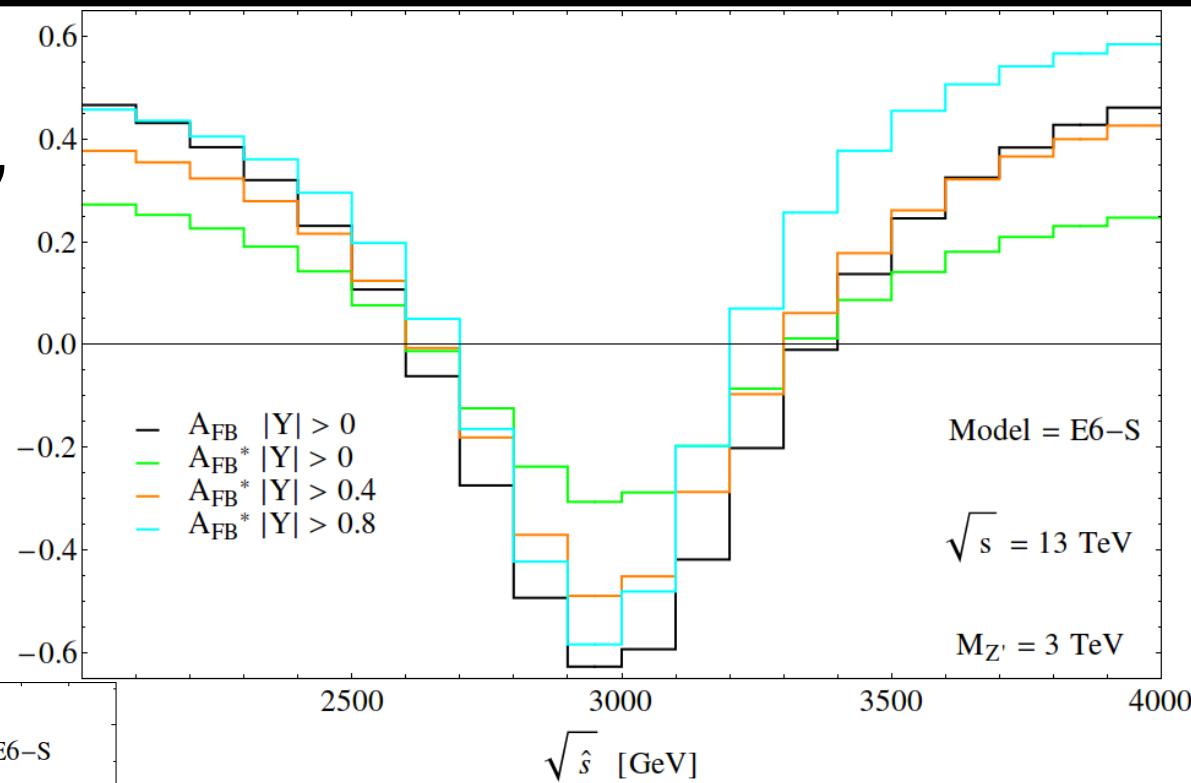
- The AFB maintains a visible shape also in case of wide resonances
- Being a ratio of cross sections, part of systematics cancel out

[CMS Collaboration, Eur. Phys. J., C76 \(2016\) 6, 325](#)

Still few data points in the high invariant mass region.
 Statistical uncertainty dominates

The AFB*

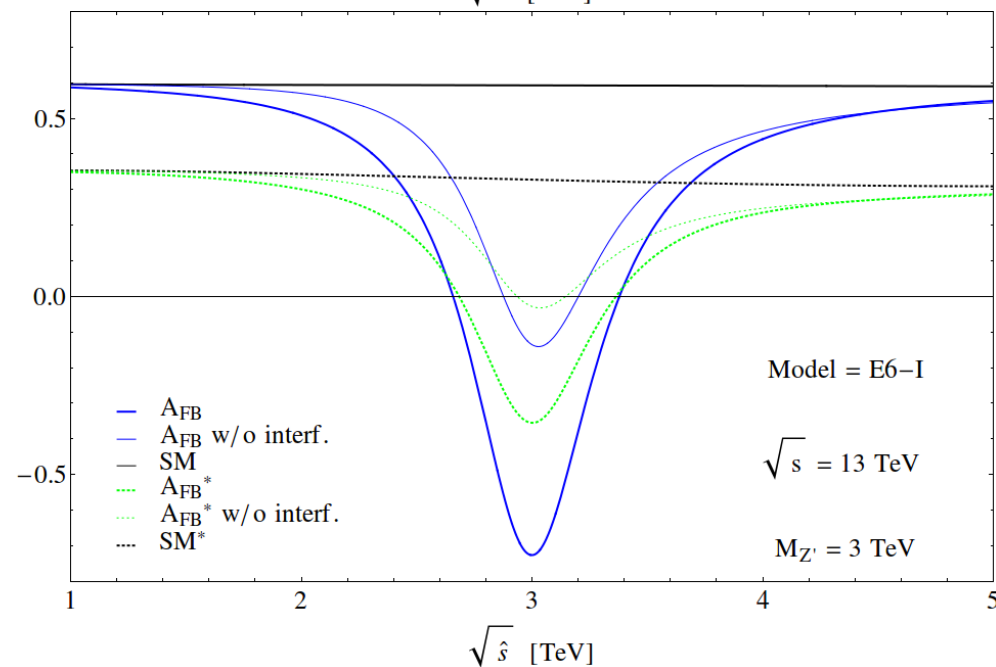
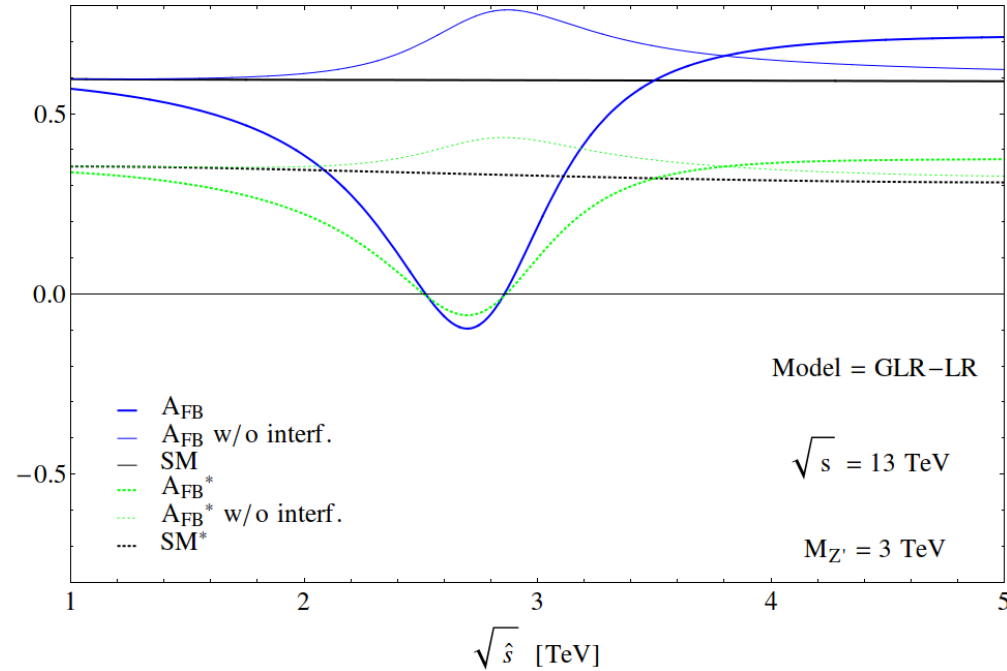
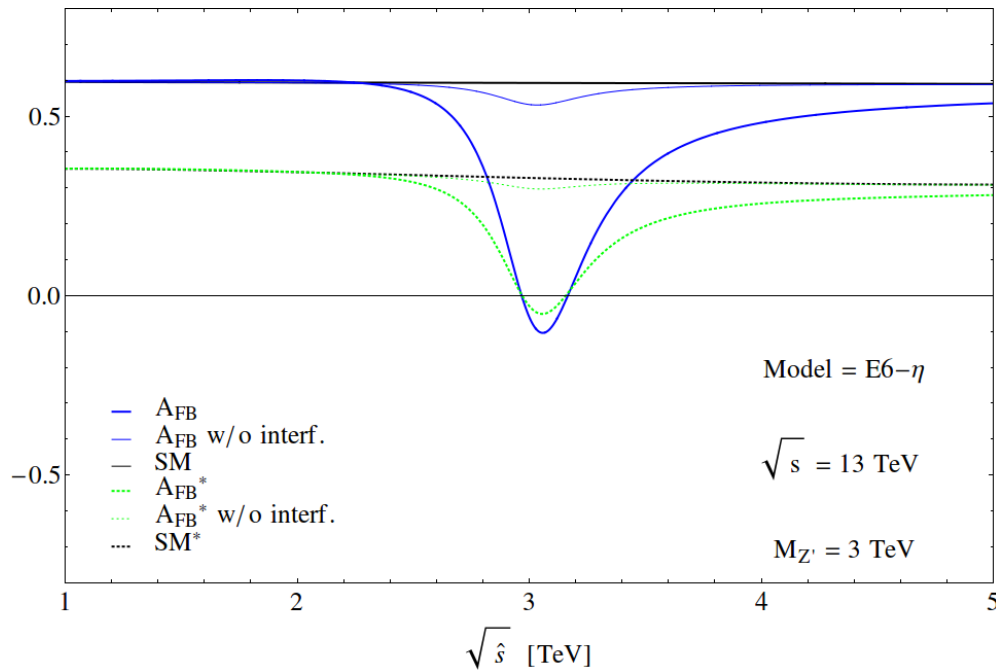
The shape of the reconstructed AFB is smeared, still we can recover a more pronounced shape by applying rapidity (Y) cuts.



Yet the rapidity cuts reduce the statistic of the sample of events. Overall the AFB is more reliable without the rapidity cuts.

[Accomando, Belyaev, Fiaschi, Mimasu, Moretti, Shepherd-Themistocleous, JHEP, 01 \(2016\), 127](#)

The AFB*



Interference between SM neutral bosons and the Z' plays an essential role in determining the shape of the AFB.

Totally model dependent shape

Accomando, Belyaev, Fiaschi, Mimasu, Moretti, Shepherd-Themistocleous, JHEP, 01 (2016), 127

Usage of the AFB*

Features:

Consequence:

AFB as diagnostic tool

- AFB depends on different combination of the couplings, with respect to the cross section → • Complementary information about the chiral couplings, with respect to the cross section
- The shape of the AFB is affected by strong interference effects → • The model dependent shape of the AFB can help in distinguish between different models

Rizzo, JHEP 0908 082 (2009)

Usage of the AFB*

Features:

Consequence:

AFB as diagnostic tool

- AFB depends on different combination of the couplings, with respect to the cross section → • Complementary information about the chiral couplings, with respect to the cross section
- The shape of the AFB is affected by strong interference effects → • The model dependent shape of the AFB can help in distinguish between different models

[Rizzo, JHEP 0908 082 \(2009\)](#)

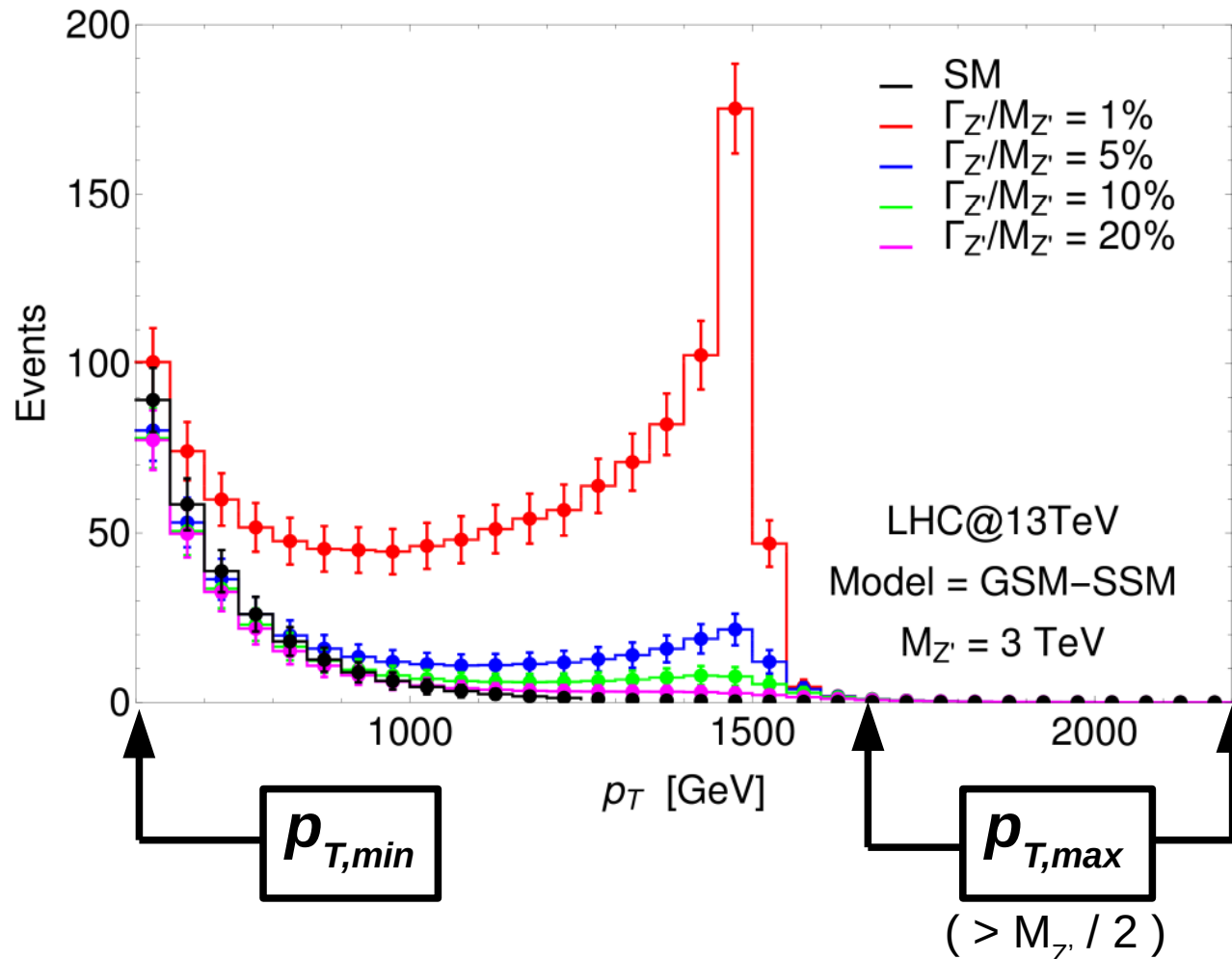
AFB as search tool

- It comes from the ratio of cross sections → • Systematic uncertainties cancel (PDFs, luminosity, etc.)
- For both narrow & wide resonances AFB can be used together with the bump search → • Off-peak effects due to interference are sizeable and can be observed

The p_T spectrum

Lepton transverse momentum distribution

One single Z' benchmark model with different values of its width



At tree-level the two leptons in the final state have the same transverse momentum, thus there is no ambiguity.

1

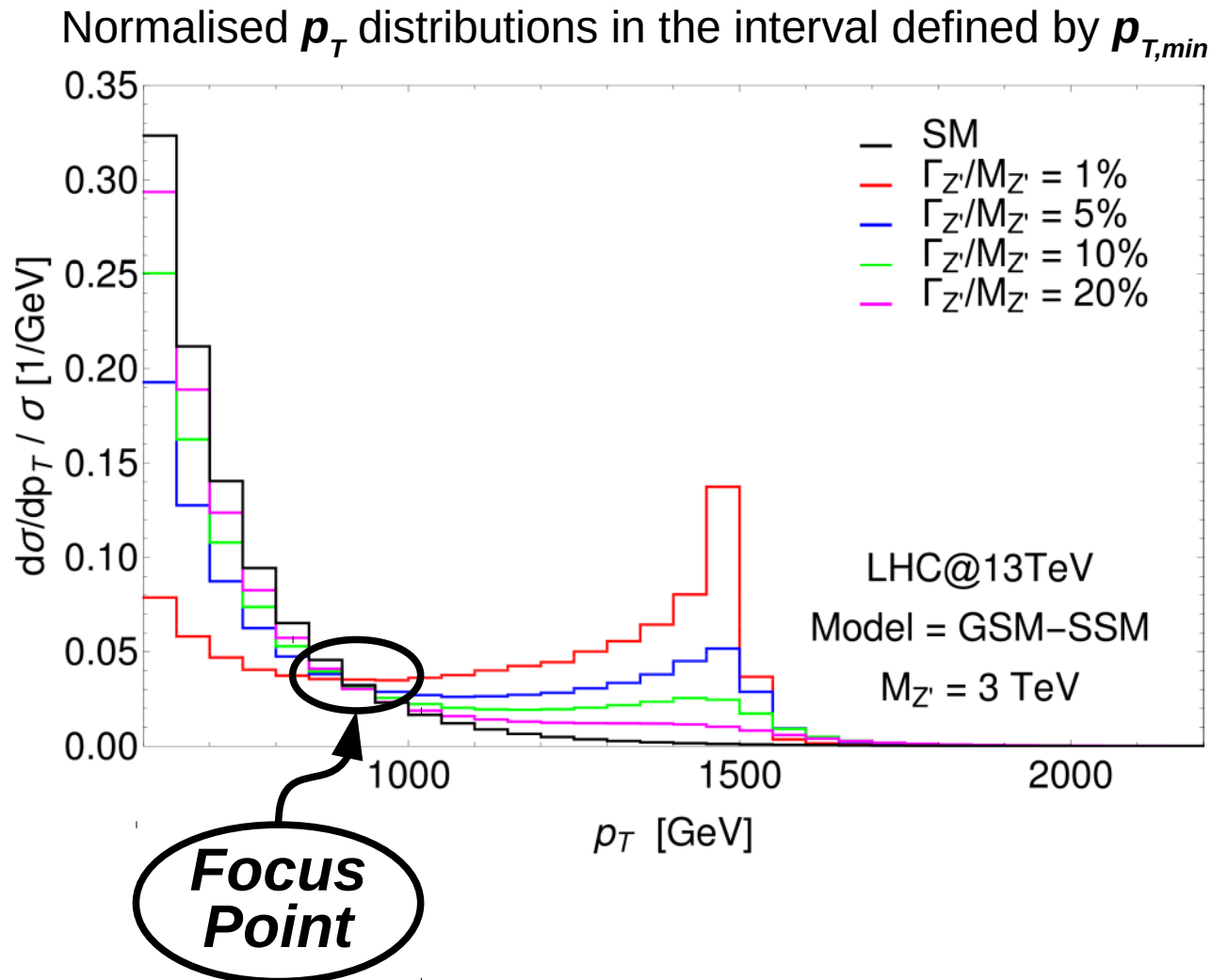
Consider an interval in the p_T spectrum that we want to probe

Normalise the distributions in the selected interval

[Accomando, Fiaschi, Moretti, Shepherd-Themistocleous, Phys. Rev. D 96, 075019 \(2017\)](#)

The p_T spectrum

Normalise the curves



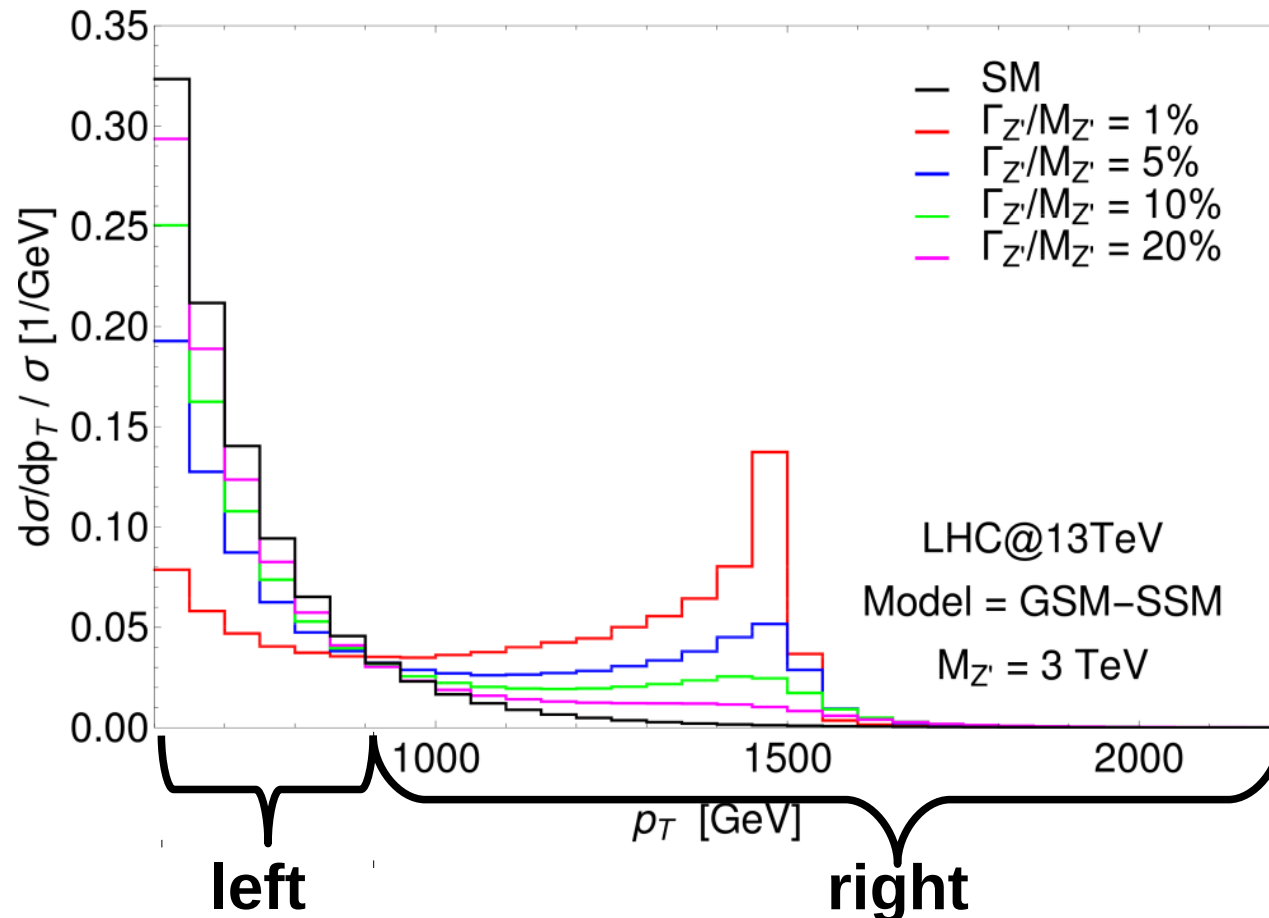
All the curves cross the same point, independently on their width. The Standard Model as well follows the same behaviour.

A Focus Point (FP) appears

The p_T spectrum

Define two integration regions

The **FP** divides the p_T spectrum in two regions



2

For each curve calculate the integral in the two regions of the p_T spectrum on the *left* and on the *right* side of the **FP**.

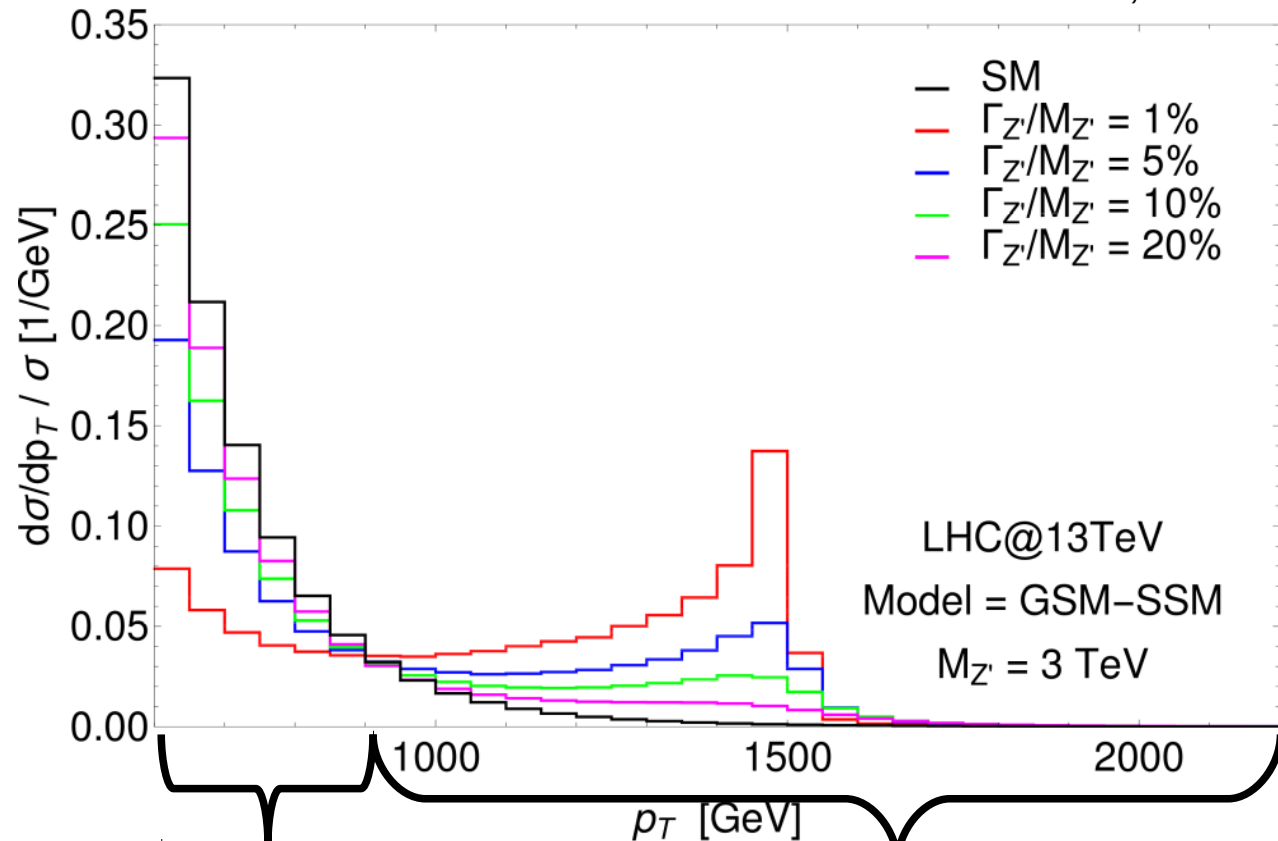
The results of the integrations will be called **L** and **R**, respectively.

The p_T spectrum

Define the Asymmetry of the Focus Point (AFP)

3

The value of the **AFP** depends on the choice of $p_{T,min}$



$$A_{FP} = \frac{L - R}{L + R}$$

This observable will provide an independent information on the resonance width, without relying on the modelling of the signal shape.

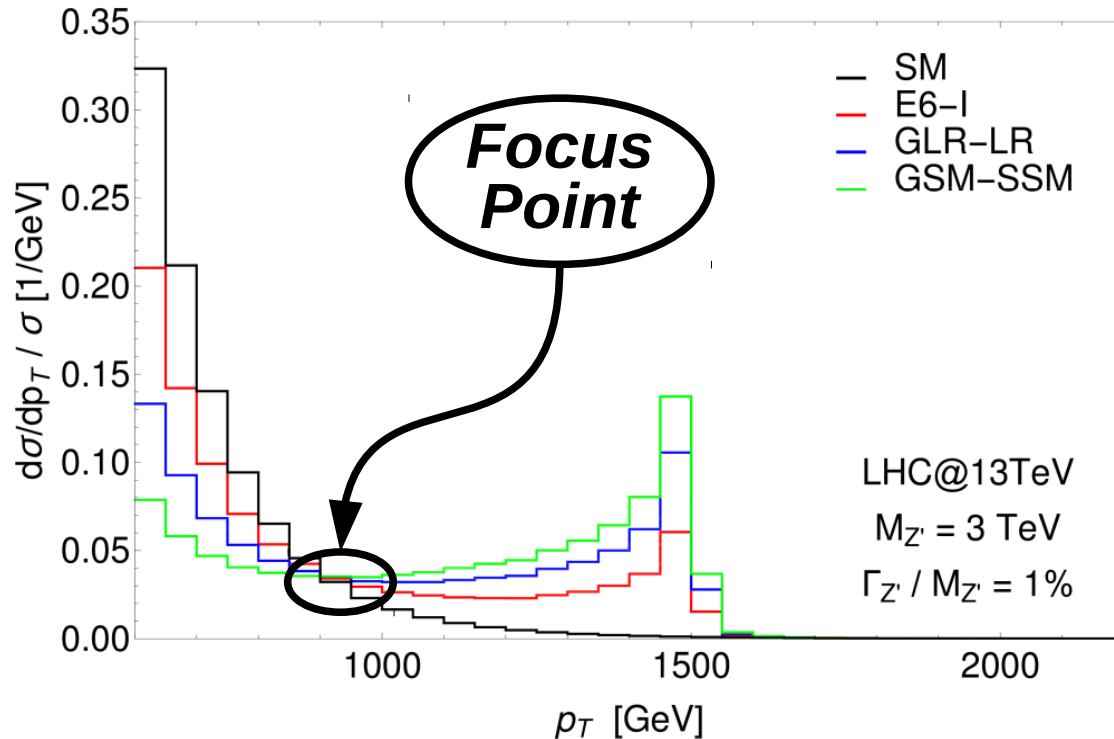
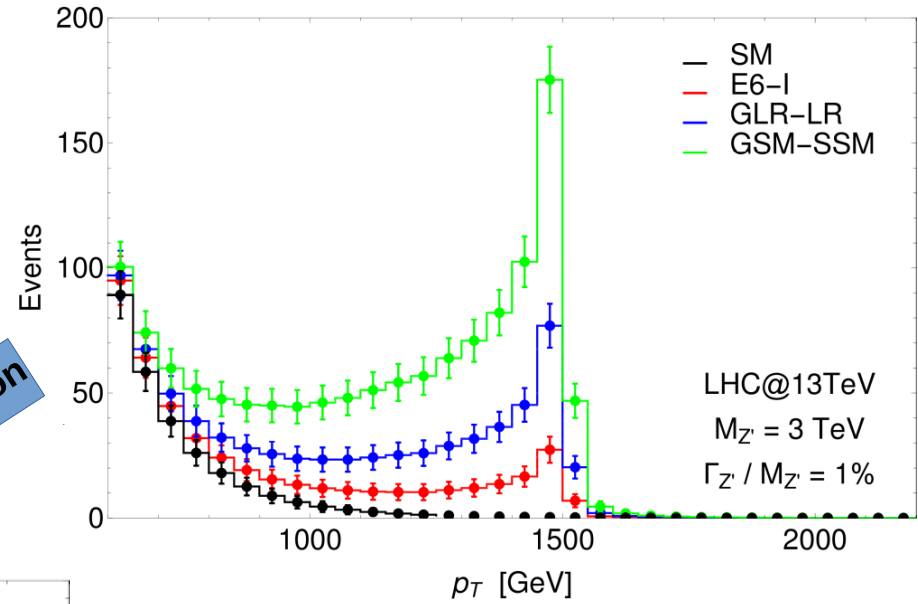
$$L = \frac{1}{\sigma} \int_{p_{T,min}}^{FP} \frac{d\sigma}{dp_T} dp_T \quad R = \frac{1}{\sigma} \int_{FP}^{p_{T,max}} \frac{d\sigma}{dp_T} dp_T$$

Properties of the Focus Point

The FP is model independent!

Fix the resonance width and normalise the p_T spectrum for each model.

Normalization

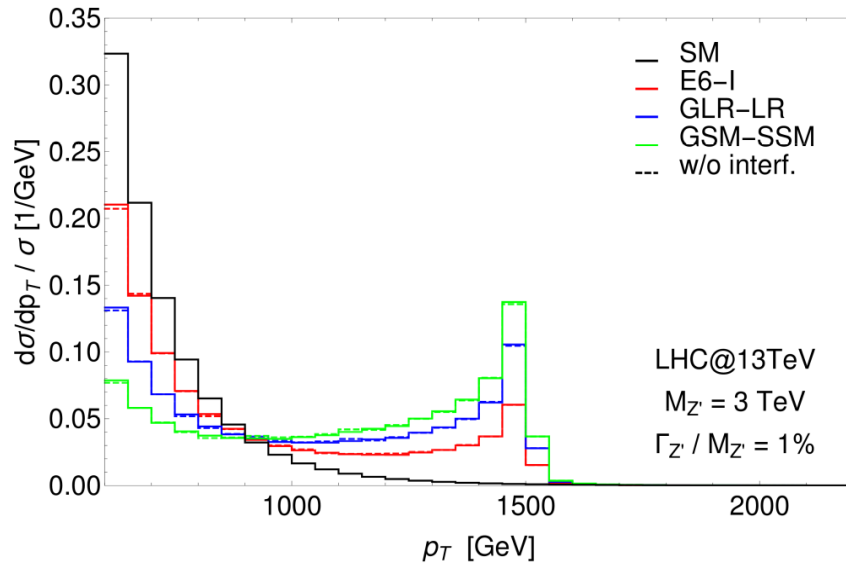


The model dependence contained in the couplings cancels out in the normalisation.

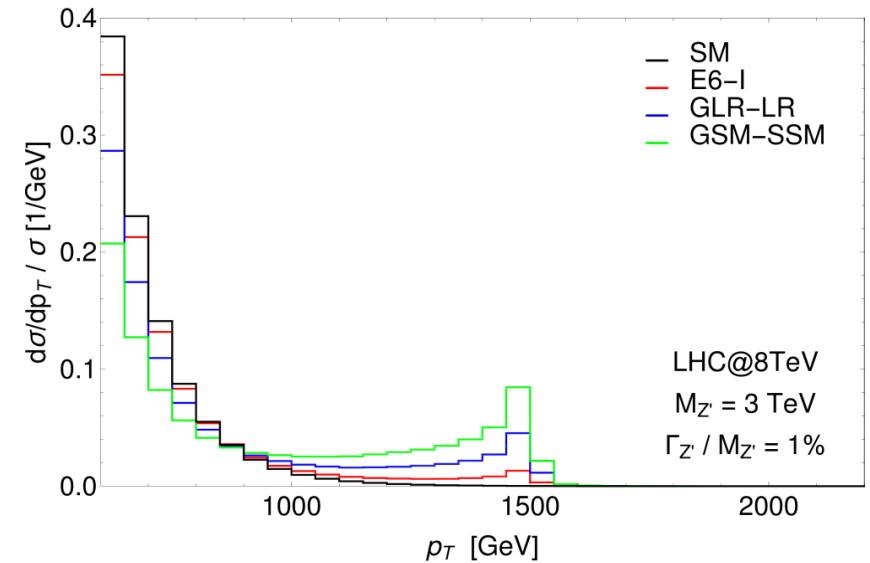
The normalisation will naturally reduce other sources of systematics (PDFs, Luminosity)

Properties of the Focus Point

The FP is model independent!



The FP depends on the collider energy and on the Z' mass

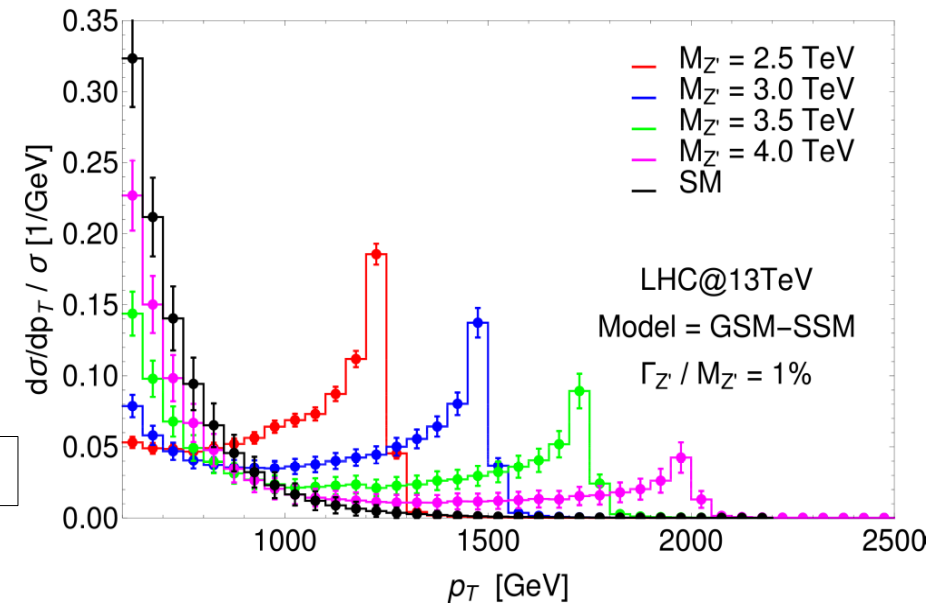


The p_T spectrum is marginally affected by the interference. Its model dependent effect on the curves is negligible.

For a fixed c.o.m. energy, the position of the **FP** depends only on the **Z' mass** and on the **choice of the $p_{T,min}$**

Empirical relation valid for the LHC@13TeV

$$FP = p_{T,min} + 10\%M_{Z'}$$



The AFP

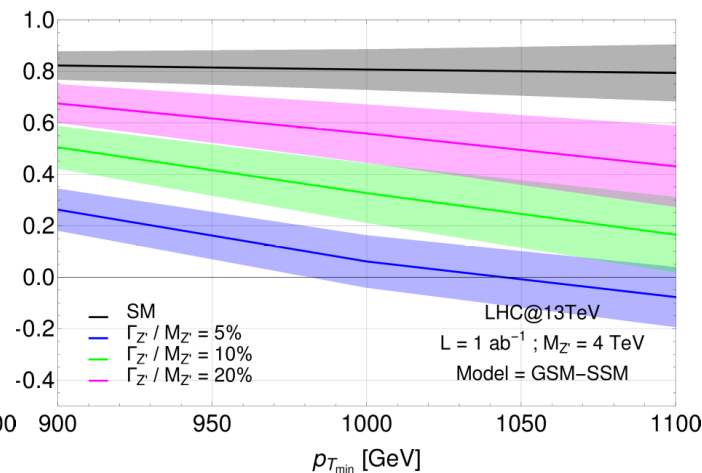
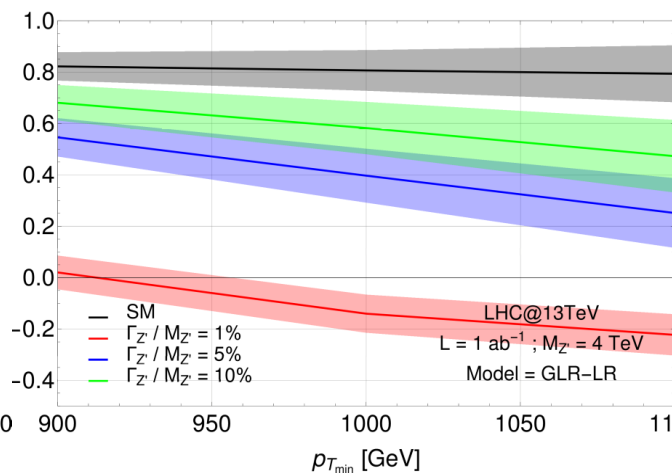
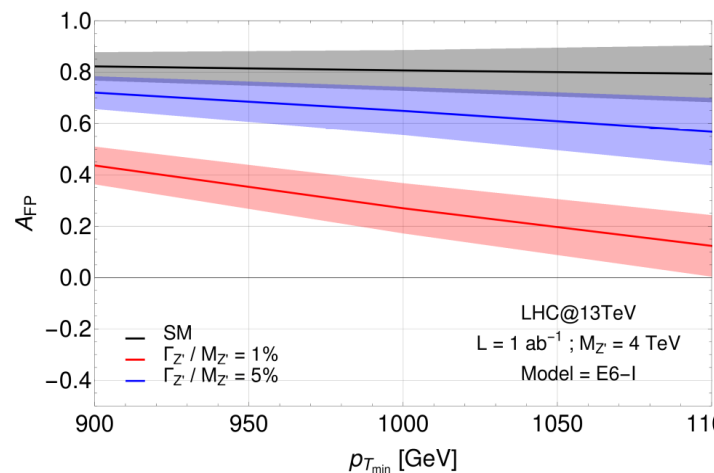
Predictions for the AFP

Statistical error
evaluated for
 $\mathcal{L} = 1 \text{ ab}^{-1}$

$M_{Z'} = 4 \text{ TeV}$

For some models we
can constrain Z' widths
up to $\Gamma/M \sim 20\%$

$M_{Z'} = 4 \text{ TeV}$				
Model	$\Gamma_{Z'}/M_{Z'} = 1\%$	$\Gamma_{Z'}/M_{Z'} = 5\%$	$\Gamma_{Z'}/M_{Z'} = 10\%$	$\Gamma_{Z'}/M_{Z'} = 20\%$
$p_T^{\text{min}} = 900 \text{ GeV}$				
SM	0.82 ± 0.05			
E_6^I	0.44 ± 0.07	0.72 ± 0.06	0.77 ± 0.06	0.80 ± 0.06
LR	0.02 ± 0.07	0.55 ± 0.07	0.68 ± 0.07	0.76 ± 0.06
SSM	-0.29 ± 0.05	0.26 ± 0.08	0.50 ± 0.08	0.67 ± 0.07
$p_T^{\text{min}} = 1000 \text{ GeV}$				
SM	0.81 ± 0.08			
E_6^I	0.27 ± 0.10	0.65 ± 0.09	0.72 ± 0.09	0.77 ± 0.08
LR	-0.14 ± 0.07	0.40 ± 0.10	0.58 ± 0.10	0.70 ± 0.09
SSM	-0.37 ± 0.05	0.06 ± 0.10	0.33 ± 0.12	0.56 ± 0.11
$p_T^{\text{min}} = 1100 \text{ GeV}$				
SM	0.79 ± 0.11			
E_6^I	0.12 ± 0.12	0.57 ± 0.13	0.68 ± 0.12	0.74 ± 0.12
LR	-0.22 ± 0.08	0.25 ± 0.14	0.47 ± 0.14	0.64 ± 0.13
SSM	-0.38 ± 0.05	-0.08 ± 0.12	0.16 ± 0.15	0.43 ± 0.16



The AFP

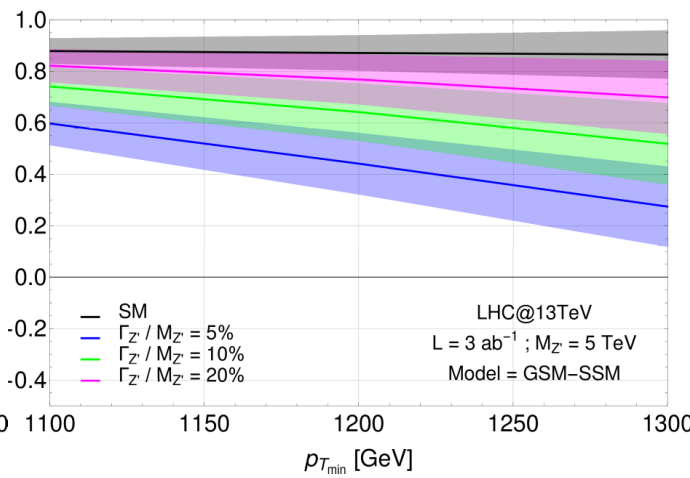
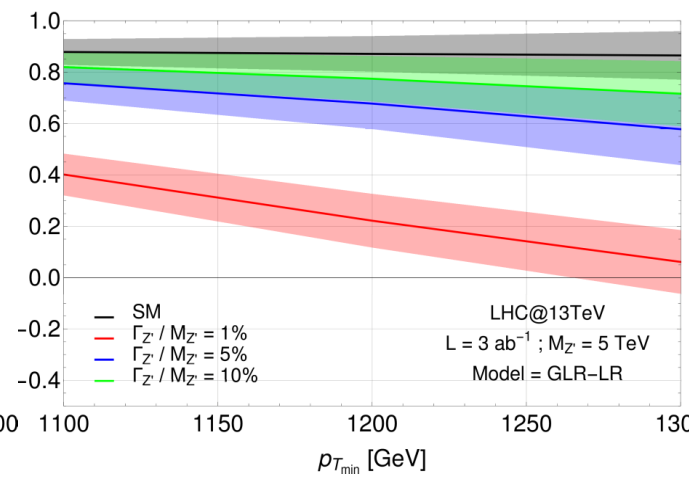
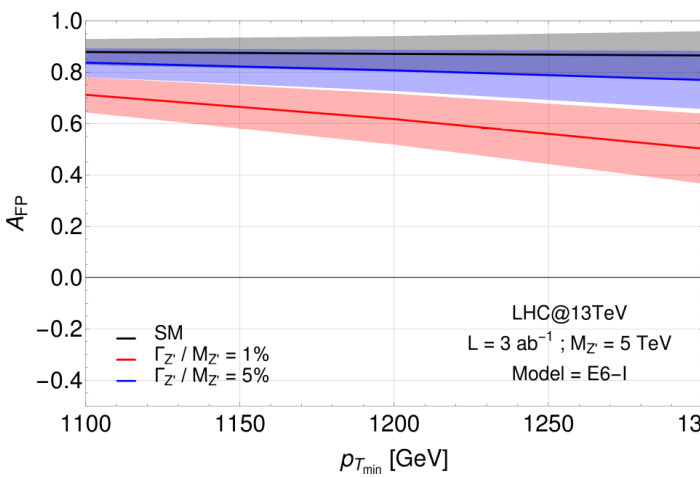
Predictions for the AFP

Statistical error
evaluated for
 $\mathcal{L} = 3 \text{ ab}^{-1}$

$M_{Z'} = 5 \text{ TeV}$

For some models we
can constrain Z' widths
up to $\Gamma/M \sim 20\%$

$M_{Z'} = 5 \text{ TeV}$				
Model	$\Gamma_{Z'}/M_{Z'} = 1\%$	$\Gamma_{Z'}/M_{Z'} = 5\%$	$\Gamma_{Z'}/M_{Z'} = 10\%$	$\Gamma_{Z'}/M_{Z'} = 20\%$
$p_T^{\text{min}} = 1100 \text{ GeV}$				
SM	0.88 ± 0.05			
E_6^I	0.71 ± 0.07	0.84 ± 0.06	0.85 ± 0.05	0.87 ± 0.05
LR	0.40 ± 0.08	0.76 ± 0.07	0.82 ± 0.06	0.85 ± 0.06
SSM	0.04 ± 0.08	0.60 ± 0.08	0.74 ± 0.07	0.82 ± 0.06
$p_T^{\text{min}} = 1200 \text{ GeV}$				
SM	0.87 ± 0.07			
E_6^I	0.62 ± 0.10	0.81 ± 0.08	0.84 ± 0.07	0.85 ± 0.07
LR	0.22 ± 0.10	0.68 ± 0.10	0.77 ± 0.09	0.83 ± 0.08
SSM	-0.14 ± 0.09	0.44 ± 0.12	0.64 ± 0.11	0.77 ± 0.10
$p_T^{\text{min}} = 1300 \text{ GeV}$				
SM	0.86 ± 0.09			
E_6^I	0.50 ± 0.14	0.77 ± 0.11	0.81 ± 0.10	0.84 ± 0.10
LR	0.06 ± 0.12	0.58 ± 0.14	0.72 ± 0.13	0.80 ± 0.11
SSM	-0.24 ± 0.09	0.27 ± 0.16	0.52 ± 0.16	0.70 ± 0.14



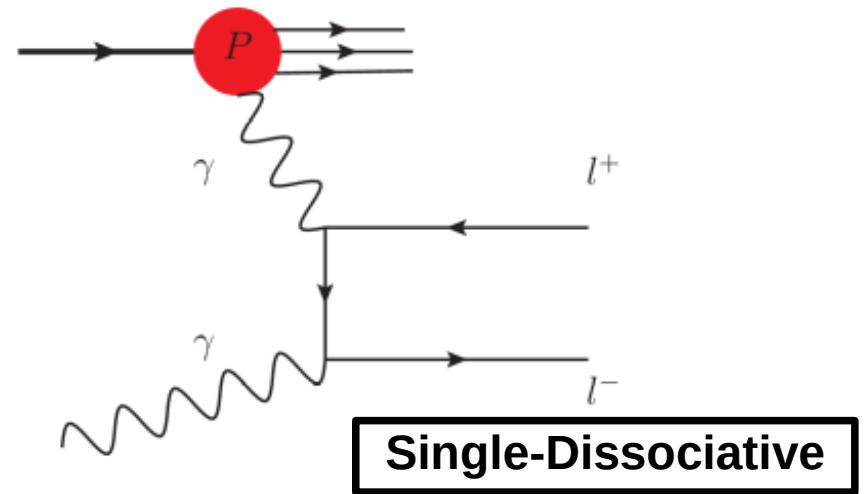
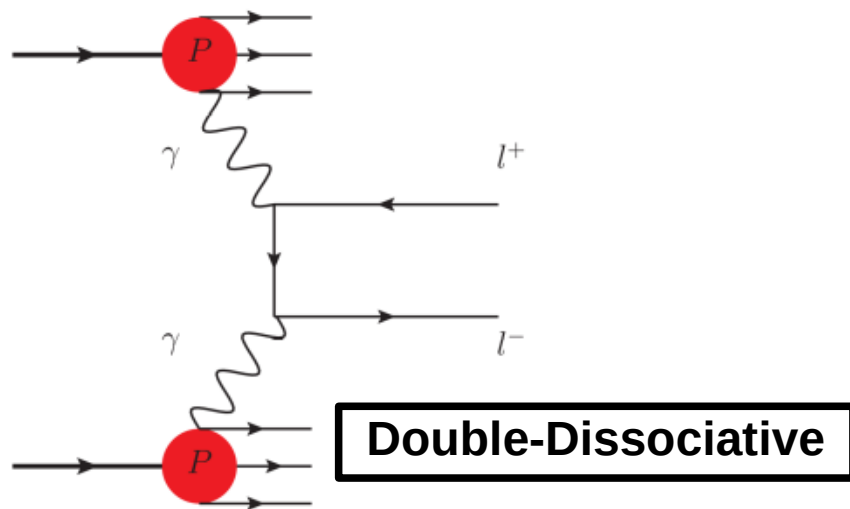
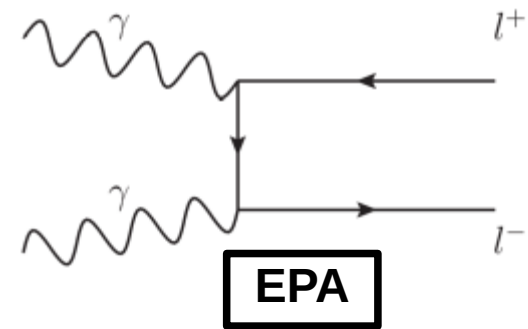
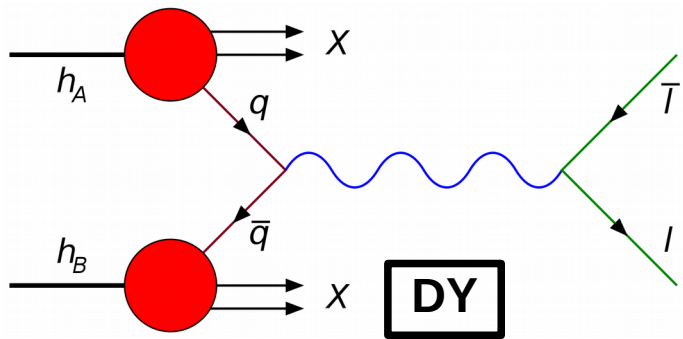
PI contribution to di-lepton channel

Drell-Yan (DY)
di-lepton production

$$q\bar{q} \rightarrow \gamma, Z, Z' \rightarrow l^+ l^-$$

Photon-Initiated (PI)
di-lepton production

$$pp \rightarrow \gamma\gamma \rightarrow l^+ l^-$$



QED PDF sets for LHC

Inelastic PDF sets:

(Virtual contributions are subtracted from photon PDF)

MRST2004QED

- First QED set with QED corrections to DGLAP evolution equation (lead to isospin violation).
- Includes HERA data.
- No update available – PDF uncertainties not available, LHC data not included.

[Martin, Roberts, Stirling, Thorne](#)
[Eur. Phys. J. C39, 155 \(2005\)](#)

CT14QED

- Includes HERA and ZEUS (with isolated photons) data to fit the ‘inelastic’ photon PDF.
- Do not include LHC data.
- The fraction of momentum carried by the photon satisfying the momentum sum rule, is constrained through fitting procedure.

[Schmidt, Pumplin, Stump, Yuan](#)
[Phys. Rev. D93, 114015 \(2016\)](#)

Inclusive PDF sets:

(Virtual contributions are included into photon PDF)

NNPDF3.0QED

- Includes HERA, ATLAS, CMS, LHCb data.
- Global fit using Neural network approach.
- QED constrains on photon PDF are included through re-weighting procedure (small violation of momentum sum rule).
- Incorporates the 2.3QED photon contribution to the 3.0 global analysis using the APFEL code for the QED correct DGLAP equations.

[NNPDF collaboration,](#)
[JHEP 1504 \(2015\) 040](#)

CT14QED_inc

xFitter_epHMDY

- Photon PDFs from ATLAS high-mass DY dilepton measurements.
- Improvements in the APFEL code for the QED correct DGLAP equations.

[xFitter Developers' Team](#)
[Eur.Phys.J. C77 \(2017\) no.6, 400](#)

LUXqed

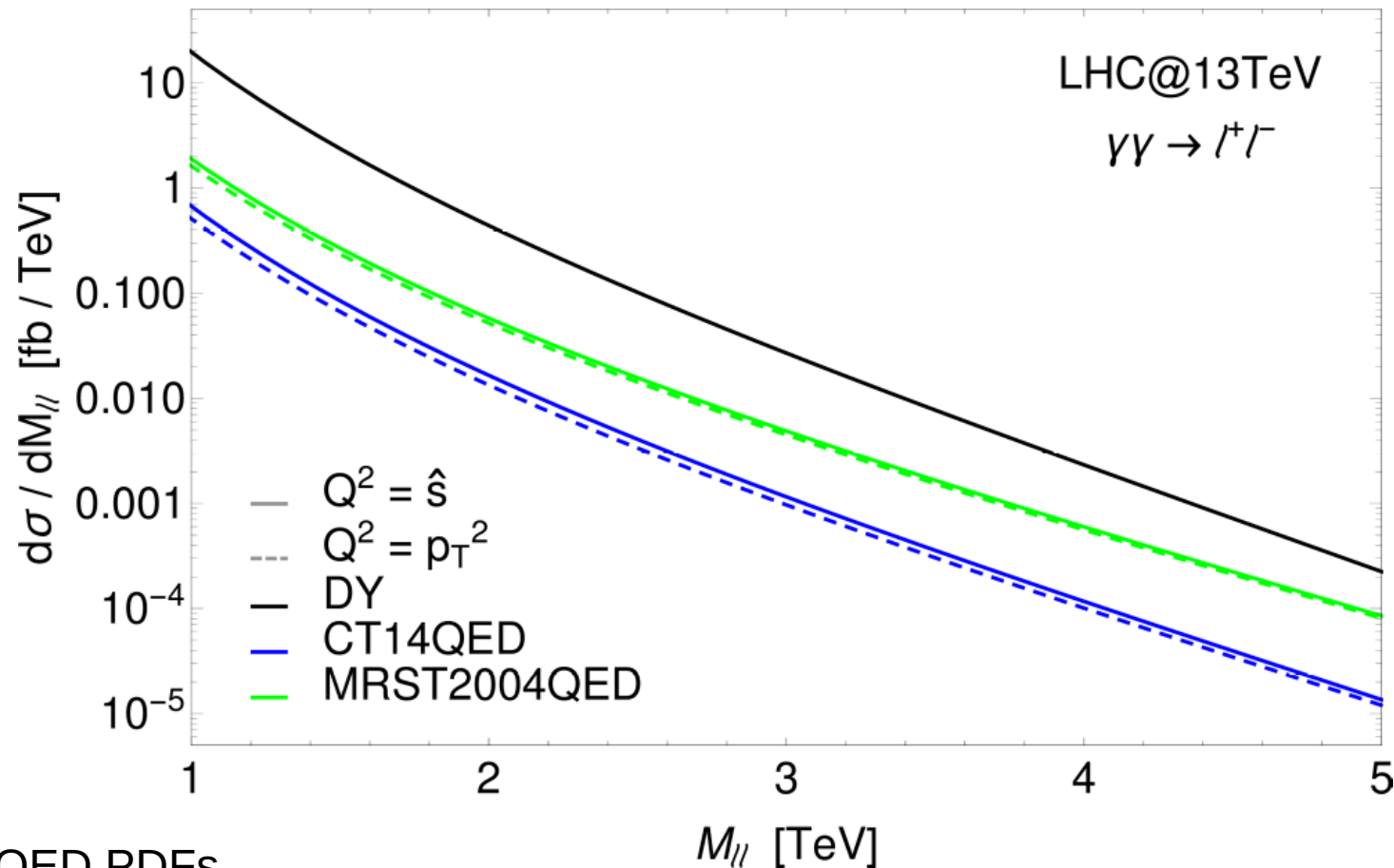
- Includes DIS data
- Do not include LHC data.
- Use a relation that connects proton structure functions to photon densities (DIS data directly constrains photon PDF).

[Manohar, Nason, Salam, Zanderighi](#)
[Phys. Rev. Lett. 117, 242002 \(2016\)](#)

Double-Dissociative

$$\frac{d\sigma_{DD}}{dM_{\ell\ell}} = \iint dx_1 dx_2 \frac{1}{32\pi M_{\ell\ell}} |\mathcal{M}(\gamma\gamma \rightarrow l^+l^-)|^2 f_\gamma(x_1, Q) f_\gamma(x_2, Q)$$

Double-Dissociative (DD) process, with **both** interacting photons from QED PDFs.



Photons extracted from the QED PDFs are **resolved**, i.e. they are **real** ($Q^2 = 0$)

Equivalent Photon Approximation

Virtual photons spectrum is included through the “Equivalent Photon Approximation” (EPA)

[Budnev, Ginzburg, Meledin, Serbo, Phys. Rept. 15, 181 \(1975\)](#)

$$dN(x, Q^2) = \frac{\alpha}{\pi} \frac{dx}{x} \frac{dQ^2}{Q^2} \left[(1-x) \left(1 - \frac{Q_{min}^2}{Q^2} \right) F_E + \frac{x^2}{2} F_M \right]$$

Virtual photons
($Q^2 \neq 0$)

$$Q_{min}^2 = \frac{m_p^2 x^2}{1-x},$$

$$F_E = \frac{4m_p^2 G_E^2 + Q^2 G_M^2}{4m_p^2 + Q^2},$$

$$G_E^2 = \frac{G_M^2}{\mu_p^2} = \left(1 + \frac{Q^2}{Q_0^2} \right)^{-4}, \quad F_M = G_M^2$$

[Piotrkowski, Phys. Rev. D63, \(2001\) 071502](#)

$$\mu_p^2 = 7.78$$

$$Q_0^2 = 0.71 \text{ GeV}^2$$

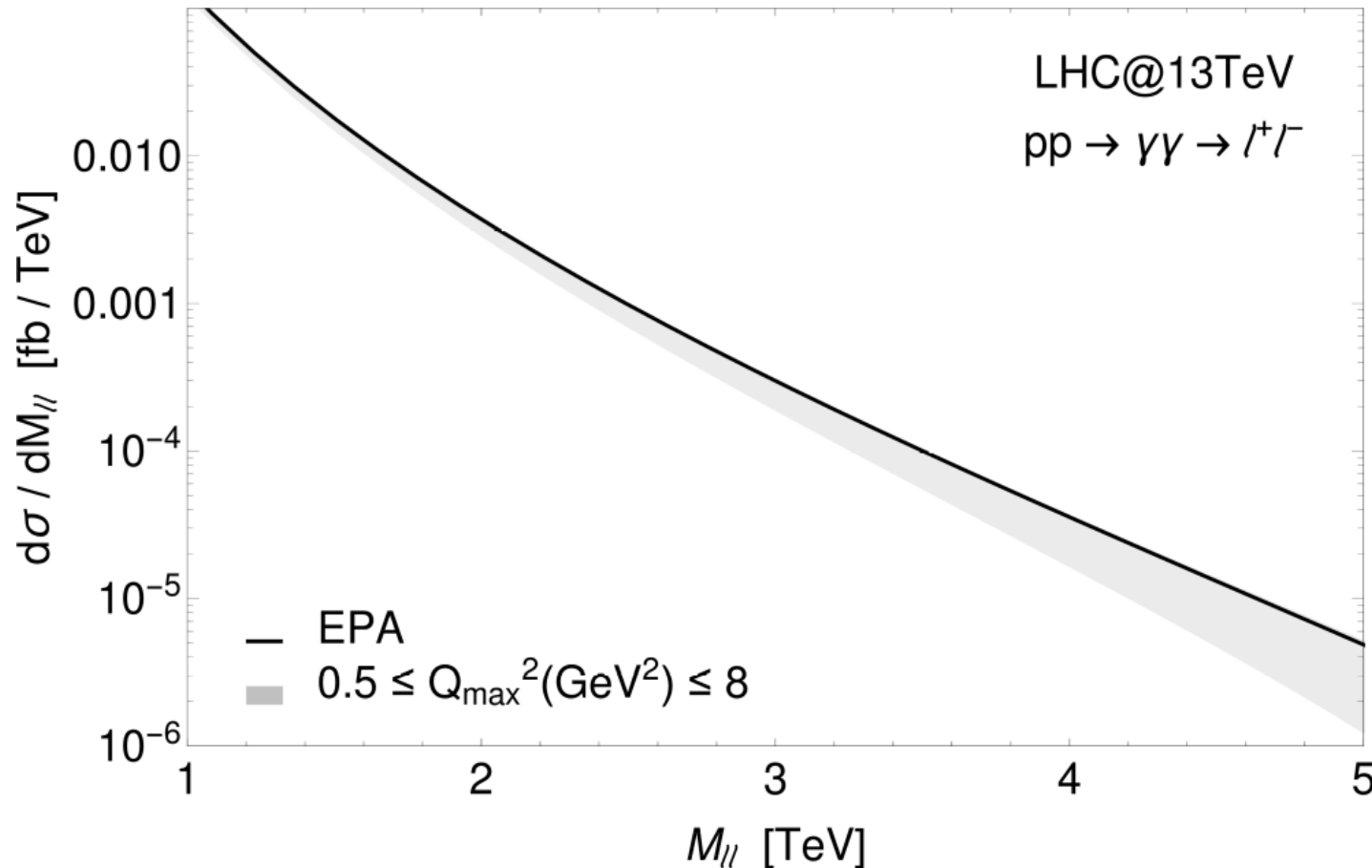
$$Q_{max}^2 = 2 \text{ GeV}^2$$

- Experimentally measured with great precision
- Value from data best fit
- We will vary this parameter to estimate the systematics

Equivalent Photon Approximation

Virtual-virtual photon interaction → EPA

$$\frac{d\sigma_{EPA}}{dM_{ll}} = \frac{dL_{\gamma\gamma}}{dM_{ll}} \sigma_{\gamma\gamma} = \int_{Q_{1,min}^2}^{Q_{1,max}^2} dQ_1^2 \int_{Q_{2,min}^2}^{Q_{2,max}^2} dQ_2^2 \iint dx_1 dx_2 \frac{|\mathcal{M}(\gamma\gamma \rightarrow l^+l^-)|^2}{32\pi M_{ll}} N(x_1, Q_1^2) N(x_2, Q_2^2)$$



Theoretical error
estimated by varying
the Q_{max}^2 parameter.

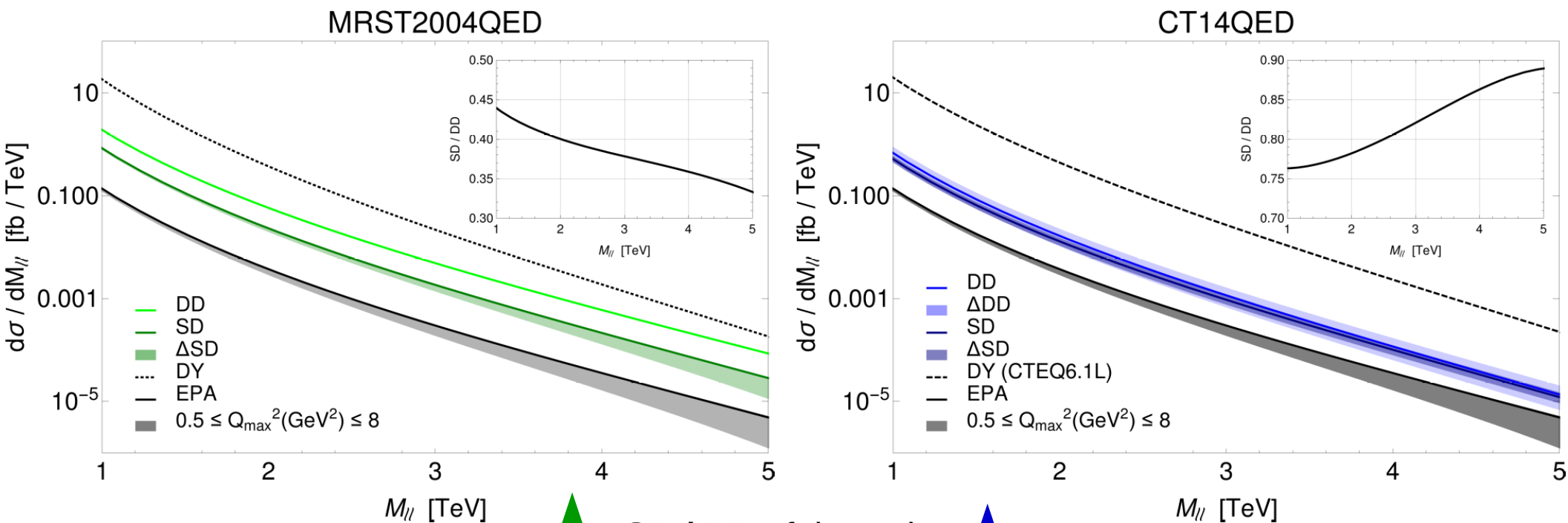
*All the results have
been calculated in the
CMS acceptance region*

CMS Collaboration,
JHEP 1504, 025 (2015)

Single-Dissociative

Real-virtual photon interaction → Single-Dissociative (SD)

$$\frac{d\sigma_{SD}}{dM_{ll}} = \int_{Q_{1,min}^2}^{Q_{1,max}^2} dQ_1^2 \iint dx_1 dx_2 \frac{|\mathcal{M}(\gamma\gamma \rightarrow l^+l^-)|^2}{32\pi M_{ll}} N(x_1, Q_1^2) f_\gamma(x_2, Q) + (x_1 \leftrightarrow x_2)$$



The **SD** contribution appears to be non-negligible

SD / DD of the order

35 – 40 %

75 – 90 %

The error bands include **both** the PDF error and the systematics on the photon spectrum

Inclusive PDF sets

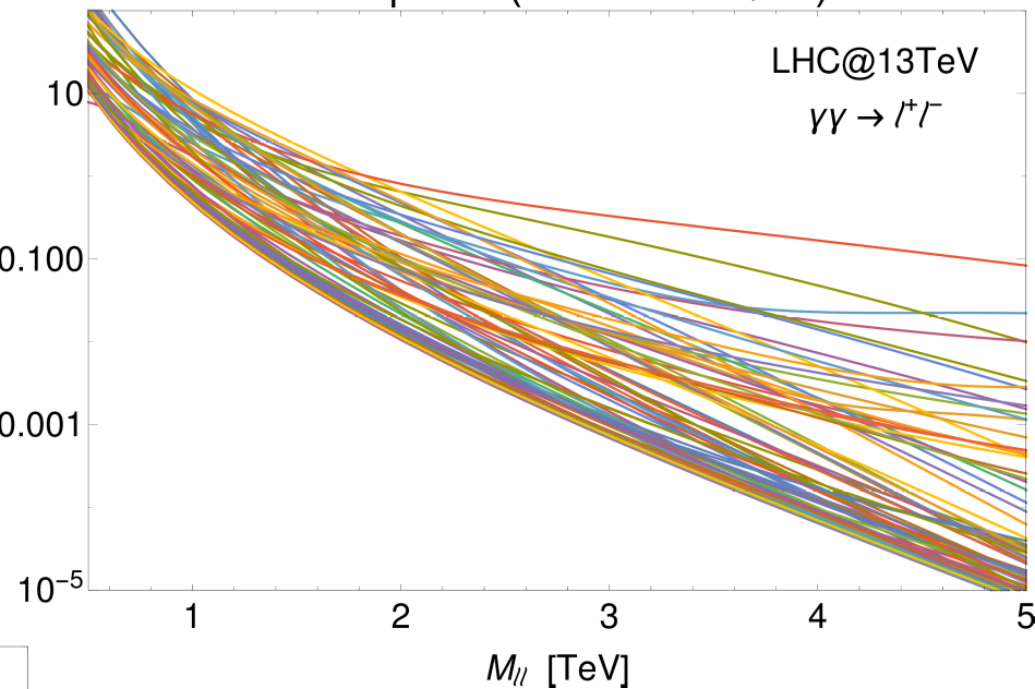
NNPDF3.0QED → 100 PDF Replicas

$$\sigma_0 = \langle \sigma \rangle = \frac{1}{N} \sum_{k=1}^N \sigma_k$$

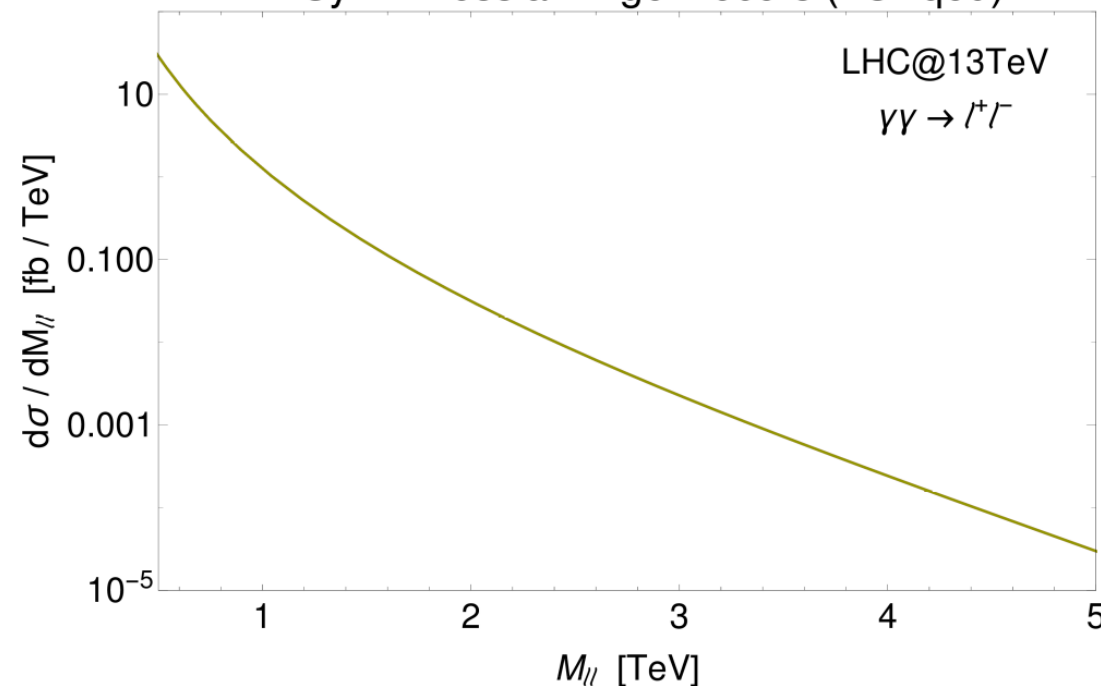
$$(\Delta\sigma)^2 = \frac{1}{N} \sum_{k=1}^N (\sigma_k - \sigma_0)^2$$

$d\sigma / dM_{ll}$ [fb / TeV]

PI Replicas (NNPDF3.0QED)



PI SymmHessian Eigenvectors (LUXqed)



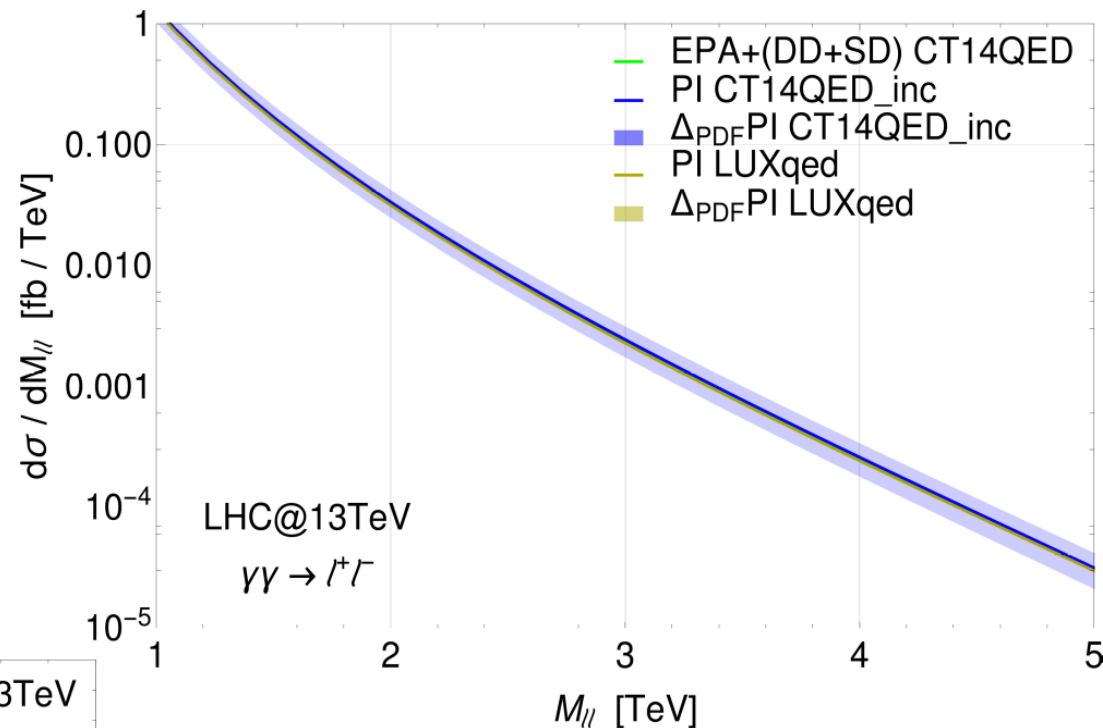
LUXqed → 100 Symmetric Hessian eigenvectors (PDF4LHC delivery)

$$(\Delta\sigma)^2 = \sum_{k=1}^N (\sigma_k - \sigma_0)^2$$

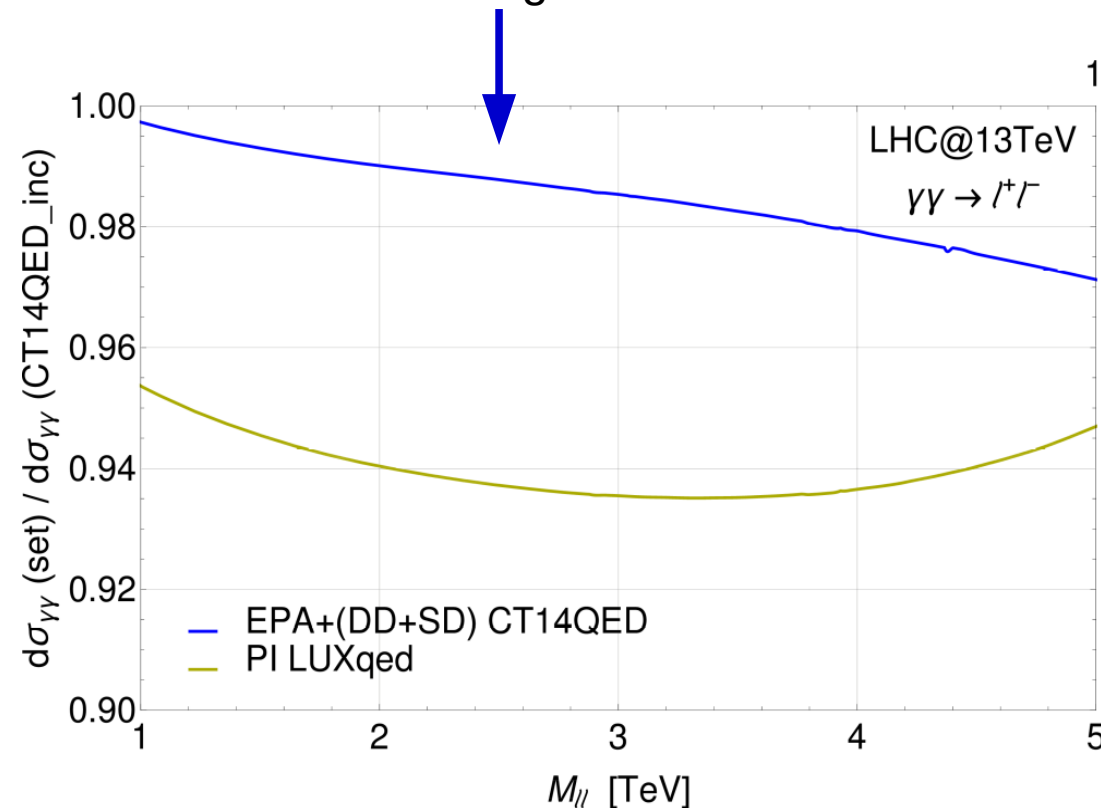
[PDF4LHC recommendations for LHC Run II, Butterworth et al., J. Phys. G: Nucl. Part. Phys. 43 \(2016\)](#)

Inclusive PDF sets

Cross check: good agreement between the three separate components **EPA+(DD+SD)** with **CT14QED** and the PI prediction obtained with **CT14QED_inc**.



Double-counting below ~3%



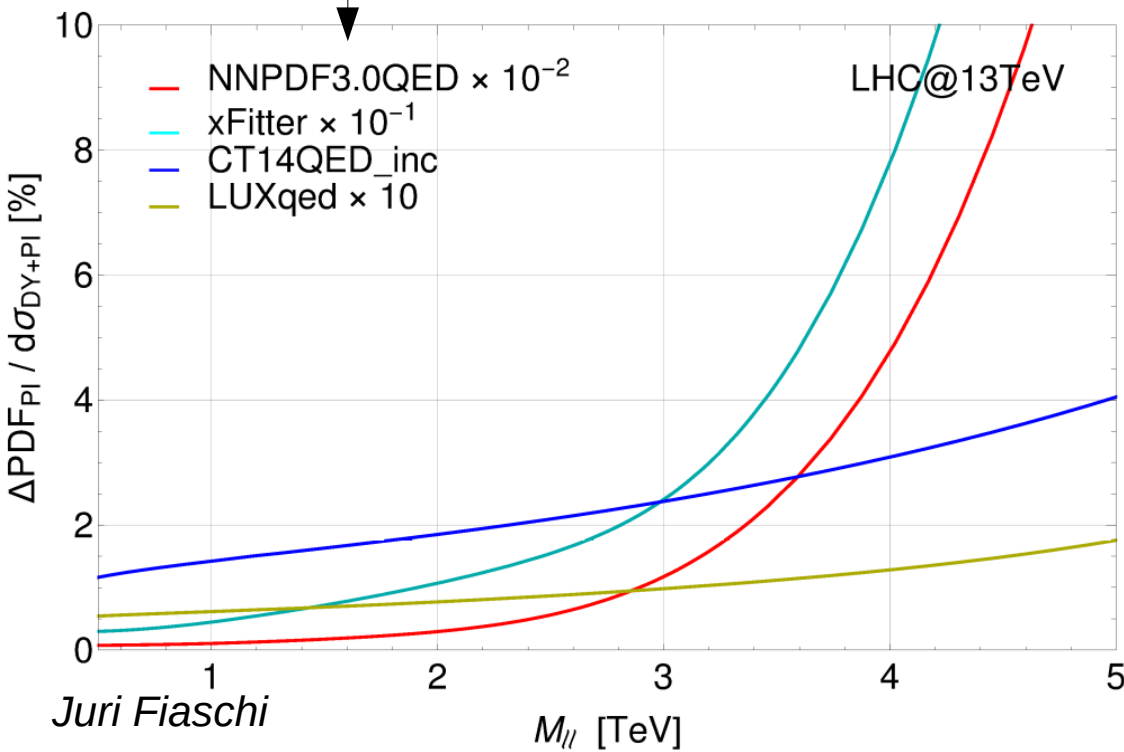
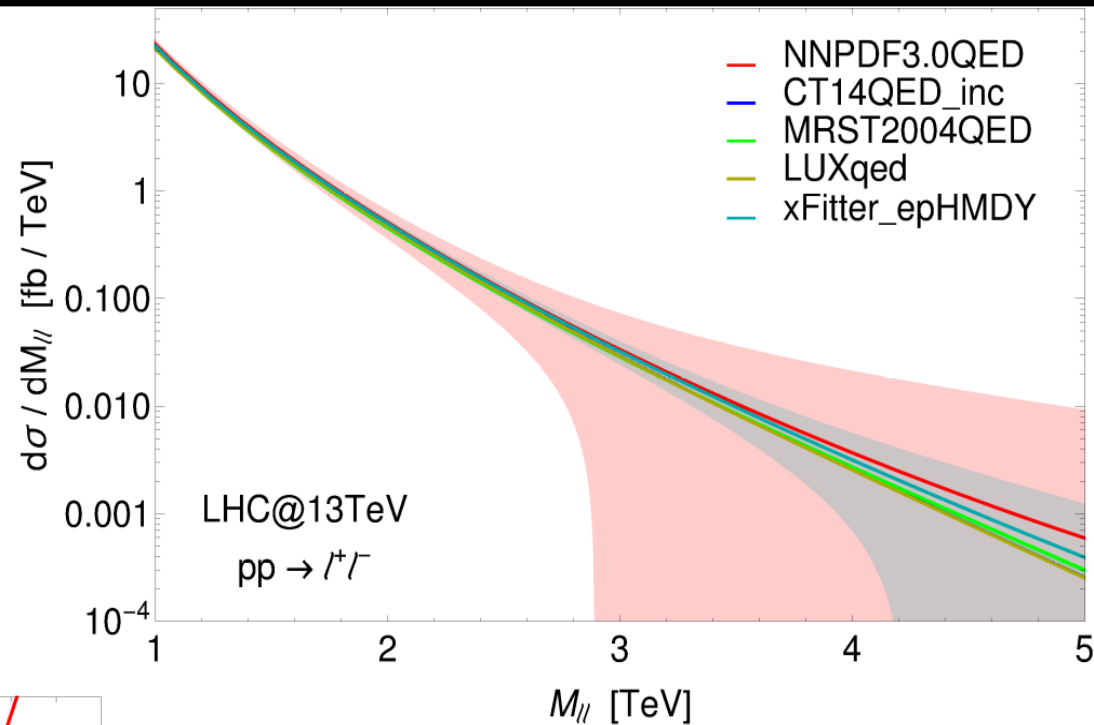
Also good agreement between the **LUXqed** and the **CT14QED_inc** predictions, consistent with the uncertainty of the latter (~20%).

Results from QED PDFs

Different QED PDF sets predicts a wide range of central values and uncertainties

Accomando, Fiaschi, Hautmann, Moretti, Shepherd-Themistocleous, Phys. Rev. D, 95 (2017), 035014, Phys. Lett. B, 770 (2017), 1-7

NOTE: different rescaling of PDF relative uncertainties.

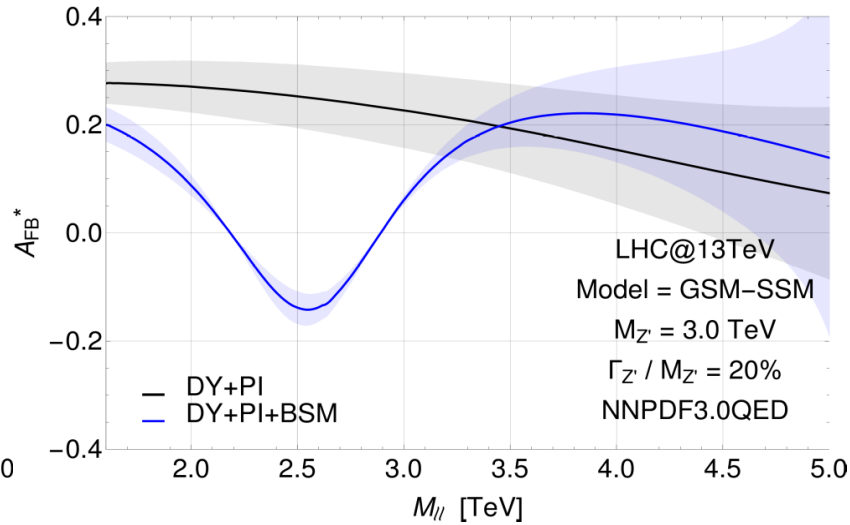
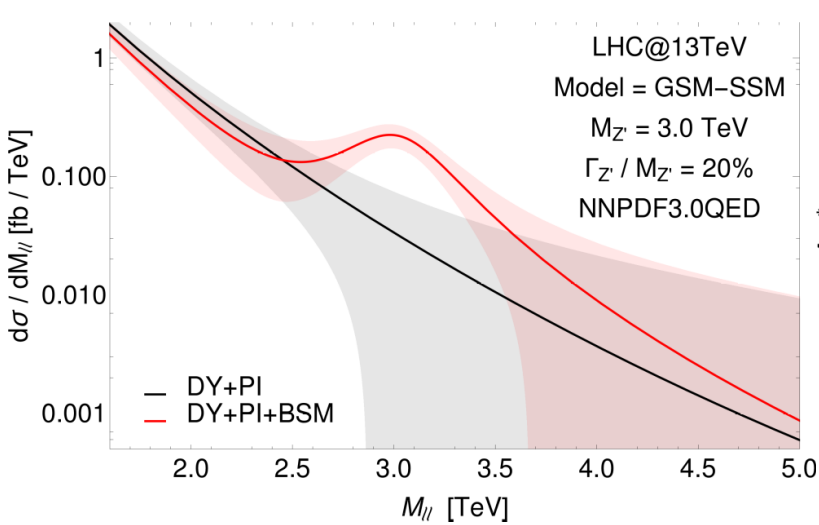


Large central value and large PDF uncertainties of PI contribution with **NNPDF3.0QED**.

Small central value and tiny PDF uncertainties of PI contribution with **LUXqed** thanks to the one to one relation between photon PDFs and proton structure functions.

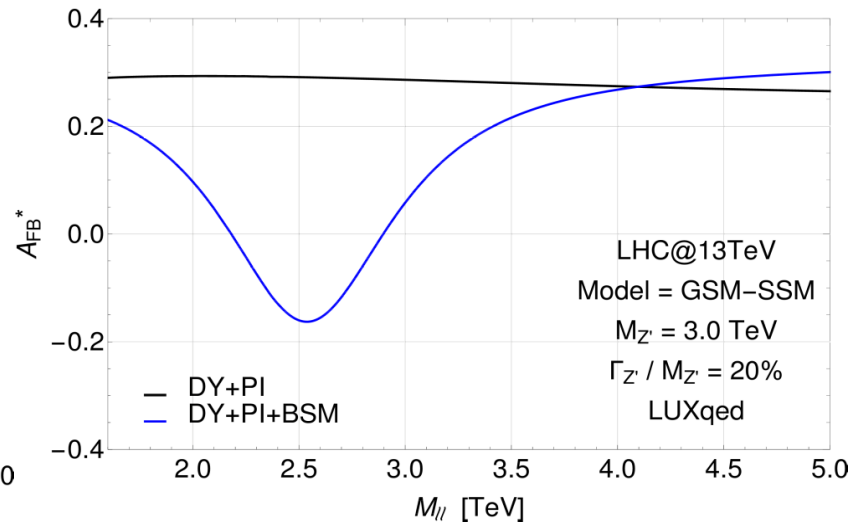
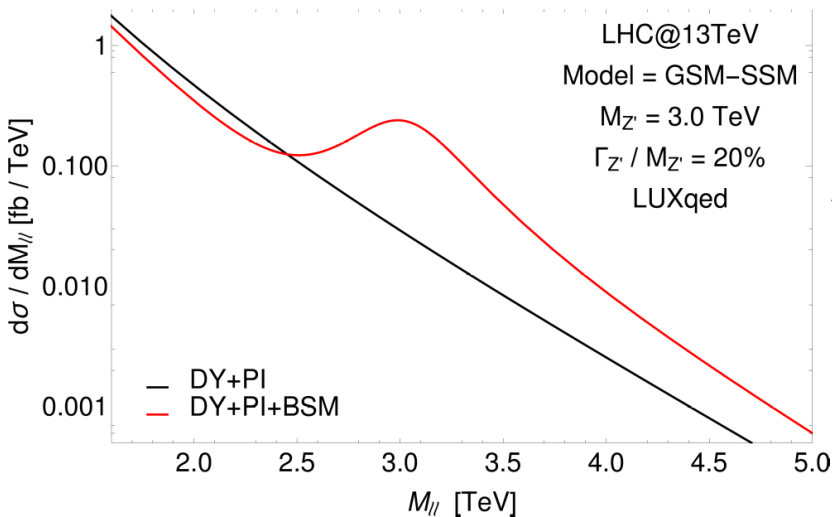
PI effects on Z' searches

Before LUX



Some concerns on the loss of sensitivity at high invariant masses due to the large PDF error.

After LUX



Small contribution from PI processes with a very small PDF uncertainty.

PI contributions remain well below the LHC sensitivity.

Other possibilities for BSM Z 's?

Single Z'

- **Extra $U(1)$**
(E6, Left-Right model, B-L motivated...)
- **Extra $SU(2)$**
(2HDM, SSM...)

Multiple Z'

- **Technicolor** (Vanilla, Running, Custodial, Walking)

[Andersen, Frandsen, Hapola, Nardecchia, Sannino](#)
[Eur. Phys. J. Plus, 126 \(2011\), 81](#)

- **Extra Dimensions** (KK excitation)
- **Composite Higgs**

Other possibilities for BSM Z's?

Single Z'

- **Extra U(1)**
(E6, Left-Right model, B-L motivated...)
- **Extra SU(2)**
(2HDM, SSM...)

Multiple Z'

- **Technicolor** (Vanilla, Running, Custodial, Walking)

[Andersen, Frandsen, Hapola, Nardecchia, Sannino](#)
[Eur. Phys. J. Plus, 126 \(2011\), 81](#)

- **Extra Dimensions** (KK excitation)
- **Composite Higgs**

- Non-Universal Large Extra Dimensions
- 4-Dimensional Composite Higgs Model

[Accomando, Barducci, De Curtis, Fiaschi, Moretti, Shepherd-Themistocleous,](#)
[JHEP, 07 \(2016\), 068](#)

The NUED model

- **Minimal version of the large Extra Dimensions class of models.**
 - Only the SM gauge bosons are allowed to propagate in the EDs.
- **Two energy scales determine the phenomenology:**
 - $M_s = l_s^{-1}$ → string length related (very high energy $\sim M_{Plank}$).
 - R^{-1} → related to the length of the extra dimensions compactified on a D-dimensional torus.
- **We can decompose the higher-dimensional space as $3 + d_{\parallel} + d_{\perp}$**
 - $3 + d_{\parallel}$ longitudinal dimension of the big brane that contains the 3D brane where the SM lives.
 - d_{\perp} indicates the EDs which are felt by the gravity and are transverse to the big brane.
- **The particle content of the model is:**
 - Gravitons: closed strings propagating in the whole space.
 - SM fermions: localized on the 3D brane.
 - SM gauge bosons: open strings propagating in the $(3 + d_{\parallel})$ brane.

[Antoniadis, Benakli, Phys. Lett. B, 326 \(1994\) 69-78](#)

The NUED model

- **We consider the case of a 5D NUED model:**
 - $D = d_{\parallel} = 1$ and periodic boundary conditions on the compact direction.
 - The states propagating in the $(4+D)$ -dimensional space are seen from the 4D point of view as a tower of resonances with masses

$$M_{KK}^2 = m_0^2 + \frac{n^2}{R^2}$$

[Antoniadis, Benakli, Quiros, Phys. Lett. B, 331 \(1994\) 313-320](#)

- **The localization of the fermions allows the direct production of KK resonances through $ff' \rightarrow V_{KK}^{(n)}$ while $VV \rightarrow V_{KK}^{(n)}$ is forbidden.**
 - In the NUED all the SM gauge group can propagate in the 5D bulk space and therefore have KK excitations.
 - In the NUED(EW) only the $SU(2) \otimes U(1)$ EW gauge group can propagate in the compactified extra dimension and acquire KK excitations.
 - The two scenarios do not differ in the purpose of our analysis.

[Bella, Etzion, Hod, Oz, Silver, Sutton, JHEP, 09 \(2010\), 025](#)

The NUED model

- **EWPT bounds from LEP data on the 5D NUED model:**

- Most recent bounds can be found in:

[Accomando, Mod. Phys. Lett. A30, 1540010 \(2015\)](#)

- Depending on the scalar sector realization they give:

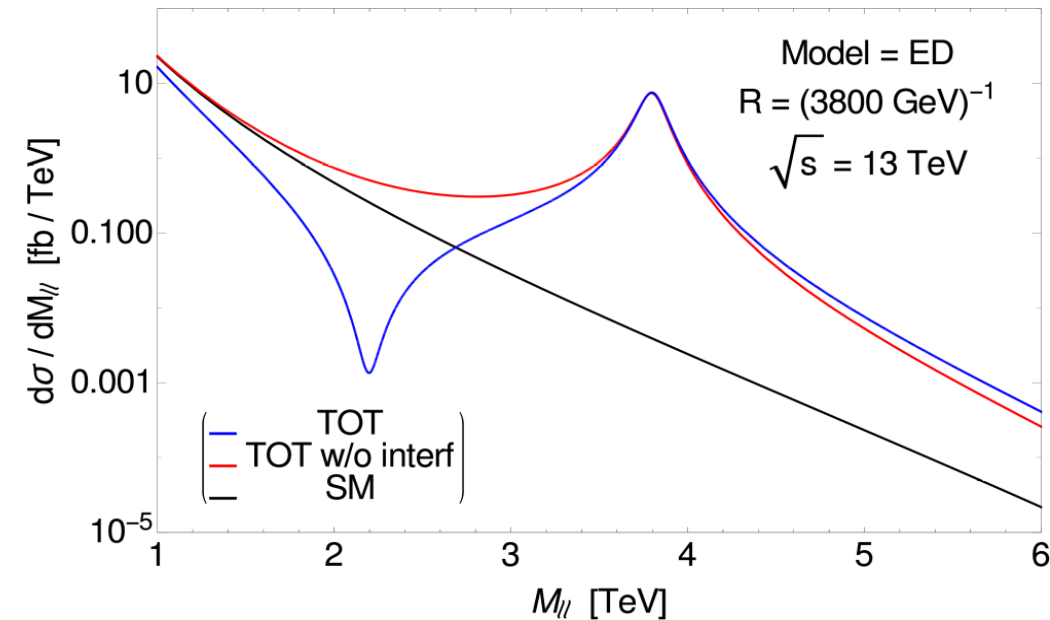
$$R^{-1} \geq 3.8 - 5.4 \text{ TeV}$$

- **LHC limits:**

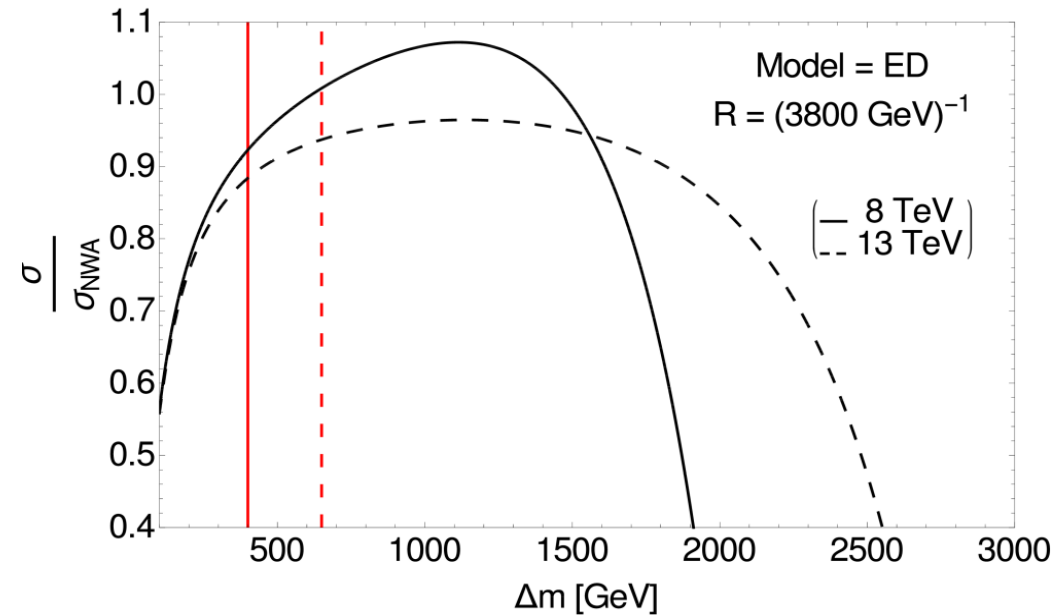
- LHC Run-I data at 20 fb⁻¹ integrated luminosity set comparable bounds

$$R^{-1} \geq 3.8 \text{ TeV}$$

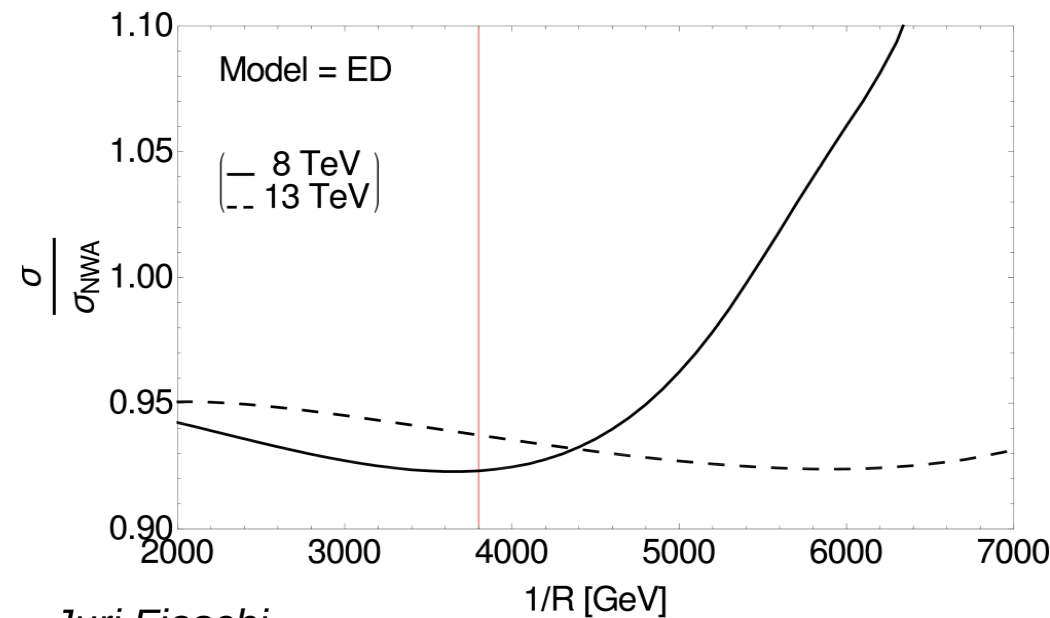
Phenomenology of NUED model



Typical profile of the ED model



In the ED model NWA works well because the dip is very far from the peak

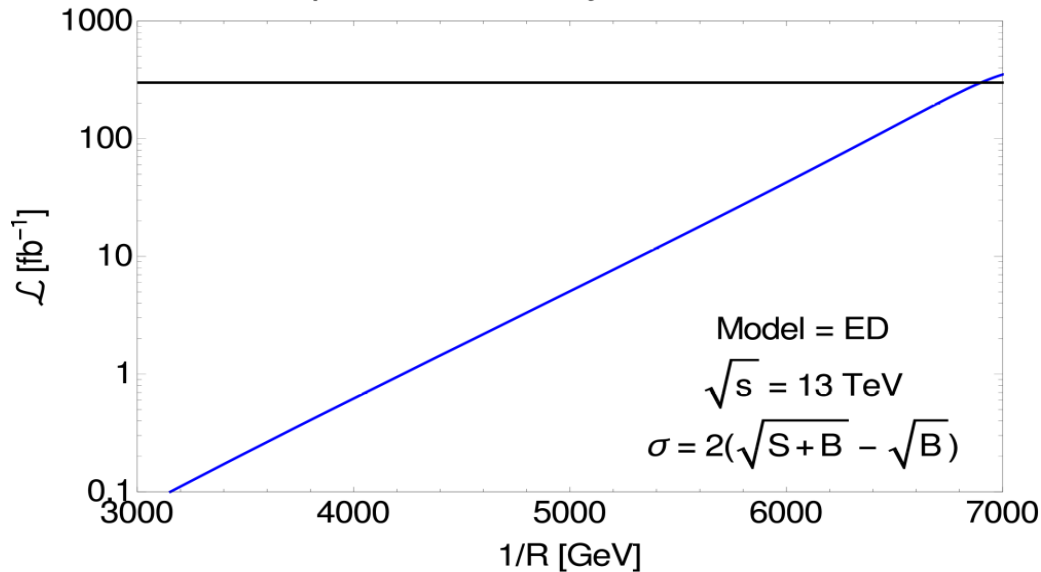


This conclusion is valid up to very high energy (R^{-1})

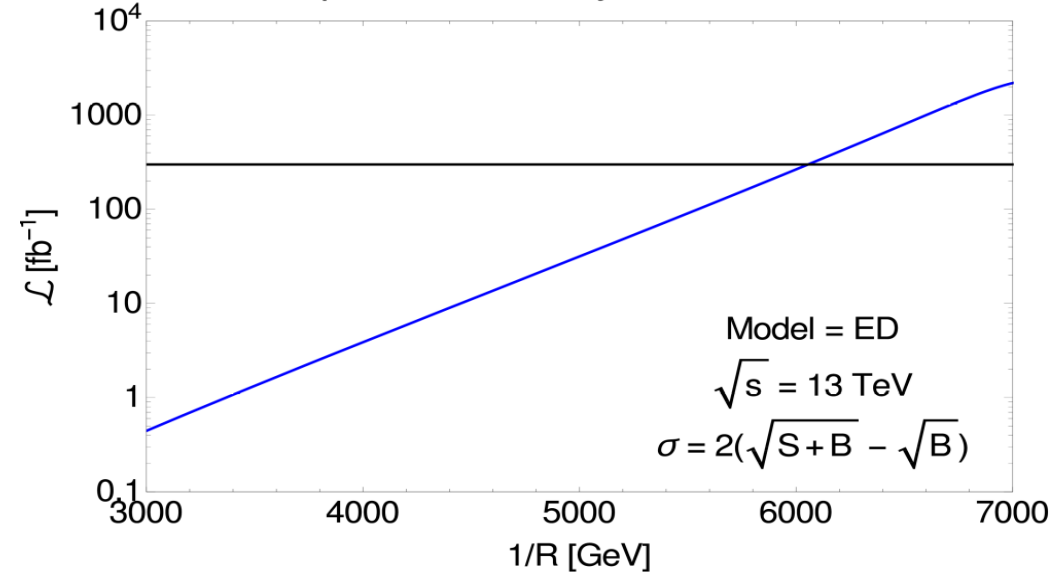
Phenomenology of NUED model

Exclusion / Discovery limits for LHC Run-II

Required Luminosity for 2σ deviation



Required Luminosity for 5σ deviation



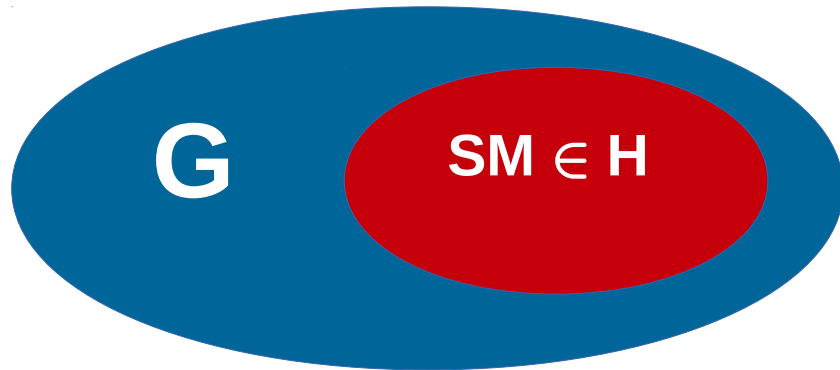
With the energy upgrade (13 TeV), and the designed integrated luminosity of the Run-II (300 fb^{-1}), we will be able to:

Exclude (2σ)
EDs with (R^{-1}) up to $\sim 6.9 \text{ TeV}$

Discover (5σ)
EDs with (R^{-1}) up to $\sim 6.1 \text{ TeV}$

The 4DCHM

- The Higgs boson is a bound state arising from a strong dynamics.
 - The Higgs boson is a pseudo Nambu-Goldstone Boson.



- Higgs from a spontaneous breaking of $G \rightarrow H$
 - The most studied in the literature is $SO(5) / SO(4)$

[Agashe, Contino, Pomarol, Nucl. Phys. B719, \(2005\), 183](#)

- The $SO(5) / SO(4)$ coset:
 - 4 Goldstone bosons.
 - Contains the $SO(4)$ custodial symmetry to protect the parameter ρ .
 - $SO(5) \rightarrow SO(4)$ at the TeV scale.
 - Minimum number of degrees of freedom that give a correct Higgs potential.
- The gauge sector of the 4DCHM is described by two non linear σ -models.
 - The introduction of the covariant derivative makes the two models interact:
 $SO(5)_L \otimes SO(5)_R \rightarrow SO(5)_{L+R} \rightarrow SO(4)$
 - In addition there is an extra $U(1)$ which crosses the $SO(5)$.

[Son, Stephanov, Phys. Rev. D69 \(2004\), 065020](#)

The 4DCHM

- **We can define an unitary gauge. The degrees of freedom are:**
 - 10+1+4 scalars provided by the two σ -models.
 - 10+1 give mass to the 5 neutral and 6 charged spin 1 physical states.
 - The 4 left are identified with the SM Higgs sector d.o.f..
- **We need to introduce a new fermion sector to misalign the vacuum. The particle content of the model is:**
 - $\underline{5 Z'}$
 - $3 W'$
 - 2 T and 2 B quarks (with exotic charges)

[Agashe et al, Nucl. Phys. B719, \(2005\), 165](#)
- **We will be interested in the phenomenology of the Z's.**
Brief recall of their properties:
 - Only three of the five Z's interact with the SM fermions, thus they will be the only one producible at the LHC (Z_2 , Z_3 and Z_5).
 - First approximation two of them have mass equal to $m_\rho = f g_\rho$, while the other has mass equal to $\sqrt{2}m_\rho$.
 - After the symmetries breaking, fine corrections to those masses arise proportional to $\xi = v^2 / f^2$ (degree of compositeness).

[Barducci, Belyaev, Brown, De Curtis, Moretti, Pruna, JHEP, 09 \(2013\), 047](#)

The 4DCHM

- **EWPT bounds from LEP data on the 4DCHM model:**

- Extra gauge bosons give large corrections to the Peskin-Takeuchi S parameter:

$$f > 750 \text{ GeV with } M_{Z'} > 2 \text{ TeV}$$

[Grojean, Matsedonskyi, Panico, JHEP 1310, 160, 2013](#)

- Corrections to the T parameter depend on the extra fermionic content. To be consistent with EWPT we need

$$M_{T'} > 800 \text{ GeV}$$

- **LHC constrains:**

- Direct DY searches of SM-like neutral heavy resonance give:

$$M_{Z'} > 2 \text{ TeV}$$

- Direct searches for extra quarks (top partner pair production, exotic charges fermions, etc.)

$$M_{T'} > 780 \text{ GeV}$$

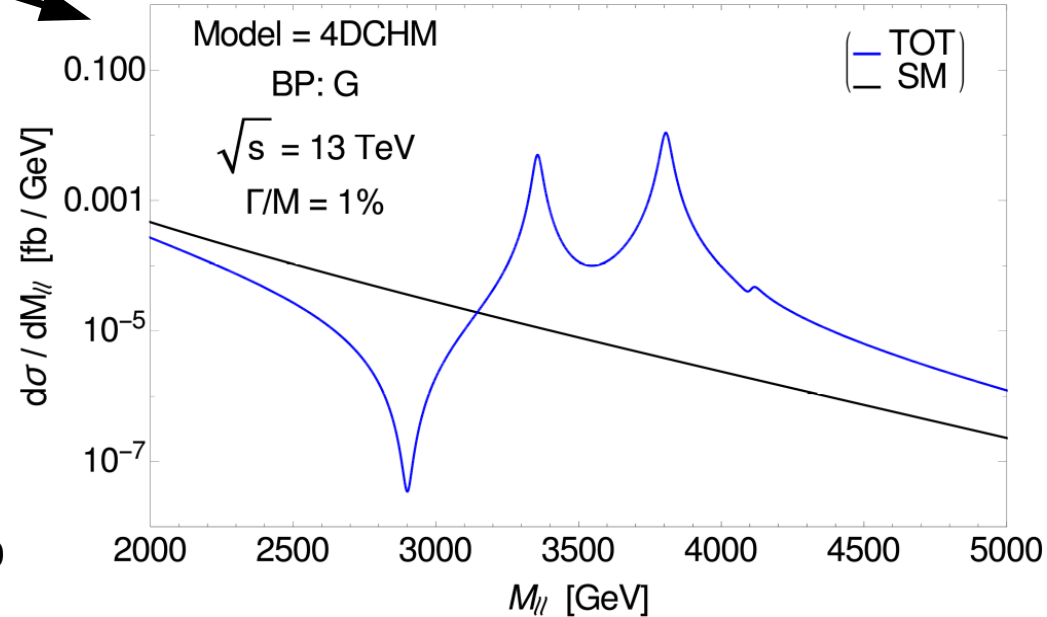
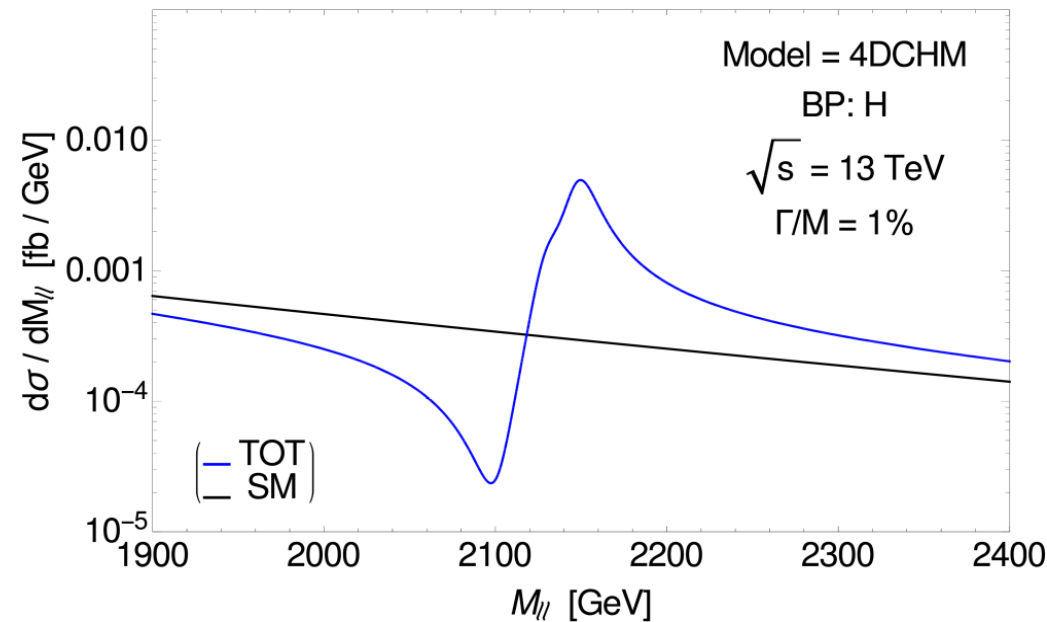
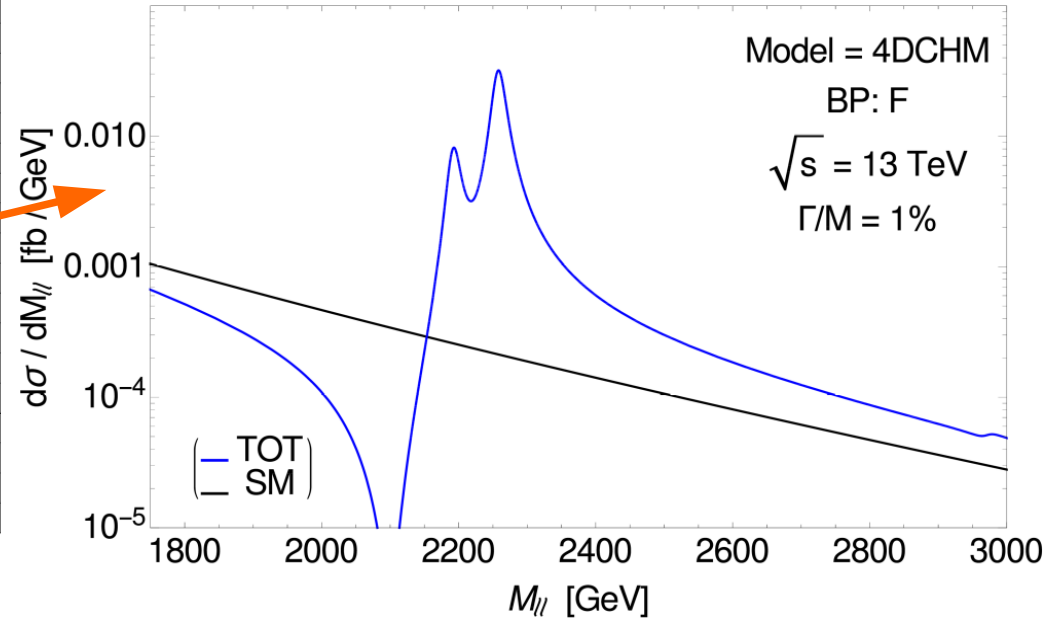
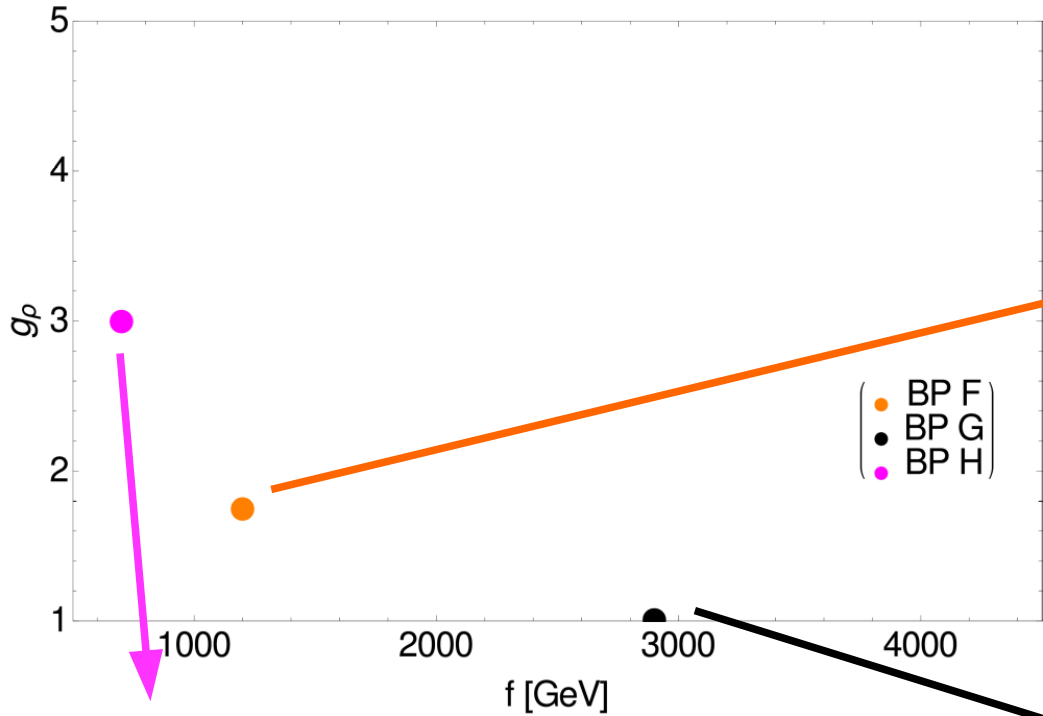
[CMS collaboration, Phys.Rev.Lett. 112 171801, \(2014\)](#)

[CMS collaboration, Phys.Lett. B729,149, \(2014\)](#)

[CMS-PAS-B2G-13-003](#)

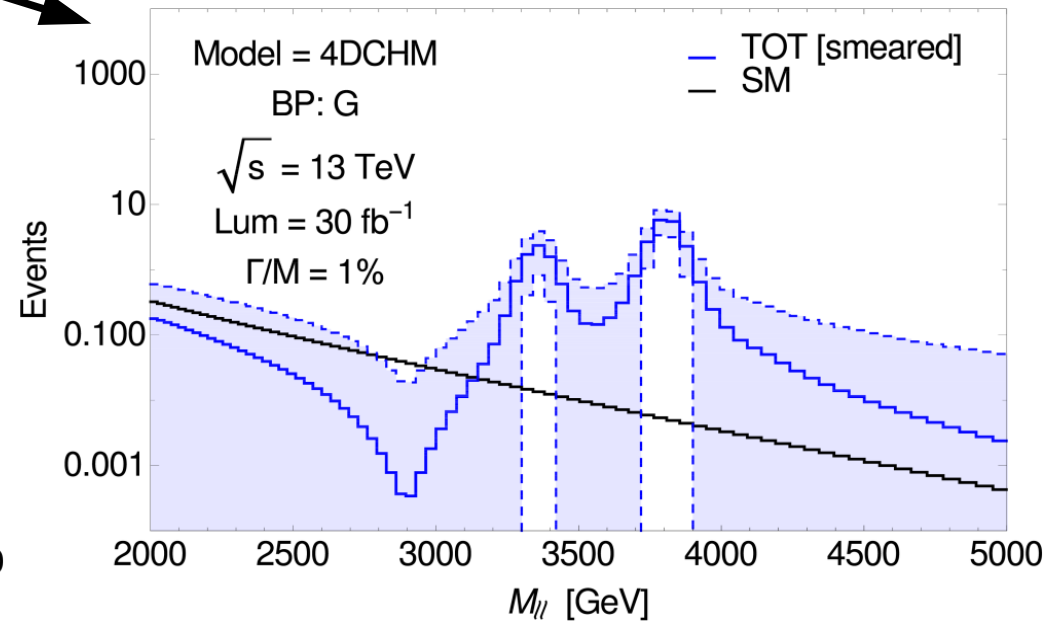
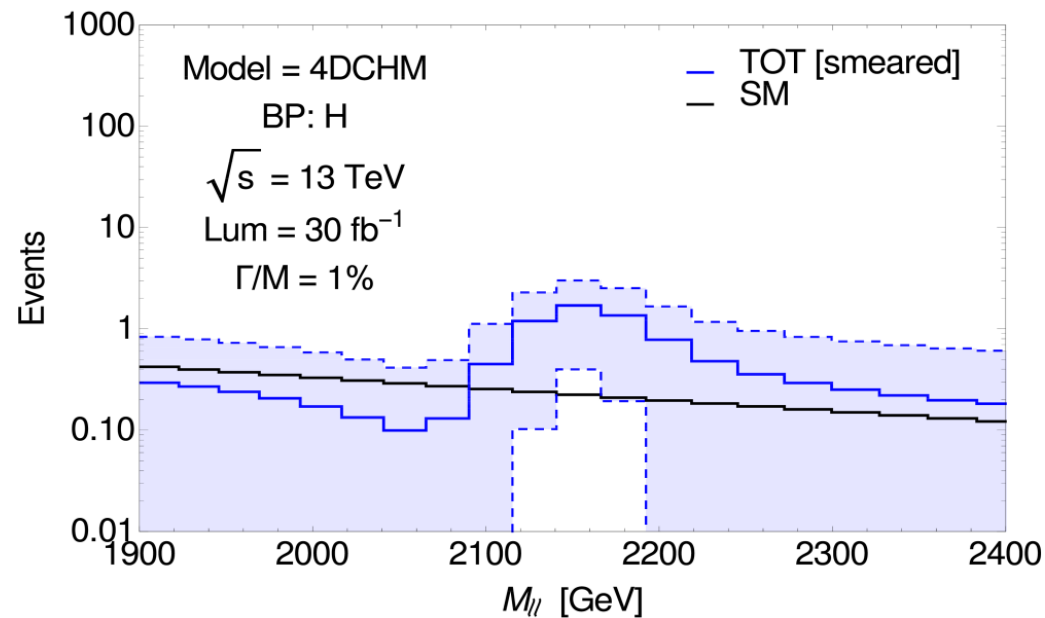
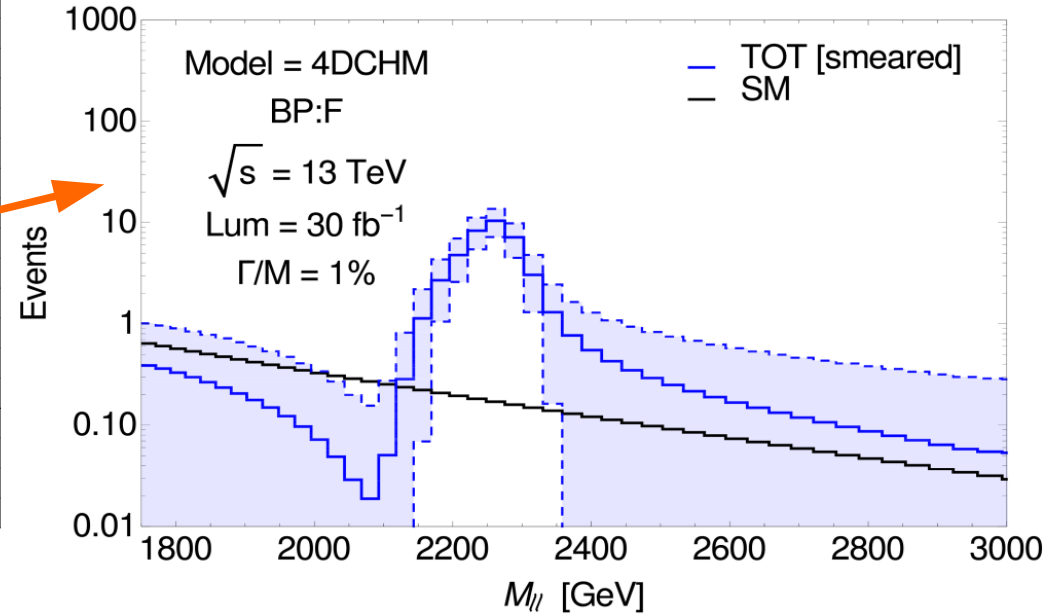
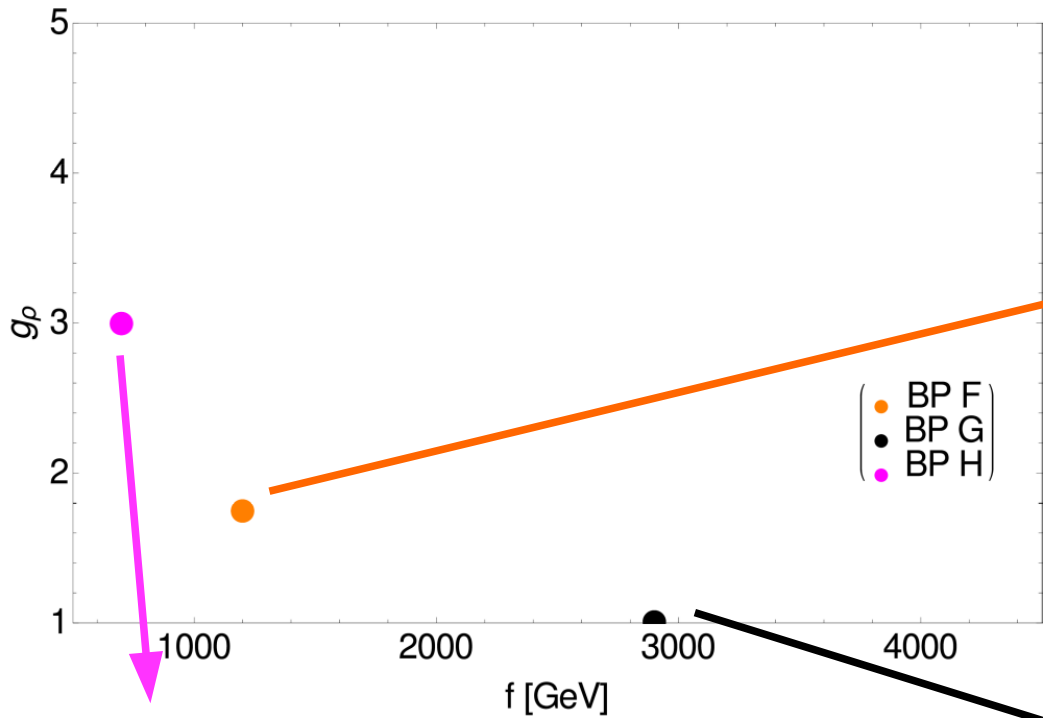
The 4DCHM – multi Z' scenario

Before the detector:



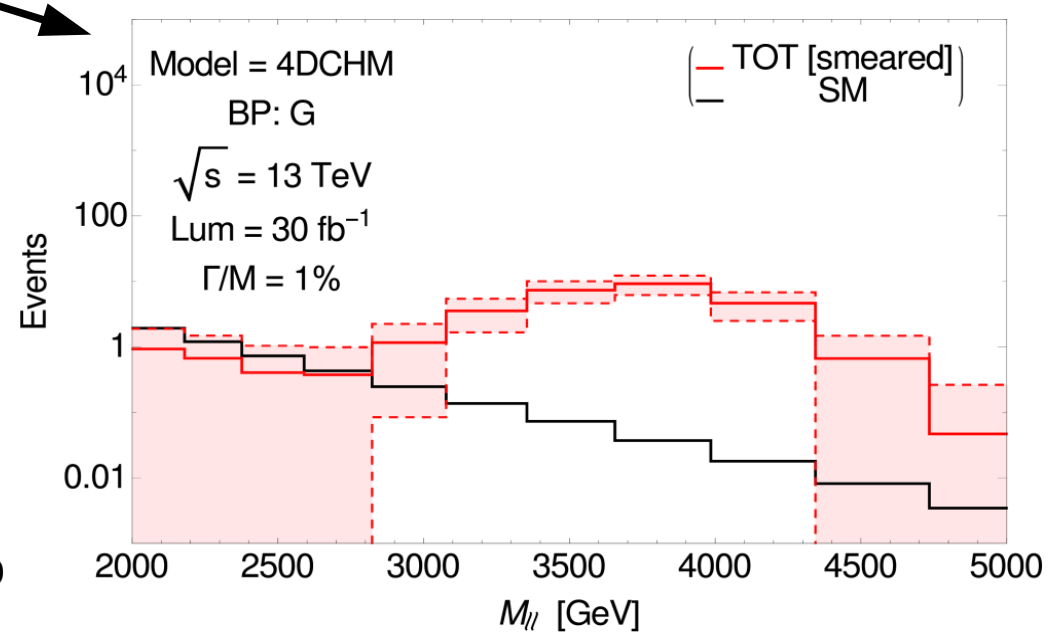
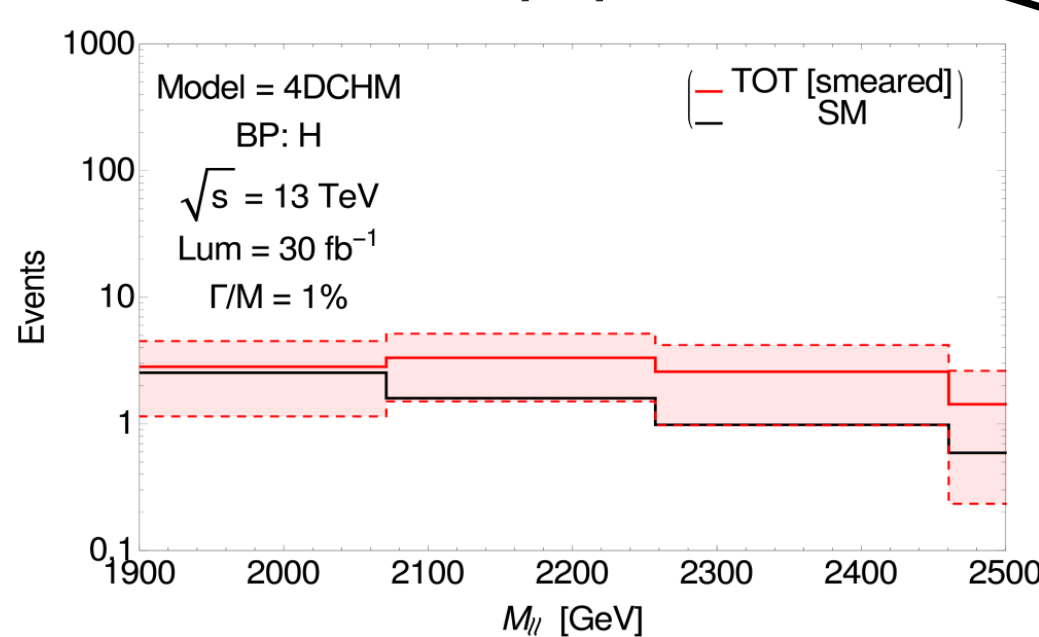
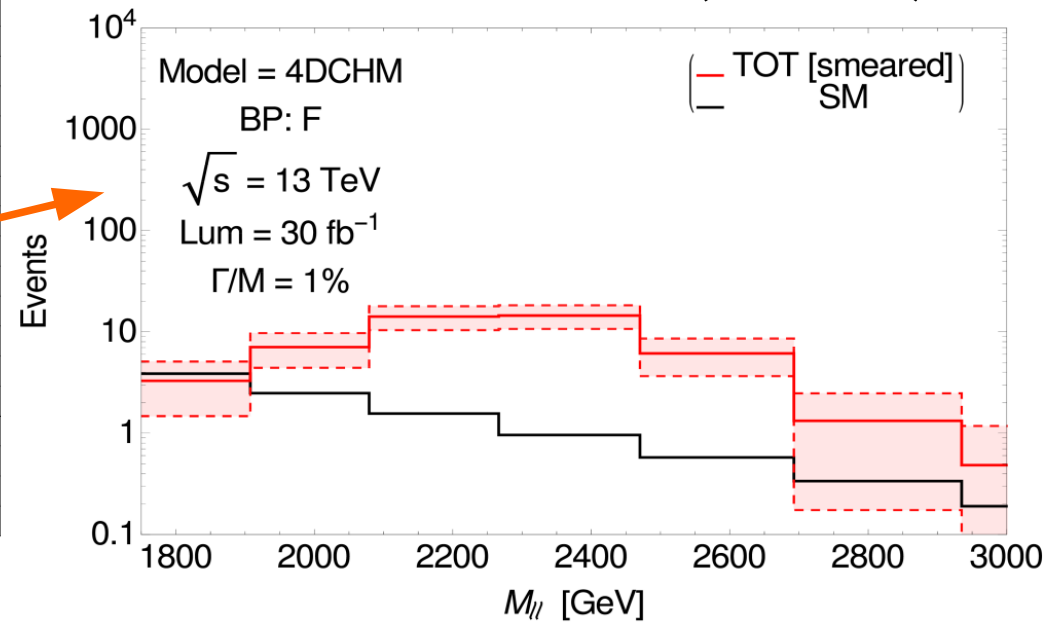
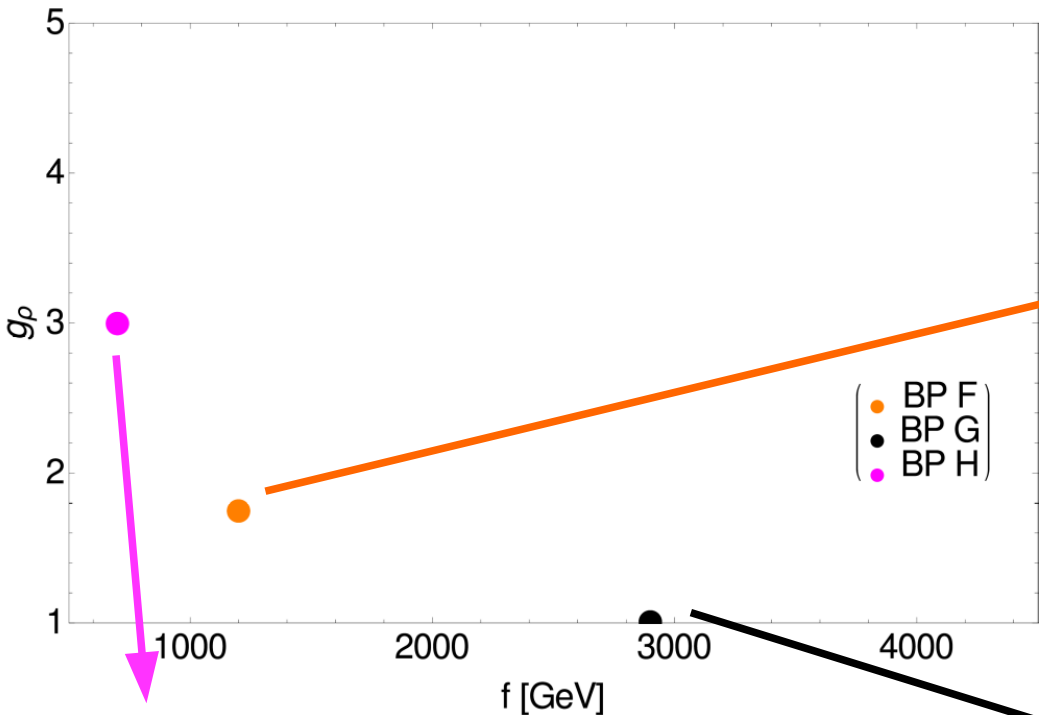
The 4DCHM – multi Z' scenario

After the detector (electron):

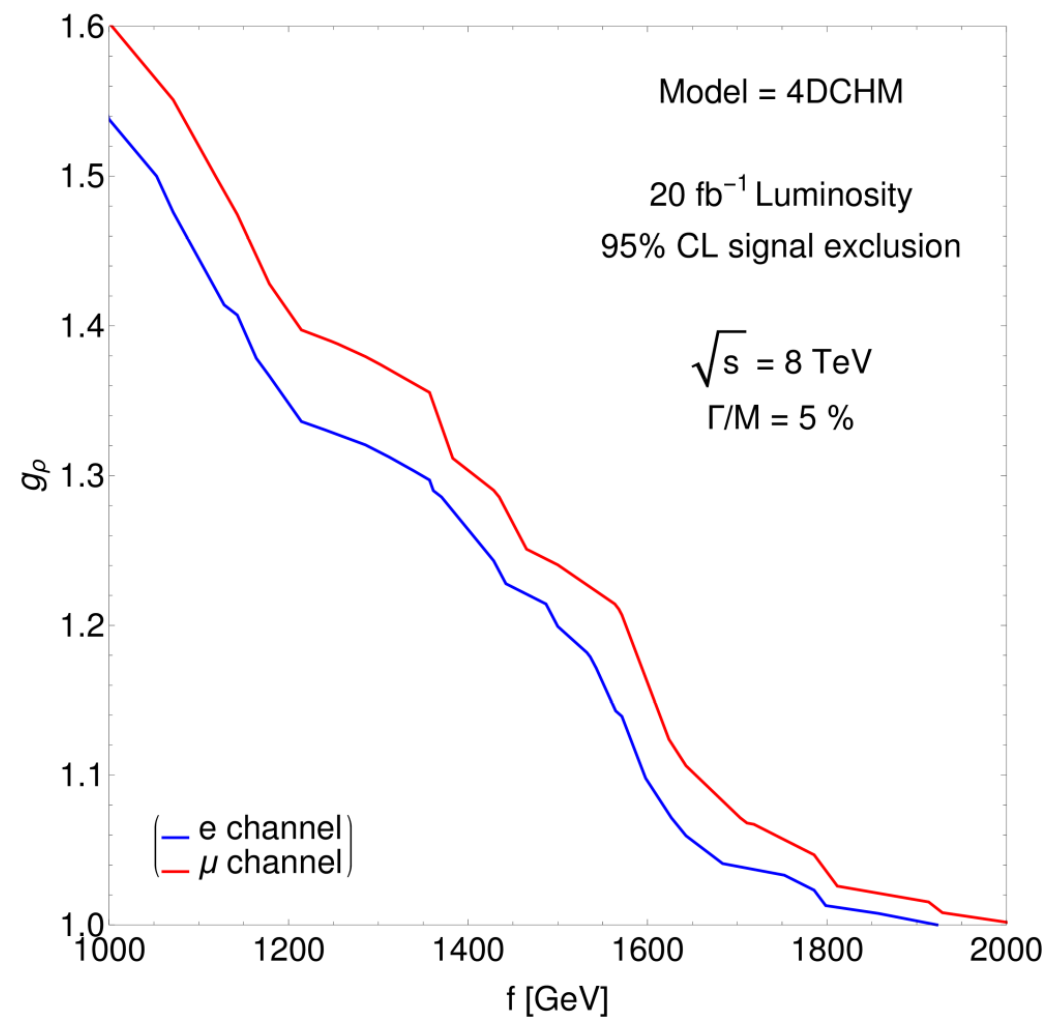


The 4DCHM – multi Z' scenario

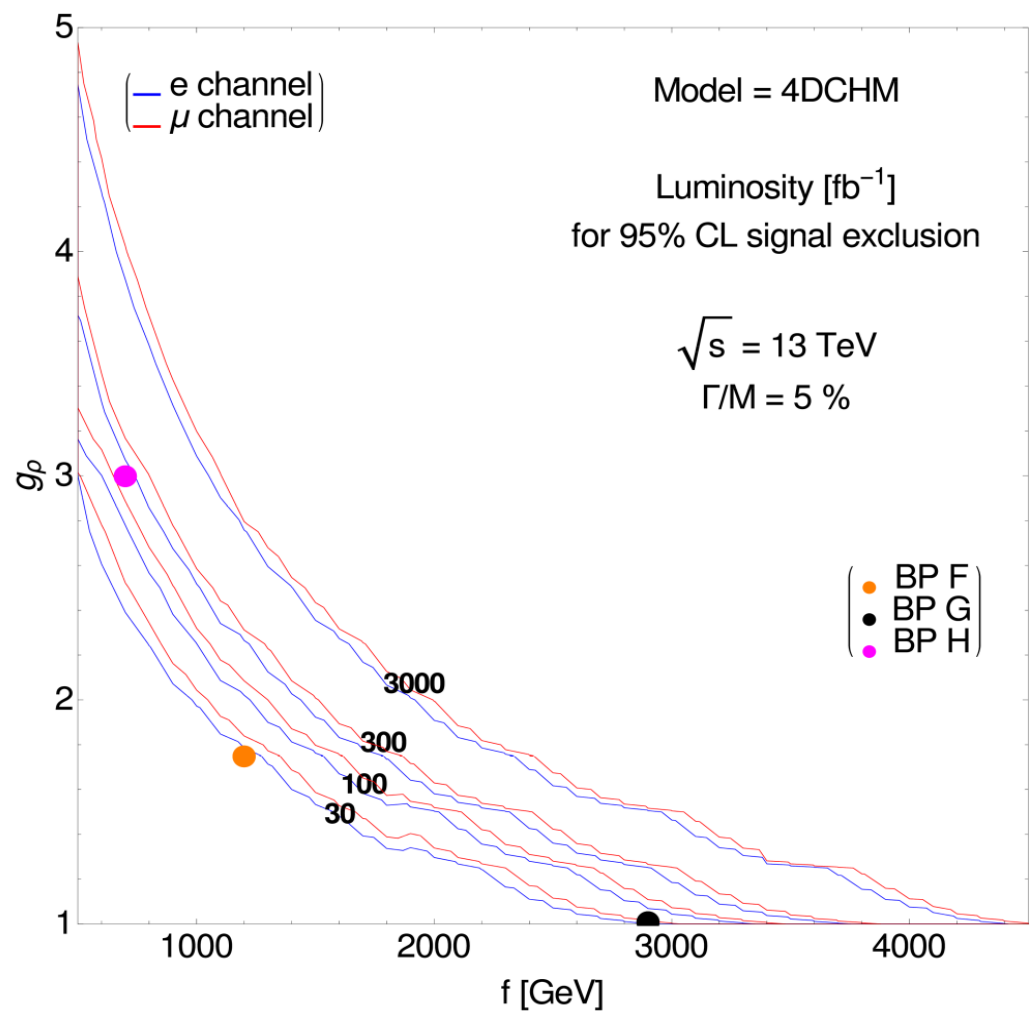
After the detector (muon):



The 4DCHM – multi Z' scenario



Exclusion Limits after Run-I



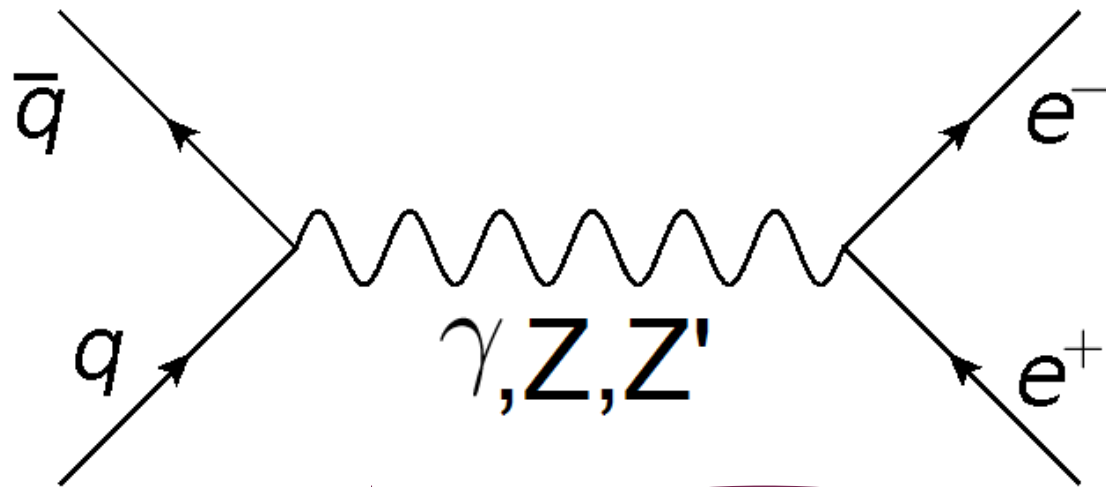
Exclusion Limits after Run-II

Conclusions

- I gave you an overview of Z' physics, from the theory to the pheno to the experimental point of view. Various phenomenological situations have been tested against the experimental strategies adopted by the ATLAS and CMS collaborations.
- We focused on the scenarios of narrow, wide and multiple resonances.
- In the context of narrow resonances we have found a good agreement between the ATLAS and CMS exclusions and the theoretical projections.
- We discussed the issues relative to experimental searches of wide resonances.
 - We proposed the introduction of extra observables (**AFB** and **AFP**) in the analysis in order to improve the sensitivity.
- We have compared the effects of PI processes (both from real and virtual photons) on the dilepton channel as predicted by different PDF sets.
 - The initial concern on the large central value and uncertainties of those contributions has been resolved adopting the parametrization proposed by the LUX collaboration.
- We explored the phenomenology of two multiple Z' models, the **NUED** and **4DCHM**.
 - The compressed spectrum and the interference effects can modify the simple Breit-Wigner shape.
 - The finite resolution of the detectors might lead to peculiar observations in the electron and muon final states.

Thank you!

Z'-bosons @ the LHC



**Bump search /
Counting strategy**

Experimentally
unobserved signal

**Excluded
cross section**

Narrow Width
Approximation
(NWA)

Optimal invariant
mass cut:
 $|M_{ll} - M_{Z'}| < 5\% E_{\text{LHC}}$

Finite width and interference
effects are kept under
control ($< 10\%$) in narrow
single Z' models

Z' mass bounds

Finite width and interference
effects are neglected

[Accomando, Becciolini,
Belyaev, Moretti,
Shepherd-
Themistocleous,
JHEP 10, 2013, 153](#)

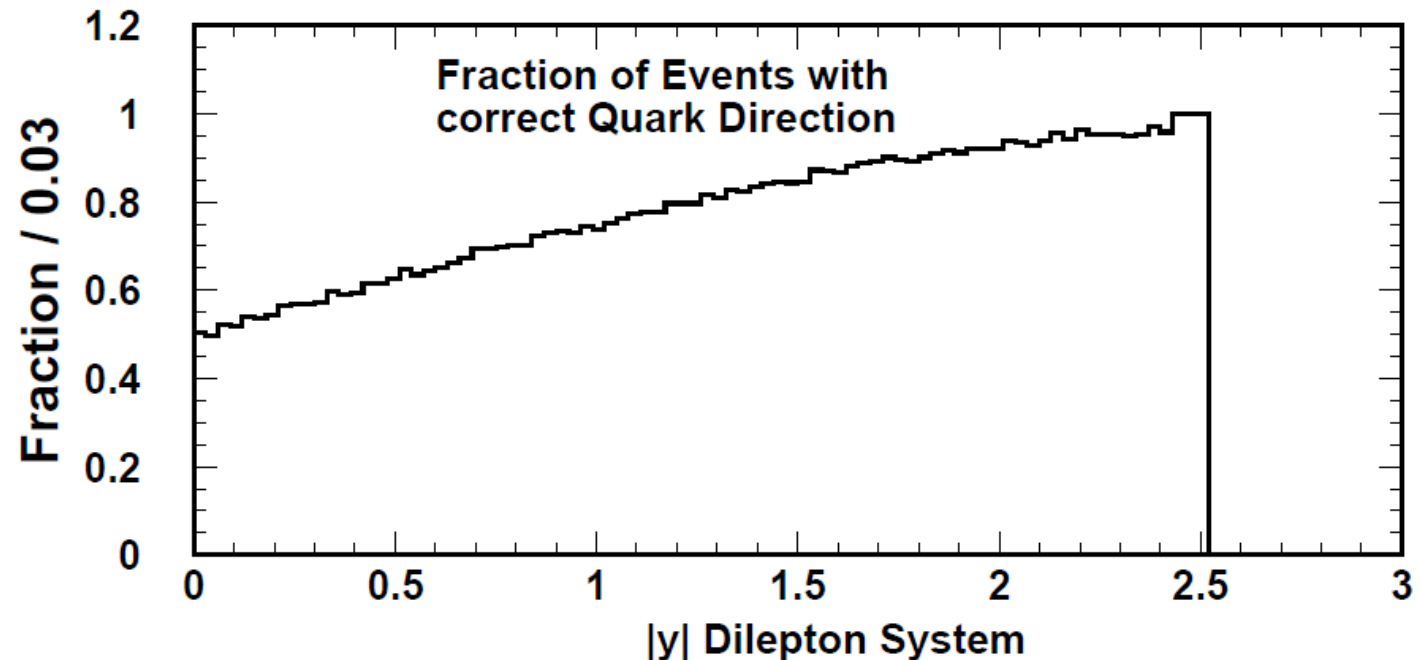
Forward / Backward

Problem in the definition of “Forward” and “Backward”:

In order to construct the asymmetry, we need to know which one is the forward direction, as in a Drell-Yan process we actually don't know from which proton the quark/antiquark comes from.

General rule:

In this case of neutral process, we expect that the dilepton longitudinal momentum marks the direction of the quark, as the latter is supposed to be more energetic than the antiquark (which comes from the sea).

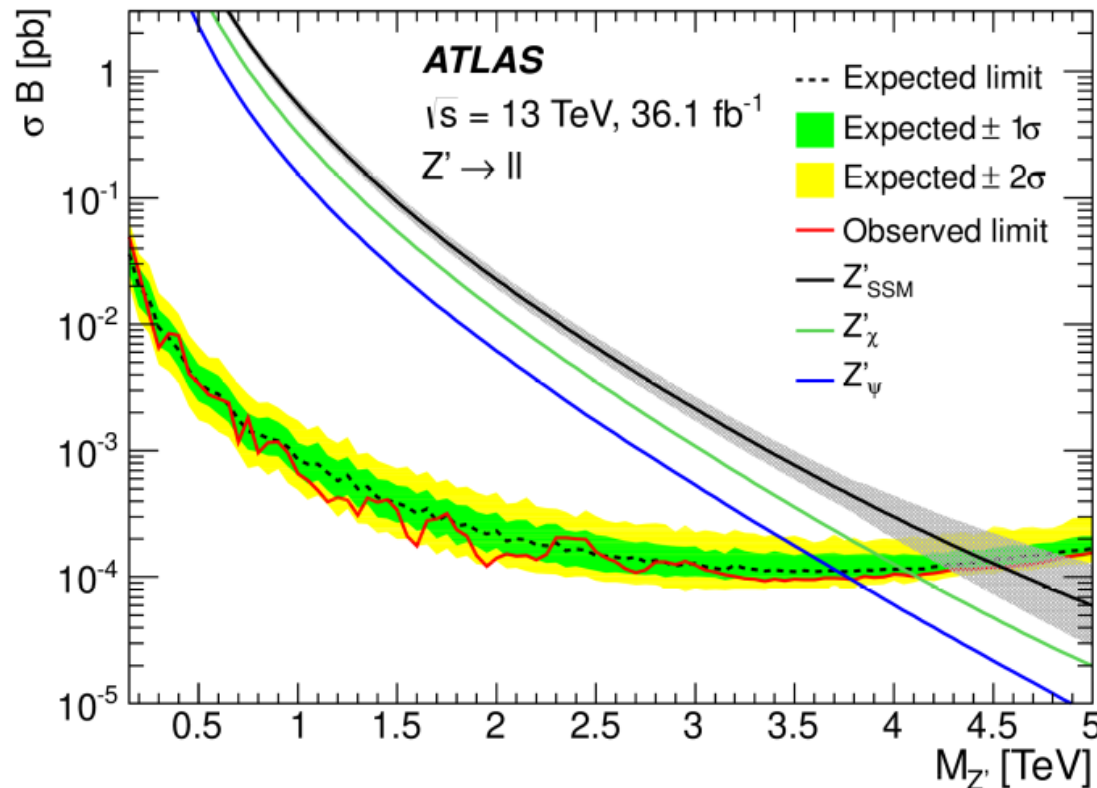
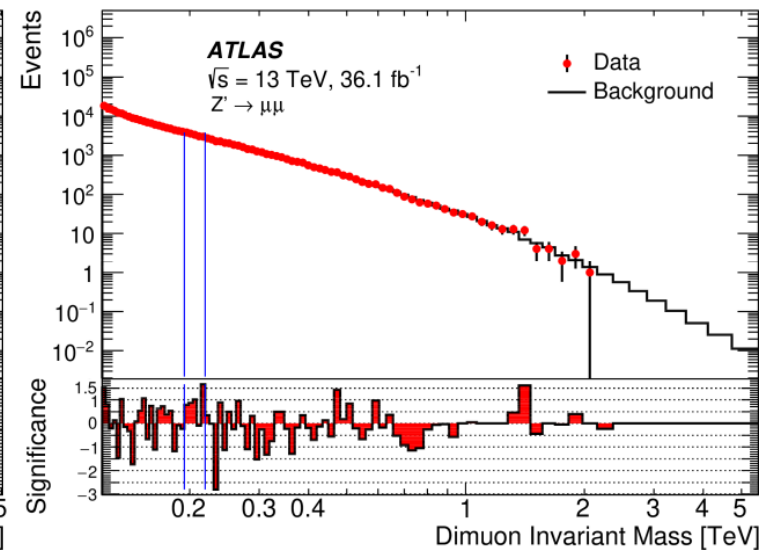
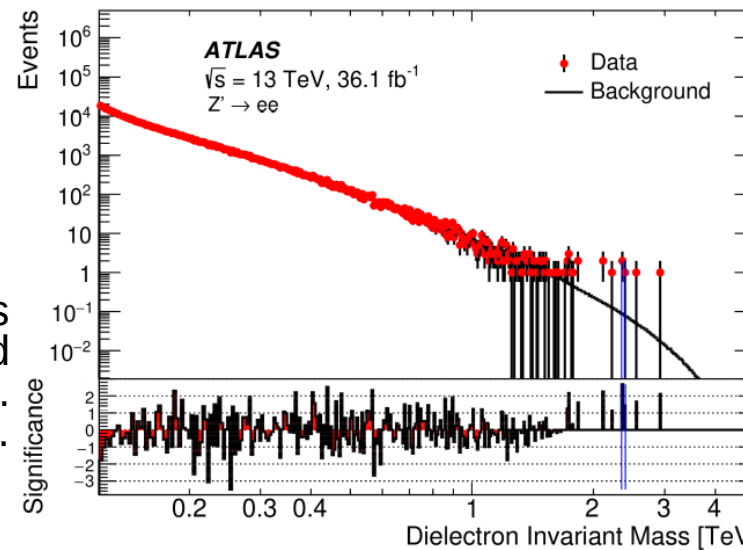


[Dittmar, Phys.Rev.D55:161-166 \(1997\)](#)

Updates from the LHC

**13 TeV data with
 $\mathcal{L} \sim 36.1 \text{ fb}^{-1}$**

Some high invariant mass events (up to **3 TeV**) observed in the **di-electron** channel. Still low significance.

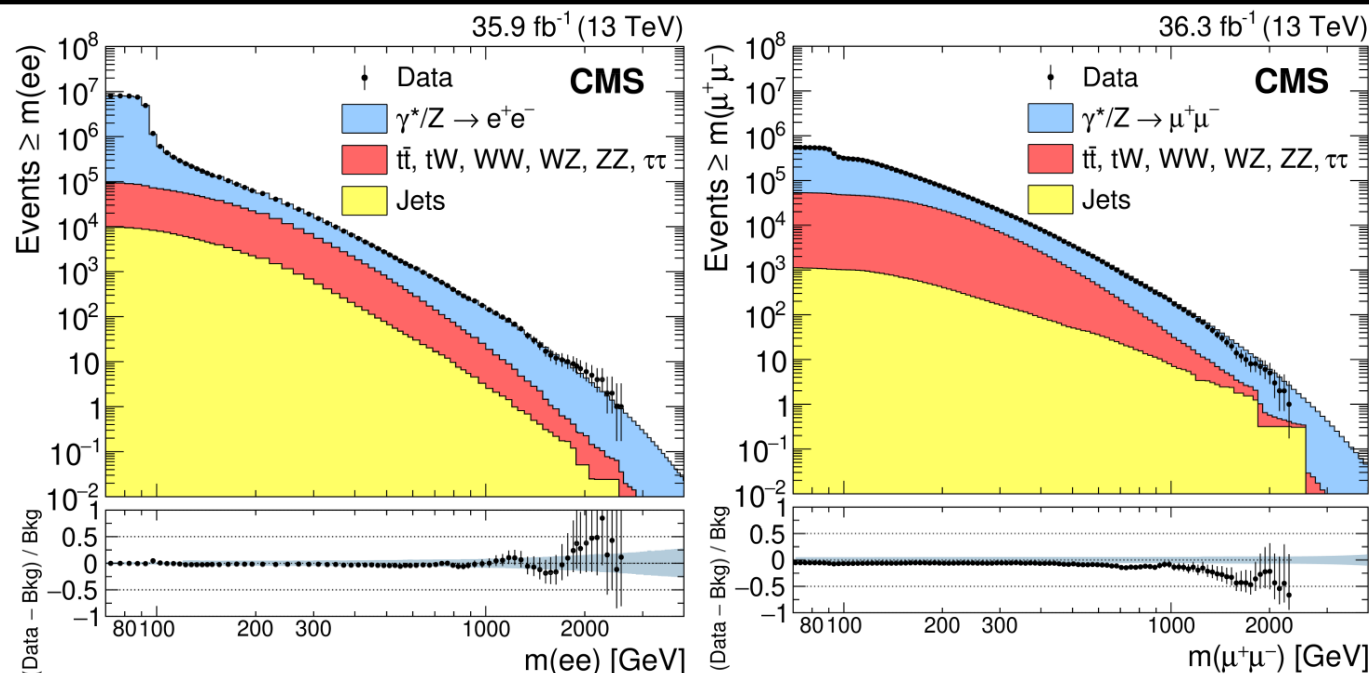


ATLAS provides the curves with the acceptance of the integrated signal in the ($M_{Z'} \pm 1$ width) region for different Z' widths. Exclusion limits can be rescaled accordingly.

Limits on Z' masses increased to **4.5 TeV**

ATLAS collaboration,
JHEP 1710 (2017) 182

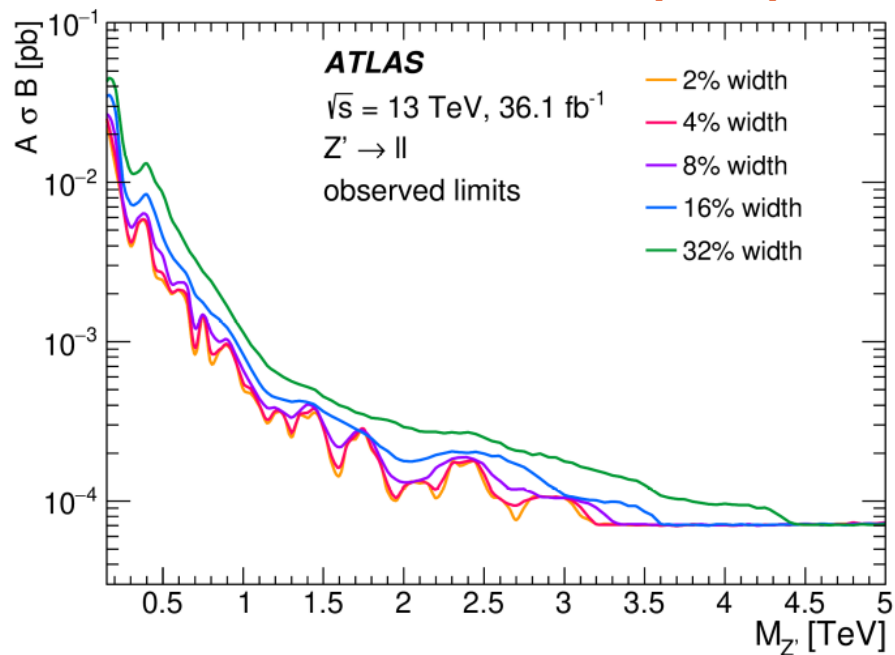
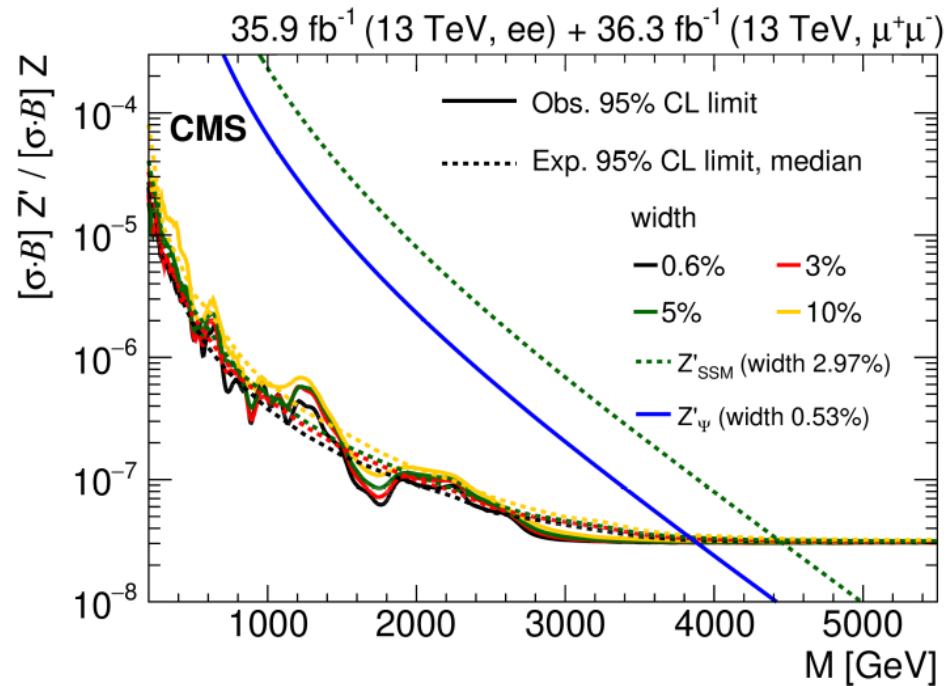
Wide Z's at the LHC



[CMS collaboration, JHEP 1806 \(2018\) 120](#)

The experimental analysis is essentially a counting experiment where we seek for an excess of events above an estimated SM background.

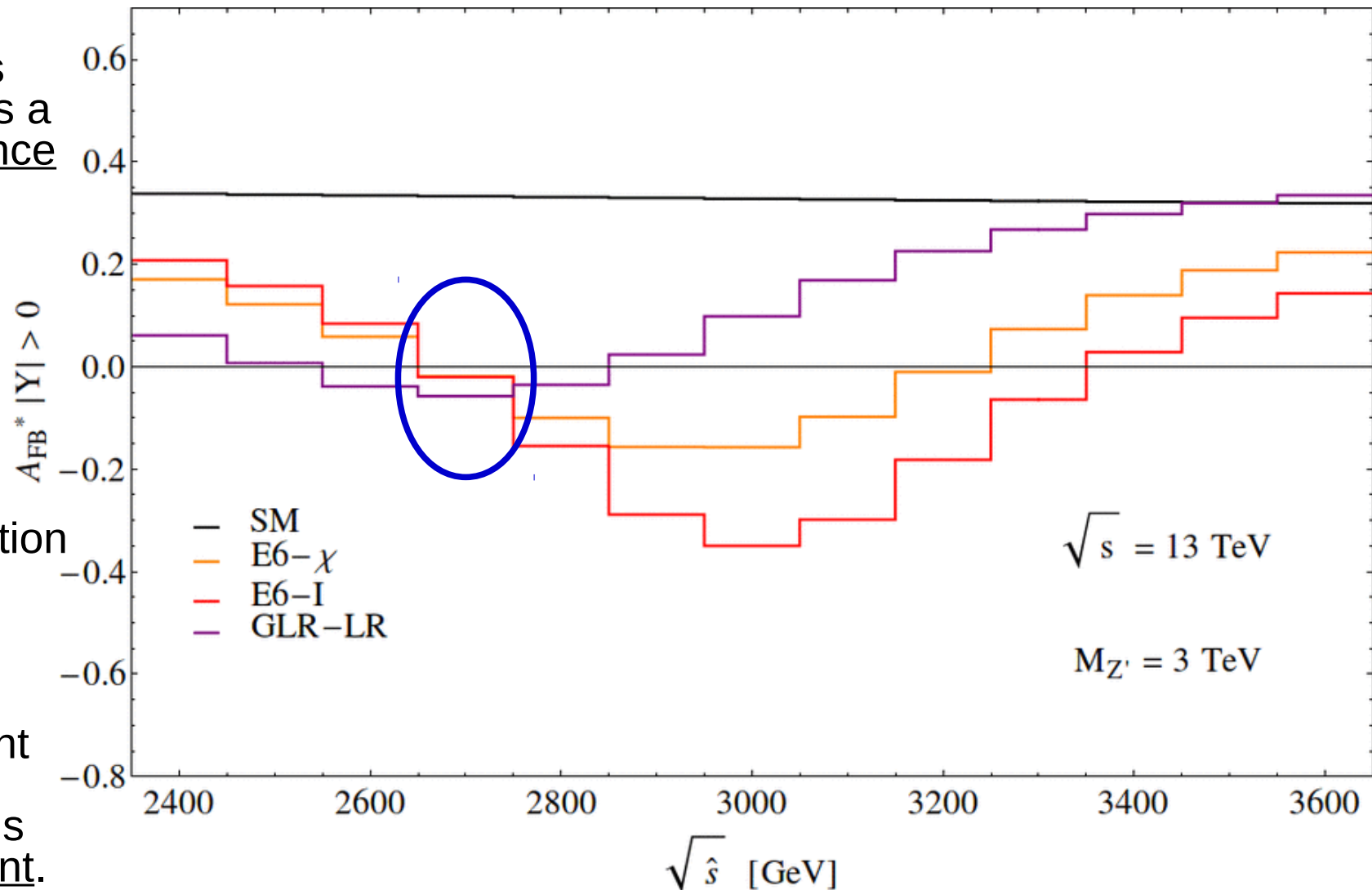
[ATLAS collaboration, JHEP 1710 \(2017\) 182](#)



Effects of rapidity cuts

The rapidity cuts bring themselves a model dependence in our analysis.

With the convention adopted in the reconstruction procedure, the probability of choosing the right direction for the incoming quark is flavour dependent.

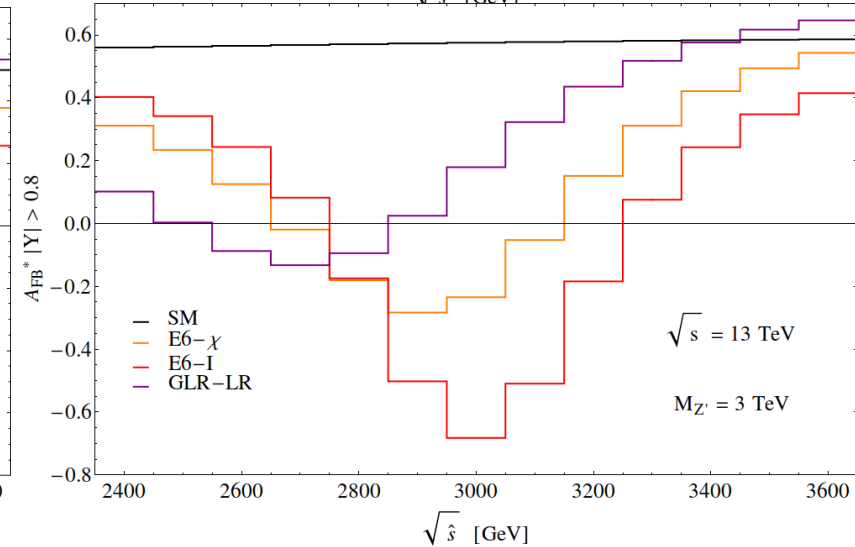
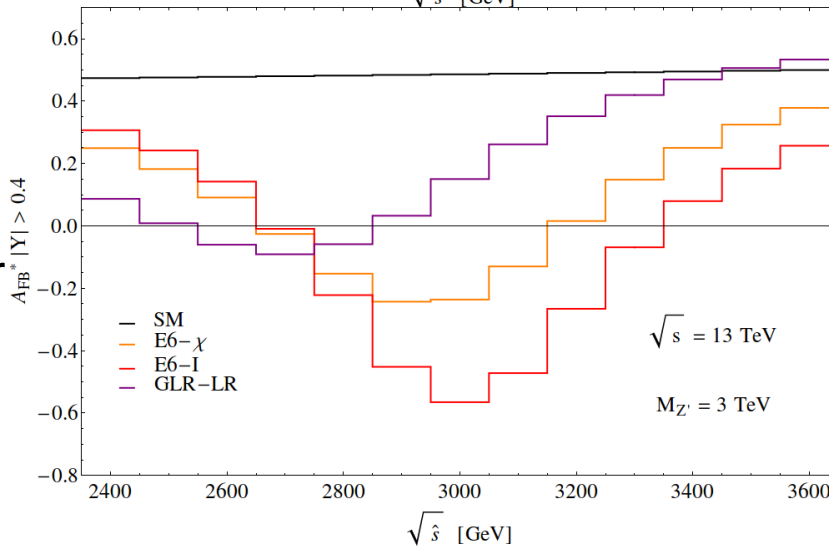
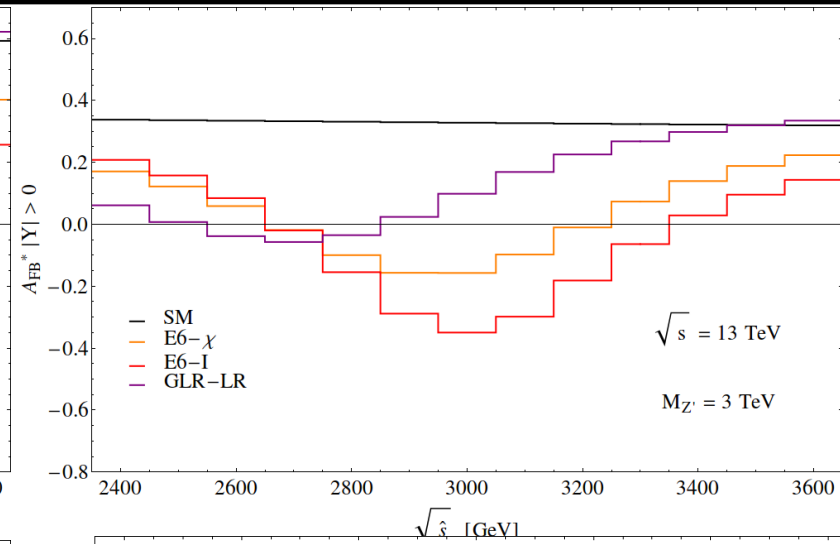
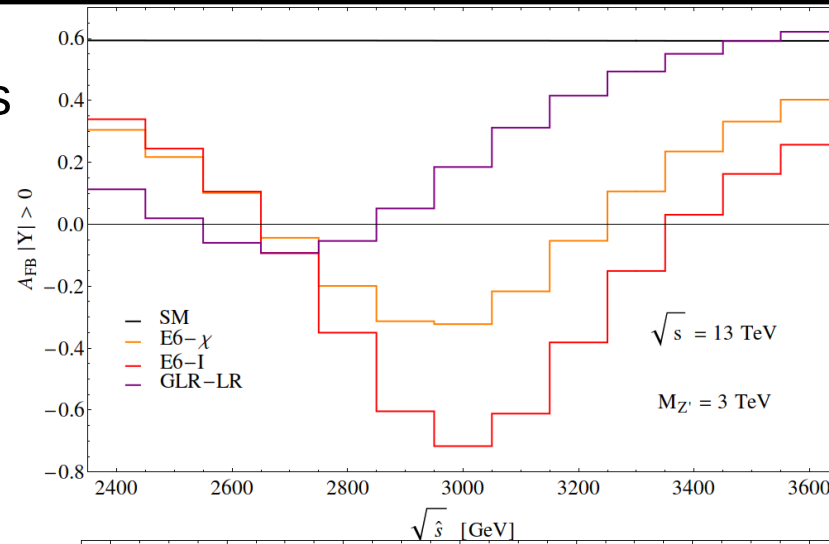


Models with different couplings to u and d quarks have a different behaviour under the application of rapidity cuts

Effects of rapidity cuts

The rapidity cuts bring themselves a model dependence in our analysis.

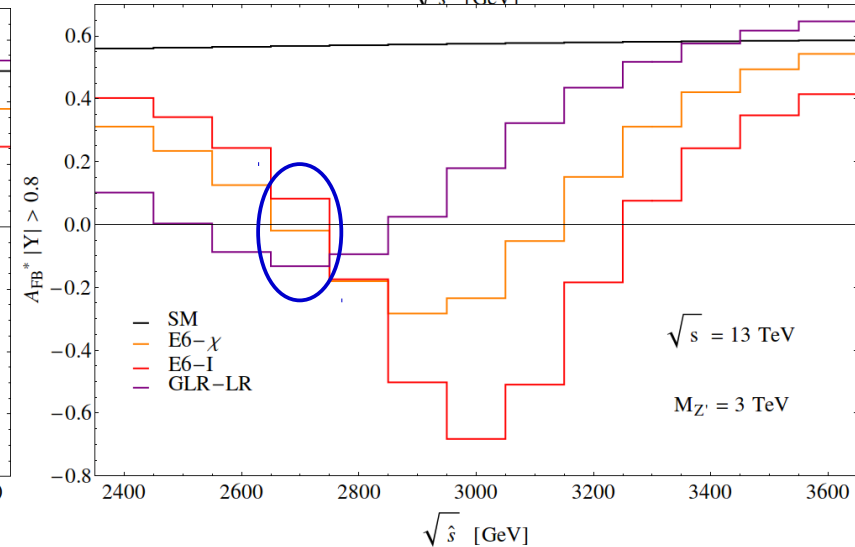
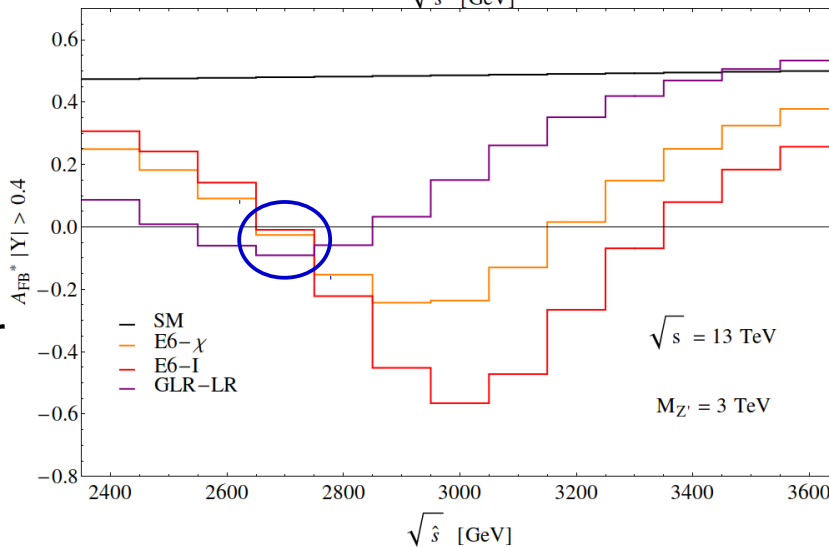
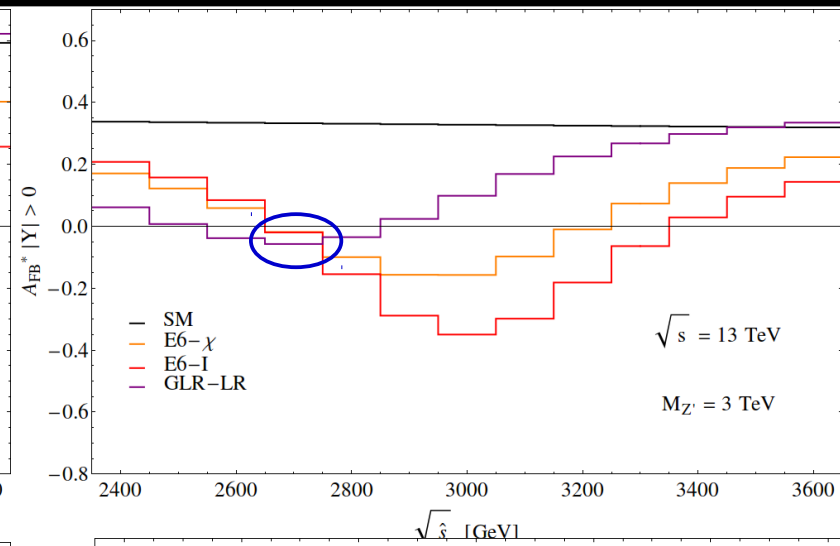
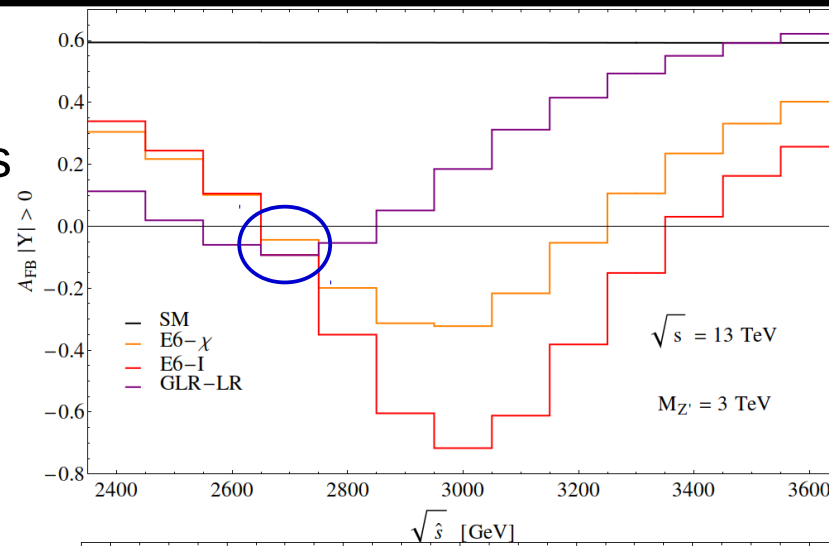
With the convention adopted in the reconstruction procedure, the probability of choosing the right direction for the incoming quark is flavour dependent.



Effects of rapidity cuts

The rapidity cuts bring themselves a model dependence in our analysis.

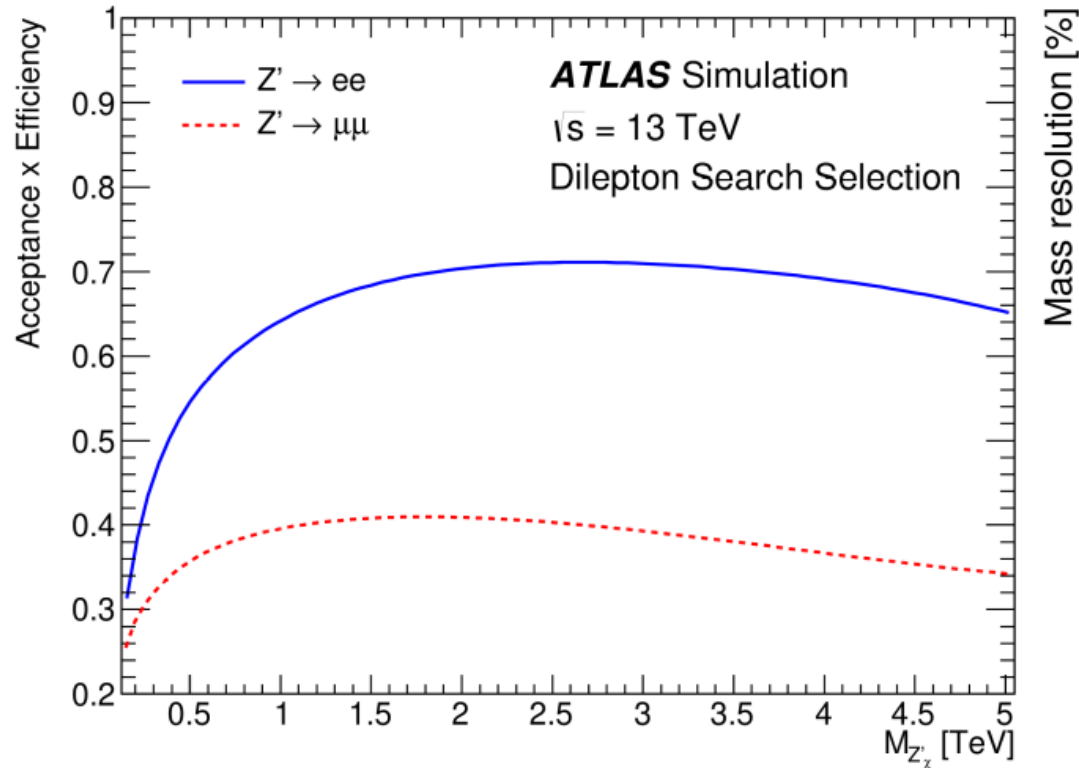
With the convention adopted in the reconstruction procedure, the probability of choosing the right direction for the incoming quark is flavour dependent.



Models with different couplings to u and d quarks have a different behaviour under the application of rapidity cuts

Detector performances

Acceptance x Efficiency



In the high invariant mass region:

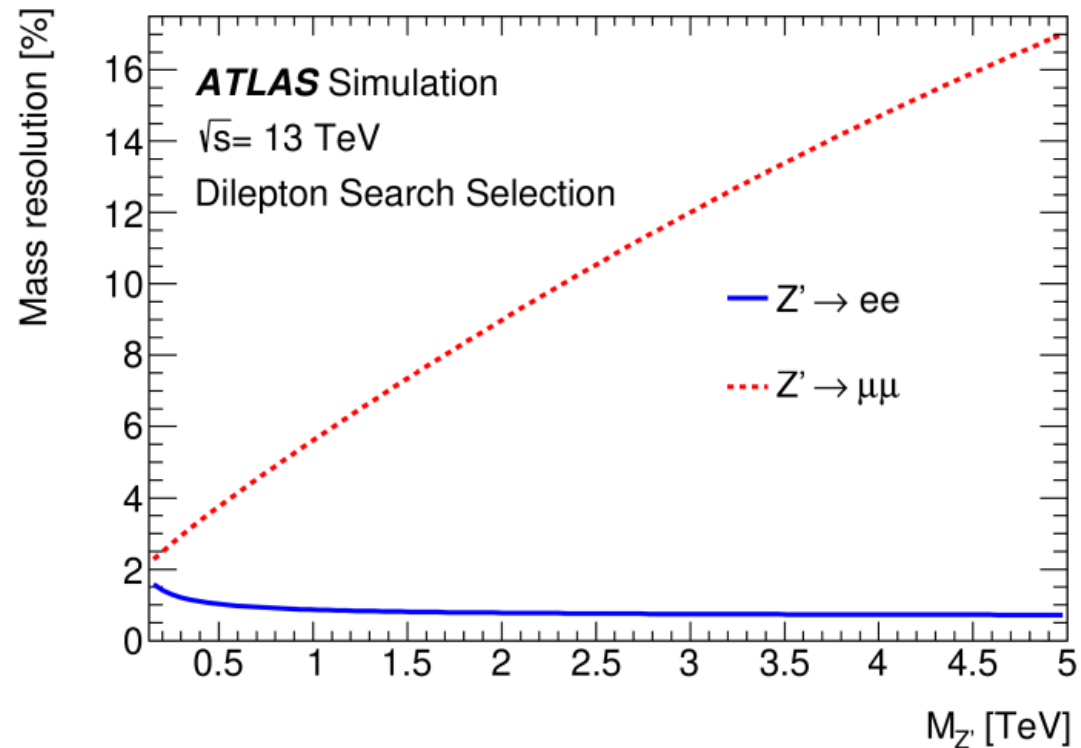
ATLAS

di-electron channel $\sim 60\% - 70\%$
 di-muon channel $\sim 35\% - 40\%$

CMS

di-electron channel $\sim 60\% - 70\%$
 di-muon channel $\sim 90\%$

Resolution



In the high invariant mass region:

ATLAS

di-electron channel $\sim 0.5\% - 1\%$
 di-muon channel \sim linear growth

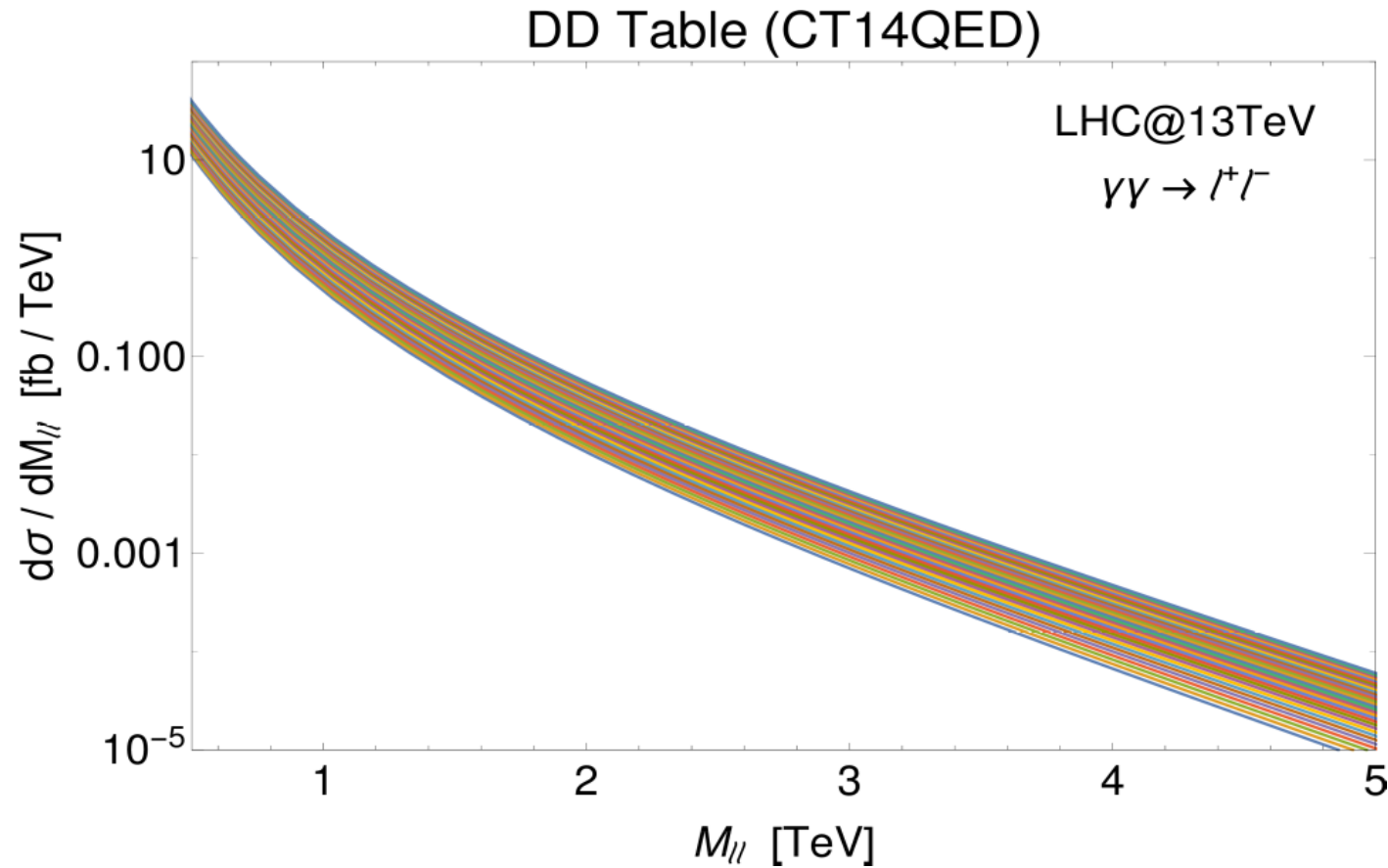
CMS

di-electron channel $\sim 1\%$
 di-muon channel $\sim 3\% - 4\%$

Double-Dissociative

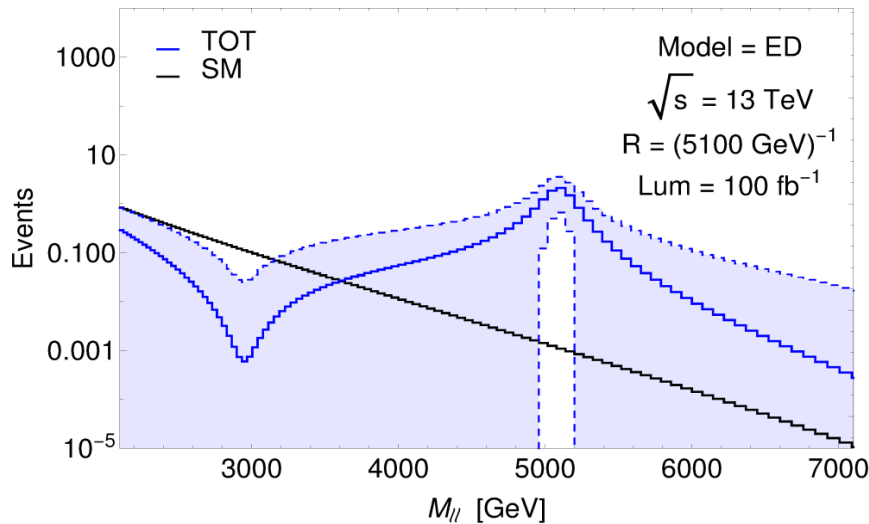
CT14QED → table of 31 PDF fitted imposing a progressive constrain on the relative momentum carried by the photon ($p_\gamma = 0.00\% - 0.30\%$)

Their analysis provides the bound:
 $p_\gamma \leq 0.11\%$ at 68% C.L.
We have considered the average of the first 12 tables as central value, and the relative 1σ error band consistently.



Phenomenology of NUED model

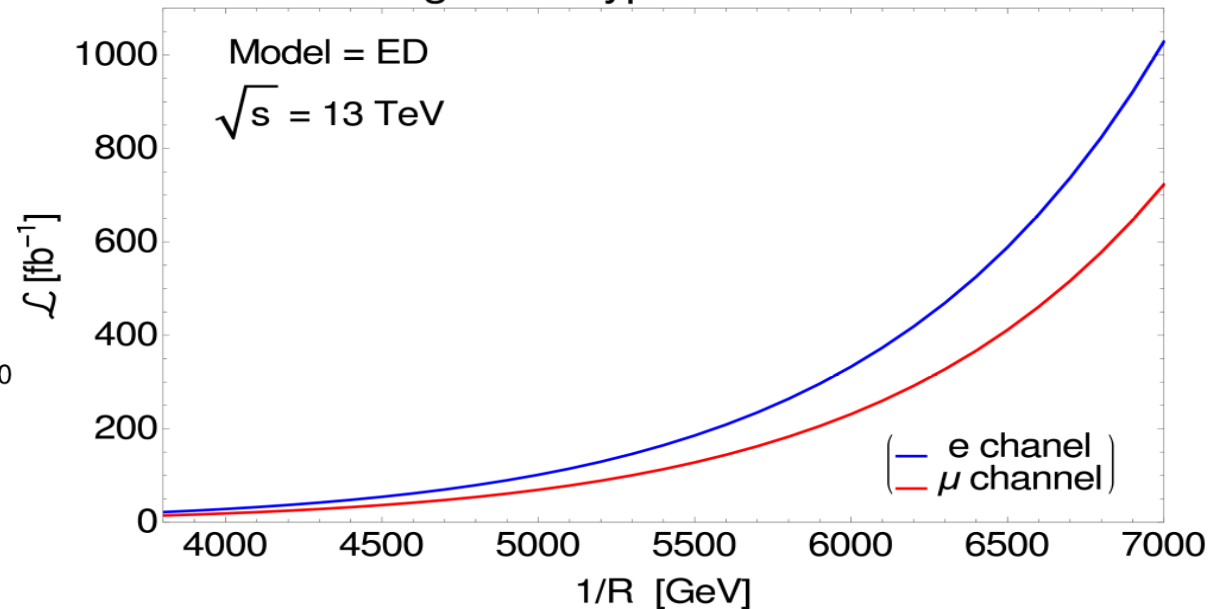
Characterization of the resonance



The interference negative contribution is larger than in a singly resonant case

We can exploit the accentuated dip to characterize the model

Required Luminosity for 95% CL background hypothesis exclusion

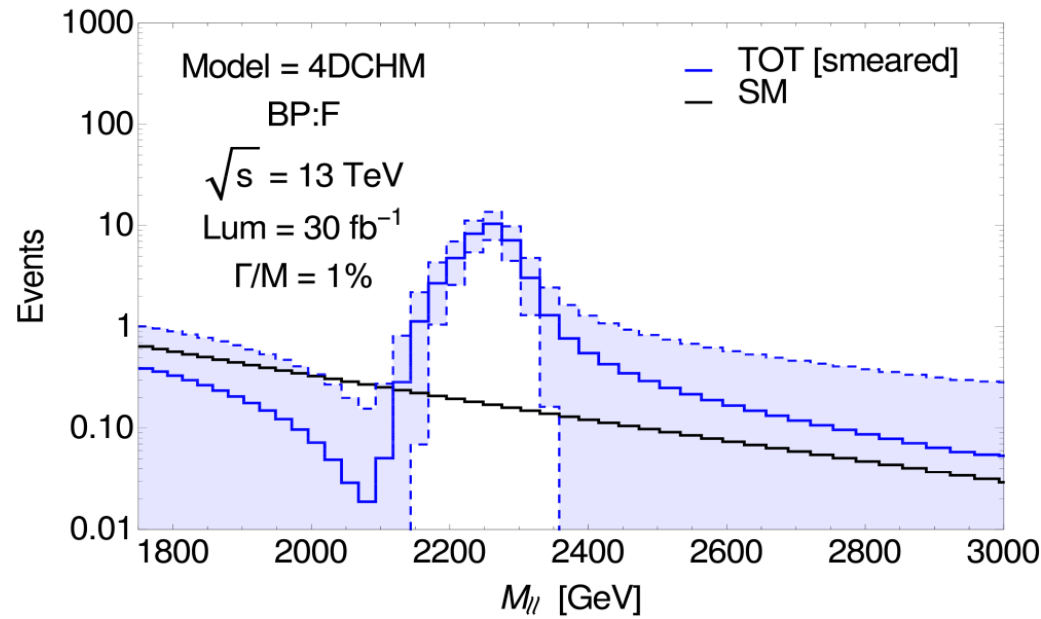


The two channels include the respective resolutions, acceptances and efficiencies

In the post discovery stage with High Luminosity (HL), we could observe the **depletion of events** produced by the interference effects

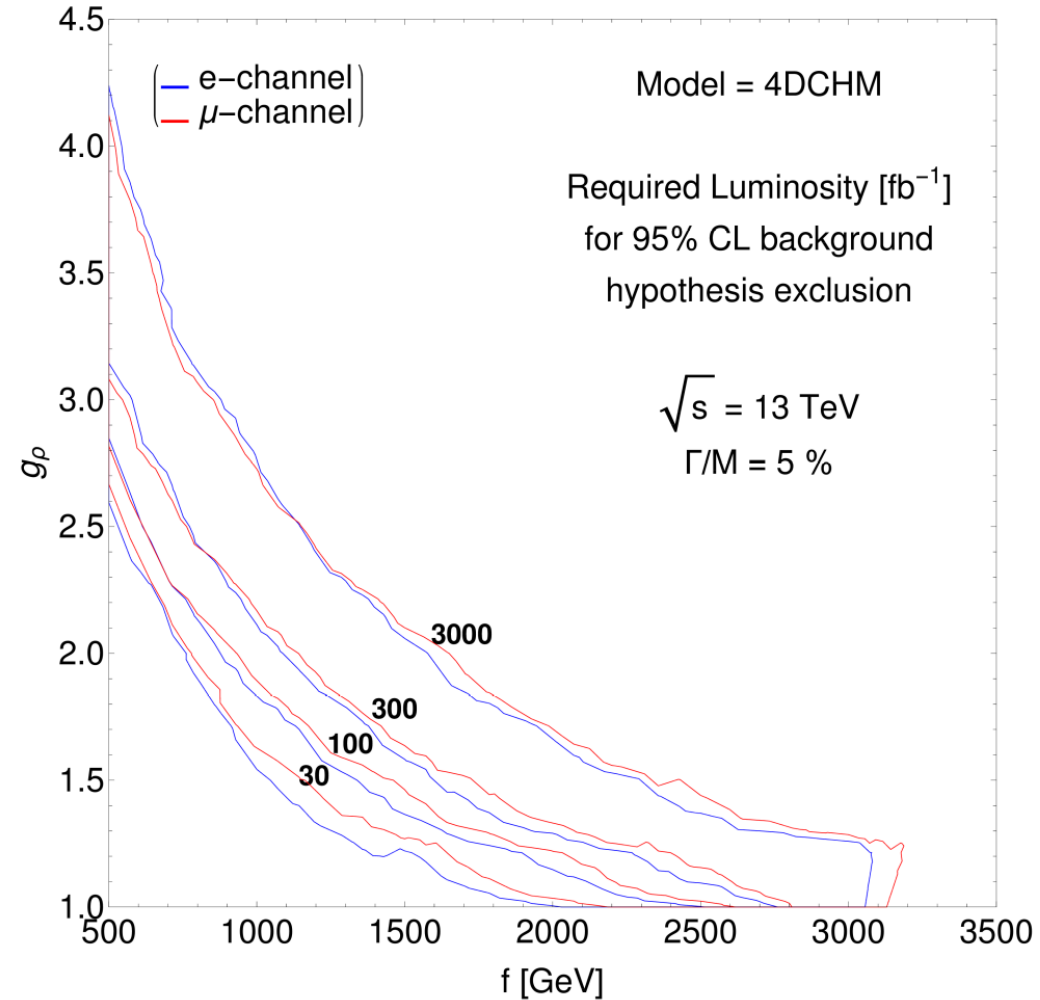
Phenomenology of 4DCHM

Characterization of the resonance



We can exploit the depletion of events to characterize the resonance

In the post discovery stage with High Luminosity (HL), we could observe the **depletion of events** produced by the interference effects

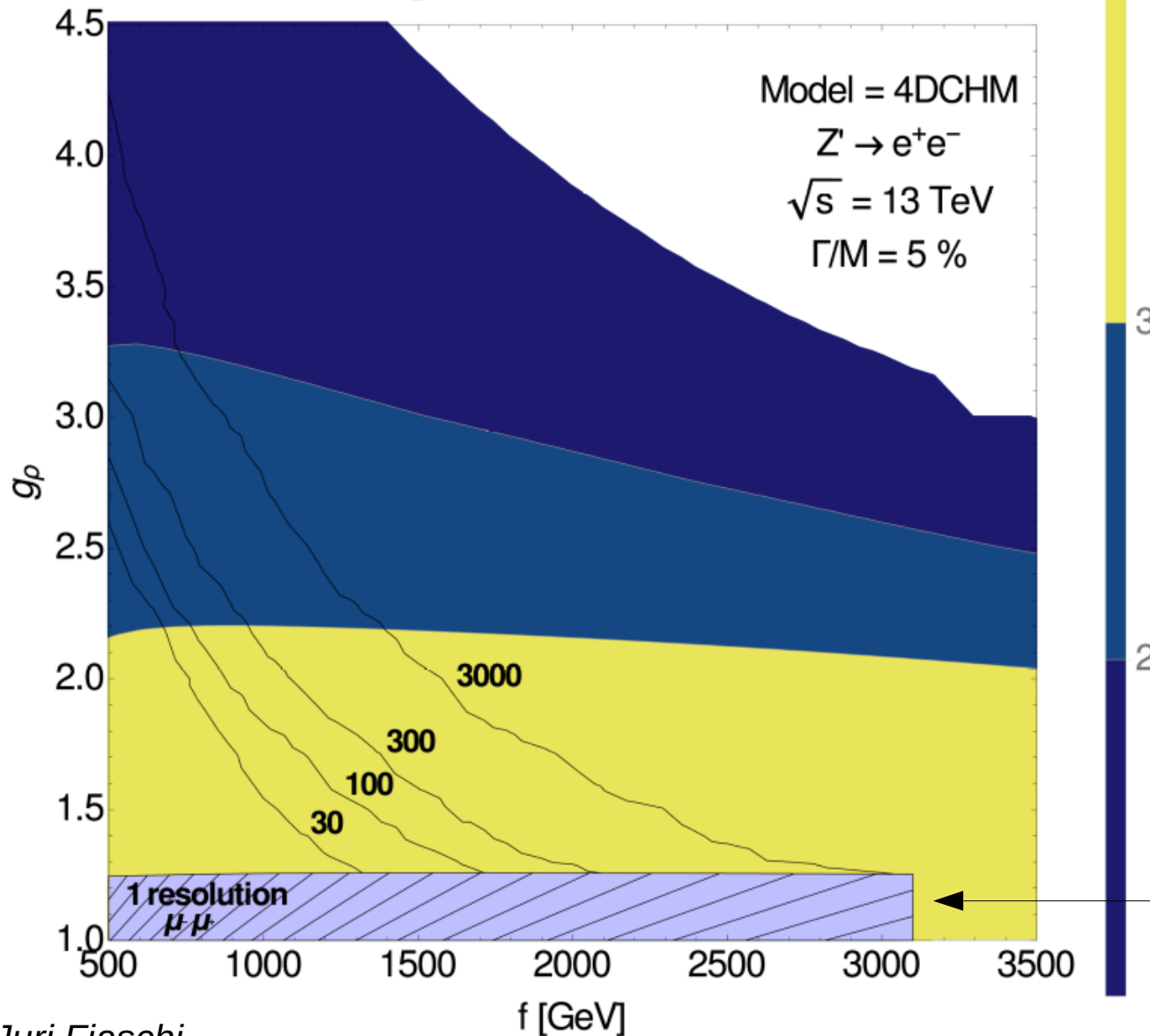


The two channels include the respective resolutions, acceptances and efficiencies

Phenomenology of 4DCHM

Characterization of the resonance

$(M_{Z_2}$ -Dip) in resolution units



Parameter space region where we are able to disentangle the peak from the dip in the electron channel (good resolution)

The muon channel does contribute to the statistic (good Acceptance x Efficiency), but do not help the diagnostic (bad resolution)